A STUDY ON MANGANESE, IRON AND DISSOLVED ORGANIC MATTER IN MOUNTAINOUS STREAMS WITH SABO DAMS

A DOCTRAL DISSERTATION

Submitted to

The UNITED GRADUATE SCHOOL OF AGRICULTURAL SCIENCE, IWATE UNIVERSITY

by

SUSAN PRAISE

March 2017

Abstract

Damming of rivers is important in various ways such as electricity generation, water supply for agriculture, industrial and domestic uses and mostly control of floods. Sabo dams have been used for many years to prevent the impact of disasters in highland areas, and their use has been expanding worldwide. Rivers and streams, on the other hand, are dynamic systems involving a variety of elements, some of which interact with each other, in continuous water movement linking terrestrial to coastal and finally to ocean ecosystems. Inland water systems receive substantial amounts of organic matter which is accompanied by high metal loading from soil erosion and rock weathering in mountainous areas. Two metals, iron (Fe) and manganese (Mn), have a significant environmental relevance and influence other metals through co-precipitation and are easily affected by changes in environmental condition resulting from damming.

This study examined changes in dissolved organic matter (DOM) composition together with Mn and Fe concentrations along the stream continuum to elucidate how the presence of sabo dams impacts on their behaviors. Water samples were collected along five mountainous streams (Mizunashigawa, Higashiiwamotogawa, Kanosawagawa, Imogawa and Maenokawasawa rivers) in Shonai district, Yamagata, Japan. The water samples were collected at four stations in each stream, which were located at the upstream, dam vicinity and the confluence to the higher order of stream. Among the sampling stations, the confluence stations only had anthropogenic influences from agricultural and domestic activities. The collected water samples were analyzed for Mn, Fe and other metals using ICP-mass spectrometry, and both total and dissolved organic carbon concentrations. DOM properties and composition in the samples were also analyzed and characterized using ultraviolet absorbance indicators; specific ultraviolet absorbance (SUVA245), spectral ratio (SR), molecular weight indicator (E2:E3), alongside excitation-emission fluorescence with parallel factor analysis (PARAFAC).

From the results, total Fe concentration varied between five streams ($F_{(4,87)}=3.01$, $p=0.022$), while total Mn concentration did not do ($F(4,87)=2.00$, $p=0.101$). A statistical analysis of all samples combined demonstrated significantly high concentrations of Mn and Fe at the stations in the dam vicinity, in other words, at the inside and below the sabo dams. The Mn concentration was also found to decrease in the downstream from the dam to the confluent stations, which could be described by the exponential equation: $[MnTot]=[MnTot]0exp(-kx)$, where k is conditional stability constant for the redox reaction and x is the distance from the dam.

Three components of DOM, namely fulvic acid-like (C1), humic acid-like (C2) and tryptophan like (C3), were successfully identified by PARAFAC analysis. These components together with fluorescence indices gave further insights into DOM dynamics. Contrary to

SUVA245, S_R, and E2:E3 values, PARAFAC components did not exhibit significant changes around the dam but rather increased at the downstream. As expected, the fulvic acid-like component was more abundant, however, the observed ratio for C1:C2 was less than our expectation (>4) based on the previous reports by other researchers. Fluorescence index (FIX) values (≥1.4) implied that DOM dominated at all stations were from terrestrial origins. Furthermore, values of biological and humification indices emphasized dominancy of terrestrial-derived DOM from vascular plants, soil pore water, and sediment source. Although DOM concentration change, which showed a significantly higher value at the confluence, along the streams was more influenced by anthropogenic activities, its aromaticity and molecular composition was mostly transformed by sabo dams. The impact of sabo dams on Mn concentration was more obvious at Mizunashigawa and Kanosawagawa. Moreover, both Fe and Mn concentrations were significantly high at stations around the sabo dams at Mizunashigawa, revealing that sabo dams may intensely affect metal transformations along the continuum through alteration of environmental conditions enhancing dissolution of stable hydroxides and oxides.

Various statistical analyses on association between Fe, Mn and DOM composition at different sections of the stream manifested strong relationships among these elements. For example, we found a significant correlation (r=0.60, p<0.05) between EEM component C1 and dissolved Mn, while dissolved Fe was not associated with this EEM component. SUVA245 was significantly correlated with both dissolved Mn (r=0.66, p≤0.001) and Fe (r=0.79, p=0.001). Principal components analysis demonstrated that the 1st and 2nd components composed of dissolved Mn and Fe, together with DOM concentration and properties, and accounted for 42.5% variation in all samples. Also, a positive linear relation was found between fulvic acid-like fractions and dissolved metals at the two stations inside and below the sabo dams, whereas, the correlation was negative at the upstream and downstream stations. Based on hierarchical cluster analysis using dissolved metals, DOM concentration and properties, the stations inside and below the dam at Mizunashigawa river were classified into a different cluster from other stations at both Mizunashigawa and Higashiiwamotogawa rivers. These two major clusters did not only emphasize the high impact of sabo dams but also further disclosed the site-specific factors such as dam size, capacity, and nature of retained materials. One of the unique characteristics of the sabo dam which may contribute to association between metals and DOM along Mizunashigawa river is that the reservoir nearly filled with sediments has become like a wetland, as well as that reservoir water was discharged from outlet vents in the dam wall.

This thesis revealed that sabo dams surely affect environmental dynamics of both trace metals and DOM through modifying DOM characteristics which enhance solubilization of metals, resulting in the increase in their concentrations. In sabo dams without overflows and large

reservoirs, the impacts may be more evident and stronger than anthropogenic inputs as observed at Mizunashigawa, however, this relies upon watershed characteristics such as vegetation and sediment delivery. Changes in these physico-chemical characteristics of watershed have a potential to alter the stream environment and ecosystem as a consequence of fates of many elements highly influenced by DOM especially in the presence of Mn and Fe. To further elaborate on this important topic, I recommend incorporating analytical techniques that can quantify both temporal and spatial changes in watershed characteristics, and other factors such as hydrological events, light penetration and residence time within the dam reservoir, and those that can examine DOM compounds in detail such as high-performance liquid chromatography (HPLC).

【和訳】

　ダムを造ることは，発電，農業や工業，都市への水供給，洪水調整などの様々な用途で重要である。砂防ダムは，高地における災害のインパクトを防ぐために使われており，その利用は世界的に広がってきた。一方で，大小の河川は，陸域から沿岸，海洋の生態系を結びつける水の連続的な動きの中で，相互作用すら有する種々な元素を巻き込んだ動的なシステムである。陸水のシステムは，山岳地帯における土壌の浸食や岩石の風化作用からの高い金属のローディングと関連する大量の有機物を受け入れている。そのうち２つの金属（鉄とマンガン）は環境への関連性が著しく，共沈作用によって他の金属に影響を与える一方で，ダムによって生じる環境条件の変化によって容易に影響を受ける。

　本研究では，砂防ダムの存在が溶存有機物（DOM）とマンガン，鉄の挙動にどのように影響を与えるかを解明するために，連続する流れに沿ってDOMの組成やマンガン，鉄の濃度の変化を調べた。山形県庄内地方の５つの山地河川（水無川，東岩本川，鹿の沢川，芋川，前の川沢）に沿って，水試料が採取された。その試料は，それぞれの河川で４地点（ダムの上流，ダム周辺の２地点，次の河川との合流地点）から採取された。それらの採取地点のうち，次の河川との合流地点だけは，農業や都市の活動による人為的な影響を受けていた。採取された試料からは，ICP質量分析法によってマンガン，鉄，その他の金属が分析され，総有機炭素および溶存有機炭素濃度が測定された。試料中のDOMの特性や組成も分析され，紫外部吸光に関する指標（SUVA254，SR，E2:E3）と，PARAFAC解析法と組み合わせた三次元励起蛍光スペクトル法によって特徴づけられた。

　その結果より，総鉄濃度は５つの河川の間で変動が見られた。一方，総マンガン濃度には変動がなかった。すべての河川からの試料をまとめた解析では，マンガンと鉄の濃度がダム周辺（砂防ダムの内部と直下の２カ所）の採取地点で有意に高いことが

示された。マンガン濃度はまた，ダムの下流から次の河川への合流地点にかけて減少し，それが指数関数（$[MnTot]=[MnTot]0$ $exp(-kx)$，ここで，kは酸化還元反応の条件安定度定数，xはダムからの距離）で表現できることが分かった。

　PARAFAC解析により，溶存有機物の３つの要素（すなわち，フルボ酸様（C1），フミン酸様（C2），トリプトファン様（C3））がうまく抽出された。これらの要素と蛍光に関する指標は，DOMの動態に関するさらなるを洞察を与えた。SUVA245，SR，E2:E3の結果に反して，PARAFAC要素はダム周辺で有意な変化を示さず，ダムの下流でむしろ増加した。フルボ酸様の要素は，予想していた通りにもっとも豊富に存在したが，C1:C2比は，他の研究者による先行研究にもとづく我々の予想（>4）よりも小さかった。蛍光指標（FIX）の値（≥1.4）は，すべての採取地点において卓越するDOMが陸域由来であることを示した。その上，生物学的な指標や腐植化の指標の値は，陸域の維管束植物，土壌間隙水，そして底質に由来するDOMが卓越することを強調した。DOM濃度は次の河川への合流点で有意に高い値を示し，この変化は人間活動の影響をより受けていたのに対して，DOMの疎水性や分子組成は砂防ダムによって変えられていた。砂防ダムのマンガン濃度に対する影響は，水無川と鹿の沢川でより明らかであった。さらに，鉄とマンガンの濃度は，水無川の砂防ダム周辺の採取地点で有意に高かった。このことは，砂防ダムが，安定な金属水酸化物や酸化物の溶解を促進するように環境条件を変えることで，河川連続体における金属の形態変化に集中的な影響を与えていることを示している。

　河川の異なる区域における鉄，マンガンとDOMの組成の関連に関する種々の統計解析により，これらの要素の間に強い関係があることが示された。例えば，EEM要素のC1と溶存態のマンガンには有意な相関（r=0.60，p<0.05）があった。一方，溶存態の鉄はこのEEM要素との関連がなかった。SUVA245は溶存態のマンガン（r=0.66，p≤0.001）と鉄（r=0.79，p=0.001）の両方に有意な相関があった。主成分分析では，第１主成分と第２主成分が溶存態のマンガンと鉄，DOMの濃度と特性で構成され，すべてのサンプルの変動の42.5％を説明していた。また，砂防ダムの内部と直下では，フルボ酸様のフラクションと溶存態金属の間には正の直線関係が見られたのに対して，ダムの上流と下流（合流点）では両者には負の相関が見られた。溶存態金属，DOM濃度と性質を用いた階層的クラスター解析にもとづくと，水無川のダムの内部と直下の採取地点は，水無川と東岩本川の他の地点とは異なるクラスターに分類された。これらの２つの主要なクラスターは，砂防ダムの強い影響を強調しただけでなく，ダムのサイズや容積，堆積物のような地点特有な因子も明らかにした。水無川の砂防ダムにおいて，金属とDOMの関係に貢献するであろう固有な特徴の一つに，その水がダムの壁に設けられた排水口から

放流されていることとともに，貯水池に土砂がたまっていて湿地のようになっていることが挙げられる。

　この論文は，砂防ダムが，DOM の特徴を変えて金属の溶解を促進することによって，確かに両方の金属と DOM の環境中での動態に影響を与えていることを明らかとした。その結果として，これらの金属濃度はダム周辺で上昇した。越流がなく大きい貯水池を有する砂防ダムでは，水無川で見られたように，その影響は人為的な流入の影響よりも明確で強いかもしれない。しかし，この比較は流域の植生や土砂輸送のような特徴に依存する。流域の物理化学的な特徴の変化は，特にマンガンや鉄の存在下で多くの要素のフェートが DOM に強い影響を受ける結果として，河川の環境や生態系を変えてしまう可能性を秘めている。この重要な課題をさらに解明するためには，流域の特徴の時間的，空間的な変化，水文学的イベント，ダム湖内での日光の透過，滞留時間などの因子を定量できる分析技術，DOMをより詳細に調べることができるHPLCのような分析技術を取り入れることを推奨する。

Table of contents

1   Introduction

1.1   Dams

Dams are hydraulic structures, barriers built across streams, rivers or a lake to store water. Dams are classified as large if their height is 15m (Wildi, 2010; Takahashi, 2009; ICOLD, Accessed Nov. 4th 2016) and above, and if, the dam of height between 5-15 m has a reservoir capacity of 3 million m^3 (Takahashi, 2009). Damming may be for various purposes such as generation of electricity, water storage for irrigation, industry or human consumption, flood control, navigation and recreation. Nevertheless, a third of dams worldwide are multipurpose. Dams have a high longevity, in developed countries, except in Japan and southern European countries where there are devastating floods and severe droughts respectively. There is a little acute need for further dam construction in Japan and southern European countries. However, the situation is opposite in developing countries where the population is on the rise hence increasing the demand for energy, food, and water, which justifies a need for more dams. Dams have so many benefits as well as undesirable impacts in relation to its location, type, capacity and purpose (Takahashi, 2009). Reservoir creation by dams transforms part of the river into a water body type with both river-like and lake like characteristics (Friedl and Wuest, 2002, Catalan et al., 2016). Reservoirs enhance in-situ primary production, evoke particle settling, decreases turbidity and affects light transmissivity (Friedl and Wuest, 2002), also affect the cycling of elements such as Carbon, nitrogen, phosphorous, silicon, iron and manganese in various ways. Some environmental consequences from dam operation are summarized in Table 1-1 below.

Table 1-1. Stream processes and   conditions affected by reservoir creation

Factor	Process	Impact
Oxygen	Depletion in deep water, and eutrophication	increase of DOC downstream, remobilization on mercury and sulfate reduction in reservoirs
Water flow	Artificial storage and increased residence time	Modifies hydrological regime, and changes in ground water level.
Sediments	Retention and accumulation of trapped suspended OM and bed load, adsorption of nutrients and contaminants in the reservoirs, trapping of coarse material and debris	Decreased downstream sediment delivery, nutrient flux Different riverbed particle size distribution between upper and lower sections
Nitrogen and Phosphorous	Nutrient loading, shift in algal communities and growth of harmful algae	Reduction in nutrients, shifts in the food web
Fish migration		Decline in migratory fish

Friedl and Wuest, 2002; Takahashi, 2009; Takao et al., 2008; Wildi, 2010; March et al., 2003)

In Japan, rapid population growth after World War II accompanied by social assets influx and occupation of lowland areas increased the risk of flooding (Yoshimura et al., 2005). About 72.7% of the land is covered by mountains (Marutani et al., 2008; Yoshimura et al., 2005), and 65.3% of the country has slopes steeper than 14% with steep rivers characterized by flashy flow regimes (Yoshimura et al., 2005). Due to the mountainous nature, debris and sediment fluxes, landslides, and cliff failures are common following heavy rainfall and sometimes typhoon-induced storms (Marutani et al., 2008). Sabo works were adopted to alleviate the impact of debris torrents from such incidences (Chanson, 2004). Use of mountain protection systems such as sedimentation dams and weirs was primarily driven by the need to minimize the impact of

floods and sediments on Japanese communities following rapid growth in 1960 (Marutani et al., 2008, Mizuyama, 2008, Yoshimura et al., 2005). Sabo is a Japanese word used to refer to erosion and sediment control works (Mizuyama 2008) or mountainous protection systems (Chanson, 2004). Sediment yields and transport in Japanese rivers is high exceeding $1000m^3km^{-2}$ for most steep catchments regardless of the watersheds being densely forested (Yoshimura et al., 2005). Hence river corridors regulation and flow regime control is necessary not only for agricultural production but also for the protection of humans and property against flood damage. Sabo dams are built in the upstream areas of mountain streams and at valley exists to accumulate and suppress the production and flow of sediments and as a barrier to debris flow. (Sabo association, 2004). Most of the rivers have been modified yet many of these rivers still experience severely disrupted ecological gradients from the existence of dams (Marutani et al., 2008). More than 80000 streams in Japan have multiple sets of sabo dams whose operation impacts on human life, property and also landscape and river health in various ways (Marutani et al., 2008). With more than 2675 big dam, Japan is the 4th and 3rd country with the highest number and greatest density of dams respectively (Yoshimura et al., 2005, Gleick et al., 2002). However, there is a need for more dams especially for flood control (Takahashi, 2009). Much as their impacts may be far greater than big dams, small dams which are approximately 80,000 worldwide have received very little scientific attention (March et al., 2003). Dam structures truncate the river altering spatial connectivity the river from its natural landscape and flow regime, impacts on the behavior of elements such as carbon, phosphorous and various trace metals as indicated in Table 1-1. Creation of areas with either disproportionately high reaction rates to the surrounding environments or short time periods with relatively higher response rates than longer time periods (McClain et al., 2003), impacts not only trace metals such as manganese concentration but also on dissolved organic matter (DOM) behavior. Changes in residence time and the hydrological regime, reduction in turbulence (Friedl and Wüest, 2002) due to impoundments affects the character of DOM exported subsequently affecting downstream areas. Furthermore, water impoundments disrupt biogeochemical cycles and cause changes which might accumulate to trigger more adverse effects.
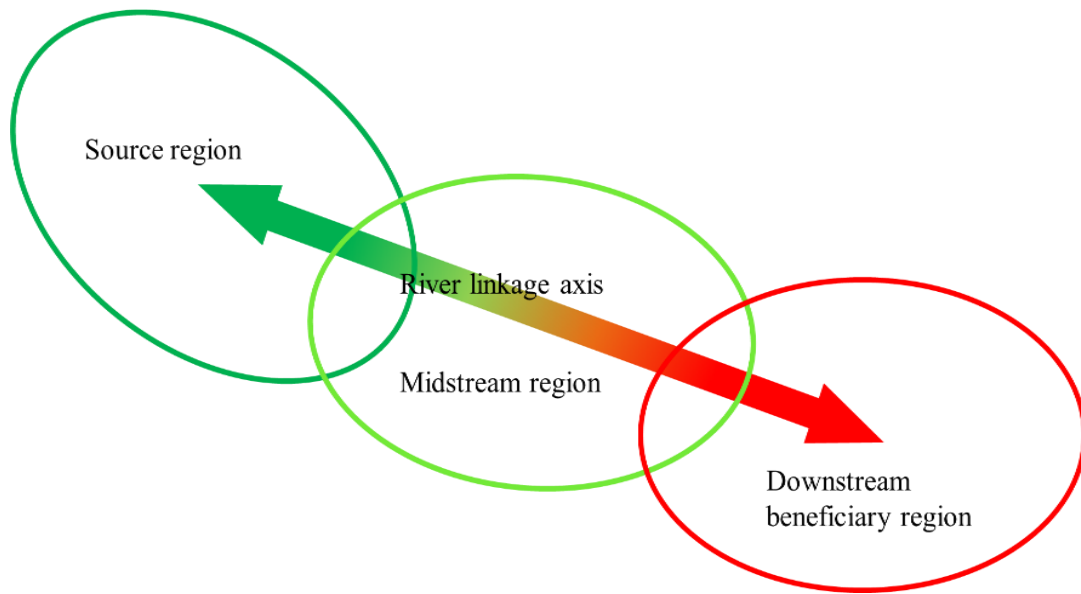
Figure 1-1. Link between upstream and downstream process modified from Yutaka 2009, pg 59

Mountainous areas have complex dissolved organic matter tendencies, in rivers and streams, downstream regions are known to depend on upstream ecosystems (Takahashi, 2009). Through processes like flood control, water supply, and environmental conservation, upstream mountainous areas support the development of downstream regions Figure 1-1. Terrestrial organic inputs are transported from upstream in a dynamic system comprising of continuous water movement while being decomposed by organisms (Takao et al., 2008). The nature of material transported sustains the ecological communities and functions of the rivers, and to a greater extent the marine environment, for example; riverine DOM export is the largest provider of reduced carbon from terrestrial sources to ocean (Spencer et al., 2012). Therefore, problems arising in the downstream reflect on the process in the upper catchment (Marutani et al., 2008). Since flood protection in urban areas is a top priority in Japan, river management for purely ecological reasons tends to remain an exception. Hence, lowland floodplains are among the most threatened ecosystems in Japan (Yoshimura et al., 2005)

Impoundments are among the most several river ecosystems modifications that interrupt material transport breaking the linkage between upstream and downstream. In addition to the effects in Table 1-1, increased residence time and autochthonous production of biomass in reservoirs alters redox conditions which subsequently affect major processes such as nutrient

cycling and potentially releasing of metals from sediments (Friedl and Wuest, 2002, Kedziorek et al., 2007; Fremion et al., 2016; Wildi, 2010). The major effects of dams on physical and biotic processes may be summarized as; (i) reduction of sediment delivery, (ii) alteration of energy base, modifications of thermal and flow regime, and (iii) disruption of aquatic species migration (Poff and Hart cited by Takao et al., 2008).

1.2 Metals and DOM in the environment

1.2.1 DOM

Natural (NOM) organic matter is classified into two forms dissolved organic matter (DOM) and particulate organic matter (POC) usually based on filtration. DOM is characterized as the part that passed through the filters size (0.2um -0.8um) (Asmala et al., 2013) and is an important control on biological, chemical and physical processes in ecosystems (Fellman et al., 2009). DOM is the largest organic matter pool in aquatic ecosystems (Cole and Caraco cited in Park et al., 2007), and at any given time, its character is the function of the source material, biogeochemical processes, and hydrology (Aiken et al., 2011; Hood et al., 2008). DOM plays a role in metal speciation ranging from alteration of surface charge of particles to having roles in the kinetics of most environmental reactions (Hood et al., 2008). And in environmental scenarios where dissolved DOM exceeds metal ion concentrations in water, DOM binds to dissolved metal ions resulting in a decrease in mineral saturation index. Also, sorption DOM to metal colloids can also enhance or inhibit dissolution (Aiken et al., 2011), in this study, filtration was done using 0.45um filters which according to Aiken et al., (2011) does not only allow DOM material but rather allows a number of components to pass through. Constituents that can go through the 0.45 um filters include DOM, dissolved metal complexes, polynuclear cluster nanoparticles, colloids, and virus.

1.2.2 Mn and Fe and other metals in the environment

Some elements with atomic mass above 50 have a biological role, often as cofactors or part of cofactors in enzymes and as structural elements in proteins (Morel and Price, 2003). Some of these trace elements such as Co, Ni, Cu, Zn, Cr and Cd exist in very low concentrations in aquatic systems delivered from weathering of rocks, atmospheric deposition and mining activities. Transportation of elements in rivers varies for each between elements for example Fe and Ni transport mechanisms in rivers are the same (Gibbs, 1973), and precipitation and co-precipitation

are important mechanisms for Ni, Fe, and Mn transportation (Gibbs, 1973). Some metals are associated with organometallic complexes (Gibbs 1973, Tribovillard et al., 2006). Although they are required in micronutrients by organisms, the fact that the metals do not undergo degradation makes them an environmental threat (Seshadri et al., 2015). Overall transport of metals is linked to sediments which serve as sources and sinks and is enhanced by storms (Seshadri et al., 2015, Karbassi et al., 2008, Vesper and White, 2003). Metal speciation is influenced by some environmental factors such as; (i) the prevailing redox conditions which is responsible for the oxidation state of metals and may also affect bioavailability and toxicity (Hill, 1997), (ii) Seasonal patterns which controls flow discharge. As observed by Nagano et al. (2003), dissolved concentrations are linked to flow discharge.

Transiting from the river to lake results into depletion of oxygen which triggers reduction of nitrate, manganese (hydro)oxides, iron (hydro)oxides and sulfate which accumulate in the deep waters and sediments (Friedl and Wuest, 2002). Bottom water and sediment organic matter decomposition induce chemical transformation which utilizes a number of oxidants such as oxygen, nitrates, manganese oxides (Mn IV), iron (Fe III) and sulfates (Ingri et al., 2011). Amorphous Iron and Manganese oxides have a high specific area which makes them efficient scavengers for metal in oxic waters (Ingri et al., 2011; Tebo et al., 2004). Fe and Mn oxides regulate the flux and behavior of other metals by providing sorption sites and reducing conditions that cause dissolution of Fe (III) and Mn(IV) to dissolved releasing the already scavenged elements (Ingri et al., 2011; Friedl and Wuest, 2002) to overlying water. Fe II and Mn II are soluble in oxygen deficient natural waters but precipitate out at higher oxidation rates (Hill, 1997), Hence Mn oxides significantly influence and control the release, transfer, and availability of many nutrient elements and organic contaminants (Feng et al., 2007). Manganese transformation between its states is important in regulating the transportation and behavior of other trace elements including Pb, Cd, Co, Cu, Ni and Zn (Ingri et al., 2011; Harvey and Fuller, 1998, Feng et al., 2007). Mn exists in many oxides states in soil and sediments whose capacity to adsorb heavy metals varies, for example; birnessite has a high adsorption capacity while hausmannite exhibits weak adsorption properties (Feng et al., 2007). The extent to which Mn oxides influences other trace metal behavior is determined by the available oxide, mineral composition and structure of Mn oxide, heavy metal ions radii, structure and coordination (Feng et al., 2007).

6

1.3   Objectives of the study

This thesis covers both trace metals and DOM behaviors in mountainous streams. Trace metals and DOM are essential elements in ecosystem functioning, therefore understanding their behavior and interactions in various environments is very crucial in pollution control and environmental management.
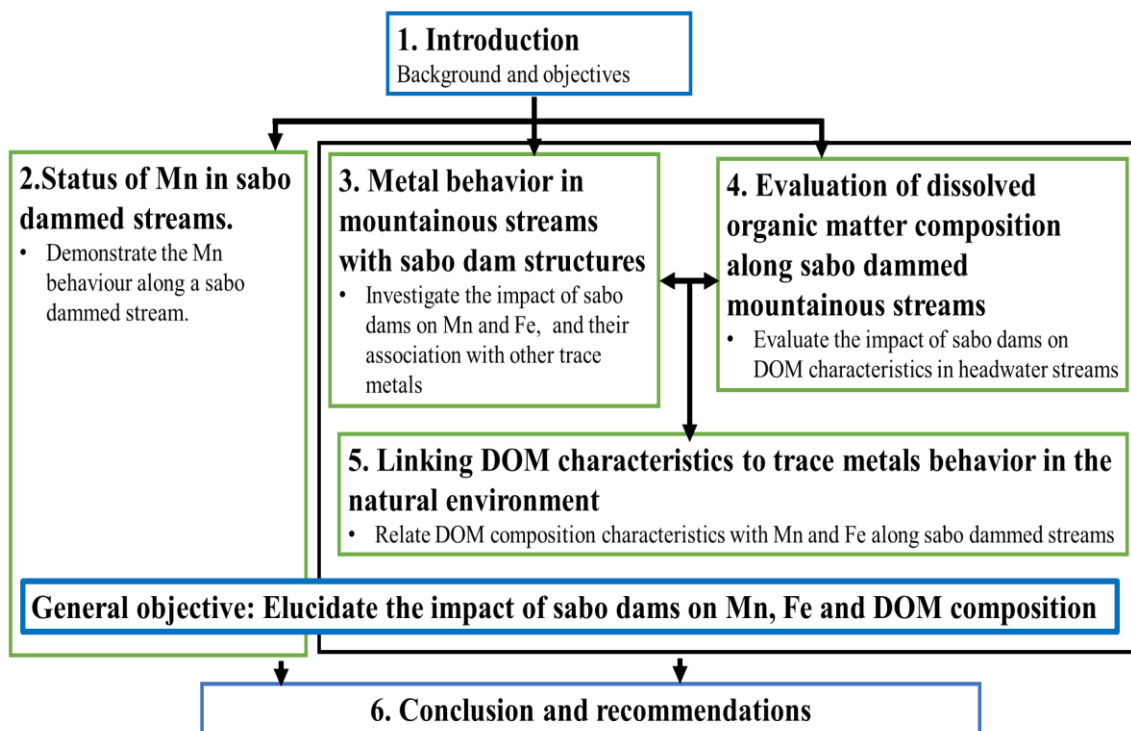
Figure 1-2 Study outline

This study was carried to elucidate the impact of sabo dams on DOM and trace metal behavior in mountainous streams with the aim to understand: (i) How do trace metal concentration vary along the stream with sabo dams, (ii) How does Sabo dams affect DOM composition and character, and (iii) Are changes in trace metals and DOM due to sabo dams related? This thesis consists of 6 chapters each covering a specific objective as shown in the study outline (Figure 1-2). Chapter 2 covers the behavior of Mn in a typical sabo dammed stream, 3 and 4 cover spatial and temporal behavior of trace metals and DOM mountainous streams with sabo dams, respectively. Chapter 5 links DOM properties to trace metal concentrations, and Chapter 6 wraps up the study with the conclusion and recommendations.

References

Aiken GR, Hsu-Kim H, Ryan JN (2011) Influence of dissolved organic matter on the environmental fate of metals, nanoparticles, and colloids Environmental science & technology 45:3196-3201 doi:10.1021/es103992s

Asmala E, Autio R, Kaartokallio H, Stedmon CA, Thomas DN (2014) Processing of humic-rich riverine dissolved organic matter by estuarine bacteria: effects of predegradation and inorganic nutrients Aquatic Sciences 76:451-463 doi:10.1007/s00027-014-0346-7

Catalán N et al. (2016) Effects of beaver impoundments on dissolved organic matter quality and biodegradability in boreal riverine systems Hydrobiologia doi:10.1007/s10750-016-2766-y

Chunson, H., 2004. Sabo check dams-mountain protectine systems in Japan. International Journal for River Basin Management, 2, 301-07.

Fellman JB, Hood E, Edwards RT, D'Amore DV (2009) Changes in the concentration, biodegradability, and fluorescent properties of dissolved organic matter during stormflows in coastal temperate watersheds Journal of Geophysical Research 114 doi:10.1029/2008jg000790

Feng XH, Zhai LM, Tan WF, Liu F, He JZ (2007) Adsorption and redox reactions of heavy metals on synthesized Mn oxide minerals Environmental pollution 147:366-373 doi:10.1016/j.envpol.2006.05.028

Fremion F, Bordas F, Mourier B, Lenain JF, Kestens T, Courtin-Nomade A (2016) Influence of dams on sediment continuity: A study case of a natural metallic contamination The Science of the total environment 547:282-294 doi:10.1016/j.scitotenv.2016.01.023

Friedl G, Wüest A (2002) Disrupting Biogeochemical Cycles —Consequences of Damming Aquatic Sciences 64:55-65 doi:10.1007/s00027-002-8054-0

Gibbs (1973) Mechanisms of Trace Metal Transport in Rivers. Science 180

Gleick PH, Burns WCG, Chalecki EL, Cohen M, Cushing KK, Mann AS, Reyes RR,Wolff GH,Wong AK. 2002. Number of dams, by country. In The World's Water 2002–2003: The Biennial Report on Freshwater Resources, Gleick PH (ed.). Island Press:

Washington; 296–299.

Harvey, J.W., Fuller, C.C., (1998). Effect of enhanced manganese oxidation in the hyporheic zone on basin scale geochemica balance. Water Resources Research, 34(4),623-636

Hill JS. (1997) Speciation of trace metals in the environment. Chemical reviews Vol 26

ICOLD http://www.icold-cigb.net/GB/World_register/general_synthesis.asp Accessed 4th Nov

Ingri, L.J., et al., (2011) Manganese redox cycling in lake Imandra: Impact on nitrogen and the trace metal sediment record. Biogeosciences Discuss, 8,273-321. DOI 10.5194/bgd-8-273-2011

Karbassi AR, Monavari SM, Nabi Bidhendi GR, Nouri J, Nematpour K (2008) Metal pollution assessment of sediment and water in the Shur River Environmental monitoring and assessment 147:107-116 doi:10.1007/s10661-007-0102-8

Kedziorek MAM, Geoffriau S, Bourg ACM (2008) Organic Matter and Modeling Redox Reactions during River Bank Filtration in an Alluvial Aquifer of the Lot River, France Environmental science & technology 42:2793-2798 doi:10.1021/es702411t

March JG, Benstead JP, Pringle CM, Scatena FN (2003) Damming Tropical Island Streams: Problems, Solutions, and Alternatives BioScience 53

Marutani, T., et al., 2008. The light and dark of sabo-dammed streams in steepland settings in Japan. In: River futures: an integrative scientific approach to river repair. Edited by Gary J.Brierley and Kirstie A. Fryirs Washington, DC: Island Press, 220–236

McClain ME et al. (2003) Biogeochemical Hot Spots and Hot Moments at the Interface of Terrestrial and Aquatic Ecosystems. Ecosystems 6:301-312 doi:10.1007/s10021-003-0161-9

Mizuyama T (2008) Structural Countermeasures for Debris Flow Disasters International Journal of Erosion Control Engineering Vol. 1:38-43

Park J-H, Lee J-H, Kang S-Y, Kim S-Y (2007) Hydroclimatic controls on dissolved organic matter (DOM) characteristics and implications for trace metal transport in Hwangryong River Watershed, Korea, during a summer monsoon period Hydrological Processes 21:3025-3034 doi:10.1002/hyp.6511

Morel M, Price F (2003) The Biogeochemical Cycles of Trace Metals in the Oceans SCIENCE wwwsciencemagor VOL 300

Sabo Publicity Center., 2001. Sabo in Japan. Creating safe and rich green communities. Present state ed. Japan Sabo Association, Tokyo: Japan Sabo Association.

Spencer RGM, Butler KD, Aiken GR (2012) Dissolved organic carbon and chromophoric dissolved organic matter properties of rivers in the USA Journal of Geophysical Research: Biogeosciences 117:n/a-n/a doi:10.1029/2011jg001928

Takao A, Kawaguchi Y, Minagawa T, Kayaba Y, Morimoto Y (2008) The relationships between benthic macroinvertebrates and biotic and abiotic environmental characteristics downstream of the Yahagi Dam, Central Japan, and the State Change Caused by inflow from a Tributary River Research and Applications 24:580-597 doi:10.1002/rra.1135

Tebo, B.M., et al. (2004). Biogenic manganese oxides: properties and mechanisms of formation. Annu. Rev. Earth Planet. Sci., 32, pp.287-328.

Tribovillard N, Algeo TJ, Lyons T, Riboulleau A (2006) Trace metals as paleoredox and paleoproductivity proxies: An update Chemical Geology 232:12-32 doi:10.1016/j.chemgeo.2006.02.012

Wildi W (2010) Environmental hazards of dams and reservoirs NEAR curriculum in natural environmental science

Yoshimura C, Omura T, Furumai H, Tockner K (2005) Present state of rivers and streams in Japan River Research and Applications 21:93-112 doi:10.1002/rra.835

Yutaka Takahashi (In ed), (2009) Water Storage, transport and distribution. Encyclopedia of life support systems. Edited by Oxford, United Kingdom

2   **Status of Mn concentration in Sabo dammed mountainous streams**

2.1   **Manganese abundance and its role in the environment**

Mn, the twelfth most abundant metal in the biosphere (Nadask et al., 2010) exists naturally in various forms in environmental components such as rocks and soils, especially in Mn-containing minerals (Buamah, 2009). Mn exists as oxides and hydroxides and cycles through different oxidation states (Ingri et al., 2011; Tebo et al., 2004) depending on environmental conditions. In aquatic environments, the specific forms of Mn are determined by pH and redox potential (Howe et al., 2004). Three types of oxidation states, Mn (IV), Mn(III) and Mn(II) are common species in the environment. Among these species, Mn (IV) and Mn (III) exist as the particulate forms whereas Mn (II) exists as the dissolved form. Environmental factors such as pH, which fluctuates between acidic and alkaline conditions (Chuan et al., 1996), biological activities, carbonate species, rainfall, organic matter and anaerobic conditions all affect manganese solubility. Mn is present in most water at pH 4–7 and is often transported from terrestrial to the aquatic environment in rivers in the form of suspended sediments (Pinsino et al., 2012; Howe et al., 2004). Mn occurs mainly as the reduced soluble Mn^{2+} at lower pH and Eh while it is oxidized to form precipitates in the presence of oxygen at higher pH (Hem, 1985).

Mn is an essential trace nutrient for all forms of life but can be toxic in excess (Li et al., 2014), it is required in trace amounts for many metabolic and non-metabolic regulatory functions (Pinsino et al., 2012).The frequency of Mn uptake by living organisms depends on the environmental conditions, (Pinsino et al., 2012); for example, Mn is utilized by manganese-reducing bacteria as a terminal electron acceptor in the absence of oxygen. Moreover, Mn oxides are some of the strongest oxidants in the natural environment and play important roles in elemental biogeochemical cycles. Mn oxides participate in a wide range of redox reactions with organic and inorganic matters and can adsorb abroad variety of ions while controlling the distributions and bioavailability of many toxic and essential elements (Tebo et al., 2004).

2.2   **Overview of Mn origin in Sabo dammed streams**

Sabo dams as detailed in chapter 1, were constructed to retain coarse materials and the debris, however, reservoir creation enhances anaerobic conditions behind the dam. Sabo dams have been praised for reducing damage to property in times of disasters (Sabo publicity center,

2001). However, environmental impacts of sabo dams accompanied by reservoir creation and sedimentation (Roman and Wiejaczka, 2014), such as change in water quality (Abesser and Robinson, 2010; Ingri et al., 2011), interference with fish migration, and alteration of downstream riverbed features including riverbed discoloration to typically black or brown color, are less obvious Table 1-1. Although this river bed discoloration may be due to various factors in both the nature of river and the surrounding environments, it is likely caused by redox-related dissolution and precipitation of iron and manganese (Mn), which mainly originate in mineral rocks and experience the involvement into biotic and abiotic organic systems and dissociation from them via such as anaerobic decomposition of organic matters (Roman and Wiejaczka, 2014; Ingri et al., 2011) in addition to natural processes (e.g., catchment erosion). Also, the differences in structure and operational processes of sabo dams should have varying effects on water quality and downstream aquatic ecosystems.

Furthermore, organic matter retention, especially leaf litters trapped between the sediments and gravel (Raikow et al., 1995), intensifies redox condition and hence Mn and iron remobilization. Sources of Mn and processes of its control differ between lowland and upland catchments, which are normally used as agricultural land and forests, respectively (Heal et al., 2002). Although the deposits in mountainous streams are thought to be due to Mn deposition because of sufficient oxygen and the variety of organisms present, its behavior around sabo dams has not been investigated. Many studies have been conducted on Mn under reductive and oxidative conditions in natural environments (e.g; Heal et al., 2002; Scott et al., 2002; Harvey and Fuller, 1998; Canfield et al., 1993; Burdige, 1993). This alteration of Mn behavior induced by sabo dams can be regarded as a potential danger to benthic and planktonic organisms (Pinsino et al., 2012) though Mn has been attracting almost no scientific attention until recently.

2.3   Objective

However, the impact of sabo dams on Mn has not been extensively investigated. In this chapter, we aim to demonstrate the behavior of Mn based on the observations of several typical sabo dams in mountainous streams. Recently, occurrences of natural disasters have increased, and Sabo dams have proliferated worldwide (Sabo publicity center, 2001). This highlights the need for an extensive study of water quality in sabo-dammed areas.

2.4   Materials and methods

2.4.1   Study area

The research was conducted along Kanosawa (KSW) stream, and the reference streams shown in Figure 2-1. KSW is a second-order stream feeding the Tsuno River, a branch of the Mogami River in Shonai District, Yamagata, Japan (Figure 2-1). The study site contains a number of structures including two weirs and four *sabo* dams, three of which are closed-type dams and another is a double-slit dam. KSW basin covers an area of 15.53 km^2 in a forested environment in mountains of Tozawamura village in Shonai district with ranging 44-1,104 m above sea level. According to the Japan Ministry of Land, Infrastructure, Transport, and Tourism website, study site receives an average annual precipitation of 2,946 mm/year (MLIT, 2015). Along the 10 km stream length, six sampling stations (St.1-6) were selected from 0.67 km upstream of the uppermost dam (CDKSW 4) to 2.05 km downstream of the lowermost dam (CDKSW 1). Closed *sabo* dams are located at the distances of 0.67, 3.24, and 3.92 km from the uppermost sampling station (St.1), denoted by CDKSW 4, CDKSW 2, and CDKSW 1, respectively, and a double-slit dam (DSKSW 3) is located at the distance of 2.71 km from St.1 as indicated in Figure 2-2. River bed materials in the upper section (upstream of CDKSW 4) of the dam are comprised of gravel, alluvial sand and a mixture of sand, silt and plant material retained behind the dam wall. In addition to the main study site, samples were collected from reference streams namely; Higashiiwamotogawa (HIG), Mizunashigawa (MIZ), Maenokawa (MEK), and Imogawa (IMO) streams, focusing on a single closed dam in each stream. At the all sabo dam sites, sediment accumulation in the dam has resulted into the formation of water pathways and inundation spots, with an exception of IMO, CDKSW 2 and CDKSW 1, which are at full capacity. The state of sediment accumulation is in the advanced stage at CDKSW 4, MIZ, HIG, and MEK, though not yet at full capacity. The river beds at the downstream of the all dams consisted of mainly boulders, cobbles and course gravel. Although all the dams have water outlets within the concrete wall, only MIZ did not have any overflow over the dam crest. Closed sabo dams have small outlets (Spillways) where water flows through while sediments and other materials are retained.
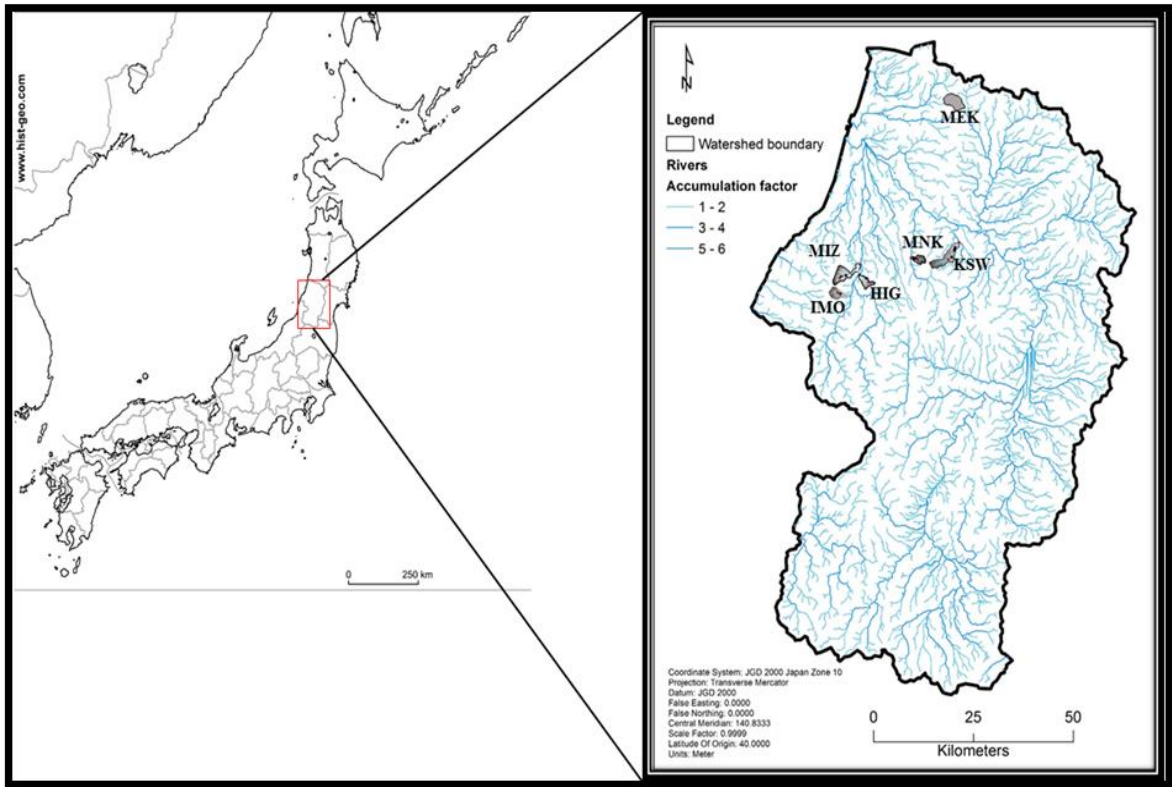
Figure 2-1 Location of the study sites (KSW, MIZ, IMO, MEK and HIG) in Yamagata prefecture in Japan
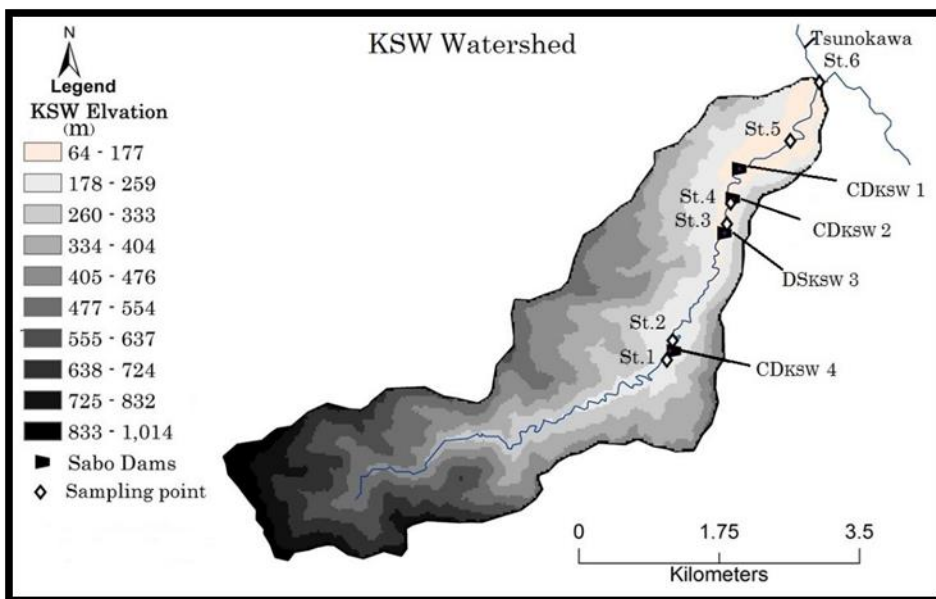
Figure 2-2 Detailed map of KSW watershed showing sabo dams and sampling stations.

(CD-closed sabo dam, DS-Double silt dam)

2.4.2   Sample collection and handling

Surface water samples were manually collected at six points (Figure 2-2) along KSW carefully with sampling bottle facing opposite of flow direction, taking care to minimize sample contamination. Sampling at the main study site was conducted in July and August 2012, May and August 2013, and June 2014; reference stream sampling was conducted randomly in 2012 and June 2014. At the time of sample collection in May 2013 and July 2012, the stream was at the end of snow melting stage.   Since the study area is located in the mountainous area, it receives a lot of snow from late November to February, and most of the snow melts by the end of May. In May 2013 and July 2012, very few heaps of melting snow were observed along the stream bank in the upper part of the stream after St. 4. In August, the stream was at around the base flow condition, and no rainfall was recorded within the weeks of samplings. At CDKSW 4 and reference streams, samples were collected from the upstream and downstream immediately after the dam. These samples were used in order to see the effect of dams on the behavior of Mn. Samples were collected at the downstream of the dam at DSKSW 3 and CDKSW 1, while the samples were collected from upstream of the dam at CDKSW 2. Flow discharge at the time of sampling was measured using current meters method (Gordon et al. 2004). The discharge date used in this paper only applies to the time of sampling since flow discharge fluctuation was not monitored.

Prior to sample collection, we thoroughly cleaned polyethylene bottles (250 ml) according to Wilde et al., (1998). All water samples were collected at a depth less than 0.5 m, kept in a cool box packed with cold insulators and immediately transported to the laboratory for further analysis. In the laboratory, filtration was performed using 0.2 and 0.45-μm Advantec mixed cellulose ester membrane filters. The filtered and unfiltered samples were then analyzed for dissolved (Mn_{Diss}) and total (Mn_{Tot}) manganese, respectively, using the formaldoxime method (Kajiwara and Goto, 1964), described below.

2.4.3   Procedure for Mn analysis

2.4.3.1   Reagent preparation

We prepared formaldoxime reagent by dissolving 8 g of hydroxyl ammonium chloride (Wako Chemicals, Japan) in 100 ml of ultrapure water (UW), adding 4 ml of 30% formaldehyde

solution (Wako Chemicals, Japan) and finally adding UW to make the total volume to 200 ml. Buffer solution was prepared by dissolving 68 g of ammonium chloride (NH_4Cl, Wako Chemicals, Japan) in 500 ml of ammonia solution (NH_3 28–30%, Cica reagent, Kanto Chemicals, Japan) and then diluted with UW to 1000 ml. A 0.1 M EDTA solution was prepared by dissolving ethylene diamine tetra-acetic acid disodium salt (Wako Chemicals, Japan) in UW. Industrial manufactured L (+)–ascorbic acid sodium salt (25%, Wako Chemicals, Japan) was used as a reducing agent. We made a calibration curve using known concentrations of Mn, prepared using its standard Mn solution (Mn 1000, Kanto Chemicals, Japan).

2.4.3.2   Sample treatment

We added 2 ml of formaldoxime reagent to 40 ml of each water sample, followed by addition of 2 ml buffer solution, and the mixture was left for 10 minutes. Then, we added 20 mg of L (+)–ascorbic acid sodium followed by addition of 2 ml 0.1 M EDTA solution. After 15–20 minutes, absorbance at the wavelength of 450 nm was measured using an absorption spectrophotometer (U1800, Hitachi, Japan) with using 5 cm path length cuvettes, the limit of detection for this method was 0.024 mg/l based on the standard deviation of the response and the slope (ICH 2005). Mn concentration was then determined for each sample the calibration curve prepared earlier with the dilution series of standard Mn solution.

Originally reported by Kajiwara and Goto, (1964), this method has been successfully used for Mn analysis of pore water (Burle and William, 1979) and seawater (Brewer and Spencer, 1971). It entails the complexation of Mn using a formaldoxime mixture within a pH range of 8–9.8. During the analysis conducted in this study, pH range was between 8.2-8.4, the red-pink complex formed is then exposed to light with 450 nm wavelength to obtain the absorbance used to determine Mn concentration. Iron interference, which is one of the limitations in acquiring correct Mn concentration by this method, was eliminated using the reducing agent and EDTA solution to break down the iron-formaldoxime complex (Brewer and Spencer, 1971).

2.5   Results and Discussion

2.5.1   Mn concentration change upstream and downstream of sabo dams

Comparing the upstream and downstream of the dams, higher concentrations of Mn_{Tot} were observed at the downstream of the closed *sabo* dams at CDKSW 4 and in the reference

streams (Figure 2-1). This indicates reduction of Mn oxides and hydroxides within the material retained on the dam wall. Especially, high percentage of increase in Mn_{Tot} concentration was observed in August and December 2012 at CDKSW 4 and HIG, respectively. With the exception of July 2012 and May 2013 at CDKSW 4, and reference sites MEK and IMO in 2014, other sites had more than 50% increase in Mn_{Tot} concentration regardless of the sampling month.
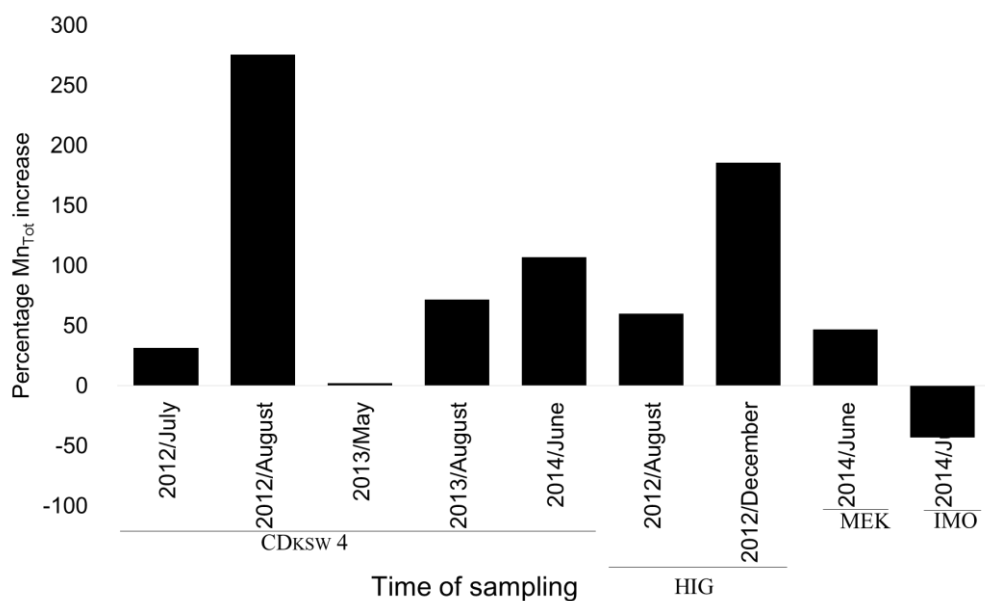
Figure 2-3 Mn_{Tot} percentage increase at closed sabo dams at KSW and reference sites. Percentage Mn_{Tot} increase $_{(y-axis)}$ was calculated using Mn_{Tot} concentration following this formula [((St.2 Mn_{Tot} − St.1 Mn_{Tot})/ St.1 Mn_{Tot}) X 100].

The differences observed in May and July between St.1 and 2 can be explained by the effect of snowmelt, which came out in the spring. As shown in Figure 2-3, we observed a large increase in Mn_{Tot} concentrations in summer and the least in spring around CDKSW 4. Highest water flow discharge was recorded in May 2013 (i.e., 1.979 m^3/s) due to the snow melting while lowest value was recorded in August 2012 at 0.159 m^3/s. July 2012 and August 2013 values were slightly higher than the lowest observed value at 0.382, and 0.326 m^3/s, respectively. (Table 2-1). The highest flow discharge observed in May corresponded to the lowest percentage Mn_{Tot} concentration increase (i.e., 2.3%). Although flow discharge did not vary a lot in July 2012, August 2013 and in 2014 (at 0.382, 0.311 and 0.326 m^3/s respectively) after the dam (CDKSW 4), percentage increase of Mn_{Tot} concentration raised by 1, 2.4 and 3.5 folds respectively. Furthermore, the highest percentage Mn_{Tot} increase was observed in August 2012,

the time when the least flow discharge was recorded. The impact of the dam on Mn_{Tot} was observed at KSW as explained above and in all the reference sites except at IMO in 2014 (Figure 2-3). Mn_{Tot} concentration increase in 2014 was slightly high at KSW (106.8%) compared to MEK and IMO at 47.1, and -42.9 % respectively. IMO at full capacity showed a decrease in Mn_{Tot} as opposed to other sites surveyed. From the observation, the impact of the dam (CDKSW 4) on Mn_{Tot} increase was clearly related to the flow discharge.

Table 2-1 Flow discharge at St.1 and percentage increase after the dam (KSW 4)

Year	Month	Station	Mn_{Tot} (mg/L)	Percent increase from St. 1 to St. 2	Flow discharge (m^3/s)	Total mas load (mg/s)
2012	July	St.1	0.035	31.4	0.382	1.34×10^{-5}
		St.2	0.046			1.76×10^{-5}
	August	St.1	0.037	275.7	0.159	5.89×10^{-6}
		St.2	0.139			2.21×10^{-5}
2013	May	St.1	0.088	2.3	1.979	1.74×10^{-4}
		St.2	0.090			1.78×10^{-4}
	August	St.1	0.067	71.6	0.311	2.08×10^{-5}
		St.2	0.115			3.58×10^{-5}
2014	June	St.1	0.059	106.8	0.326	1.92×10^{-5}
		St.2	0.122			3.97×10^{-5}

Besides flow discharge and sabo dam relations, flow discharge at St.1 may also show a link between flow fluctuations and Mn_{Tot} concentration. For example, in 2014 variations at the reference streams and KSW show correspondence between the highest Mn_{Tot} concentration and the lowest flow discharge (Table 2-2 at MIZ). The highest Mn_{Tot} observed at MIZ can be attributed to the nature of the dam as described in the 2.4.1. Also Mn_{Tot} total load at St.1 was related to the flow discharge changes, the highest was noted with high flow discharge in May at 1.73×10^{-4} mg/s and vice versa as shown in Table 2-1. In spite of such a large difference of flow discharge, Mn_{Tot} concentration hardly changed in July and August 2012 at St.1 (an increase of 0.002 mg/l while the flow discharged reduced by more than 100%). On the other hand, 95.6% increase in flow discharge in summer (August 2012 and 2013) resulted into 81.1% increase in Mn_{Tot} at St.1.

Table 2-2 Water quality parameters measured inside the dam (St.1) and in discharge flow (St.2) in June 2014

Site	Location	pH	Temp ($\circ$C)	DO	Turbidity (NTU)	Conductivity (ms/M)	Flow discharge (m^3/s)	Mn_{Tot} (mg/L)
KSW	Inside the dam	7.42	14.3	9.27	11.8	4.2	0.326	0.059
	Discharge	7.32	16.5	8.82	16.9	4	ND	0.120
MIZ	Inside the dam	6.05	14.9	7.44	3.1	4.2	0.045	0.103
	Discharge	7.23	15.1	9.02	0.2	4.1	ND	ND
MEK	Inside the dam	6.75	18.2	7.84	8.8	5.1	ND	0.017
	Inside the dam*	6.96	14	8.76	5.7	6.1	ND	0.050
	Discharge	7.42	15.3	8.4	0	6.2	ND	0.025
IMO	Inside the dam	6.83	15.7	9.09	4.6	3.6	0.674	0.028
	Inside the dam*	6.17	15.6	3.32	2.9	4.9	ND	0.100
	Discharge	6.9	16	9.07	0	3.5	ND	0.016

*Measurements were taken in the pool section with in the dam reservoir, these values were not used in calculating percentage Mn_{Tot} increase; ND- No data.
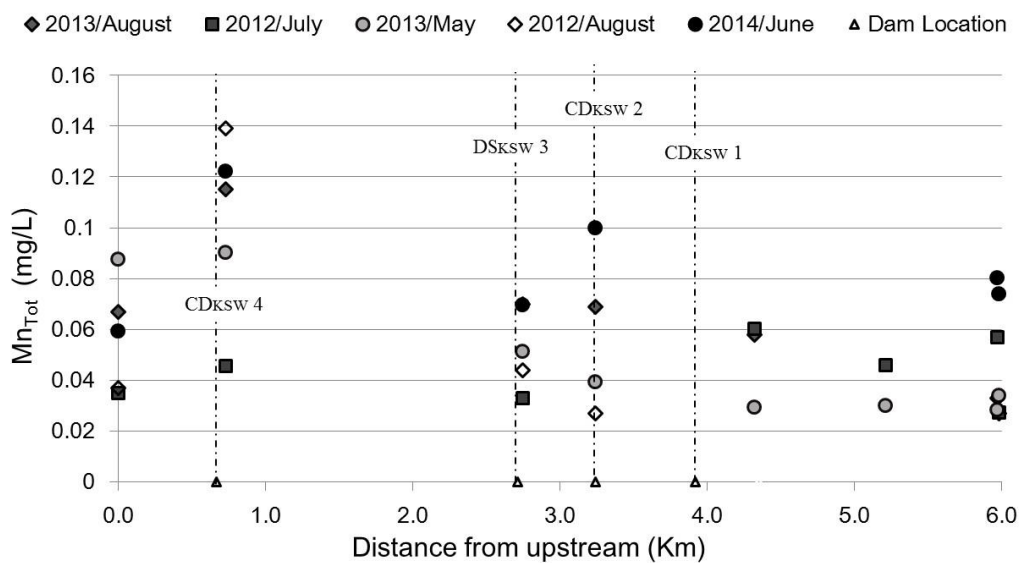
Figure 2-4 Total Mn concentration change across the study site from St.1 to St. 6. Lines show the location of sabo dams CDKSW 4, CDKSW 2, and CDKSW 1 and DSKSW 3, as indicated in in figure 2-2.

Seasonal Mn_{Tot} concentration change along the stream revealed a decrease pattern in Mn_{Tot} concentration towards downstream (Figure 2-4). Irrespective of the sampling time, Mn_{Tot}

was higher in the upper stream section before and after CDKSW 4 at St.1 and St.2 with an exception of May 2013 perhaps due to melting snow and overflow over the dam crest. Mn concentration increase after closed-type sabo dams at KSW and reference streams (Figure 2-3 and Figure 2-4) may be attributed to processes that occur in the retained material upstream of the dam. Processes such as leaf litter fall and sediment erosion in the upstream reach, followed by retention at the dam, result in the reduction of Mn oxides and hydroxides to their dissolved forms, which are easily discharged into the downstream. All the sites (KSW, MEK, HIG, IMO and MIZ) are located in mountainous areas covered by forests in the upper reach, this contributes to the nature and amount of the material retained in the dam. The degree of Mn increase noted around sabo dams (Figure 2-3) may be attributed to the season and nature of the stream. For example, over 276% increase at CDKSW 4 in August 2012 may be due to basal flow conditions while 180% at HIG in December may be linked to leaf litter inflow and breakdown following autumn leaf fall and heavy rains.

Bilby and Likens (1980) found that the layers of organic matters were buried under inorganic sediments in particulate form. By contrast, large particles were easily broken down and decomposed into fragments. This can be easily linked to the Mn_{Tot} change at CDKSW 4 and reference sites where a similar pattern was observed. In addition to formation of such layers, reduction of stable oxyhydroxides of Mn is enhanced. Vertical Mn remobilization profiles in sediments according to Fones (2004) and Zhang et al., (2002) show raise in Mn concentration at the water-sediment interface and at a shallow depth respectively. The former rise relates to Mn diffusion from the underlying sediments to the surface while the latter is due to the readily available Mn oxyhydroxides in the sub-oxic layer. In mountainous streams, and especially in autumn, there is high organic matter inflow from the surrounding vegetation in form of leaf fall. Factors such as vegetation stage may intensify decomposition and solubilization of organic matters (Astel et al., 2008). Vegetation cover change due to seasonal and climatic effects may cause erosion during rain storms characterized by sediment flushing and increased transportation of organic matters and, hence, the observed monthly variation in Figure 2-4. Closed *sabo* dams retain and store organic matter along with inorganic sediments, under such conditions, stable Mn oxides are reduced according to the following reaction (Buamah, 2009).

$$1/2\ MnO_2(s) + 2H^+ + e^- \longrightarrow 1/2\ Mn^{2+}(aq) + H_2O \qquad\qquad (2\text{-}1)$$
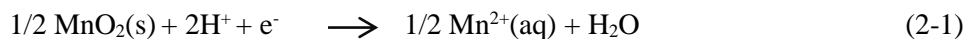
The increase in Mn_{Tot} percentage around *sabo* dams at KSW 4 and reference streams in Figure 2 and Figure 2-4 could be attributed to this process. We observed the greatest increase in Mn_{Tot} of 275.7% in summer (August 2012) and the lowest (3.0%) in spring (May) at CDKSW 4.
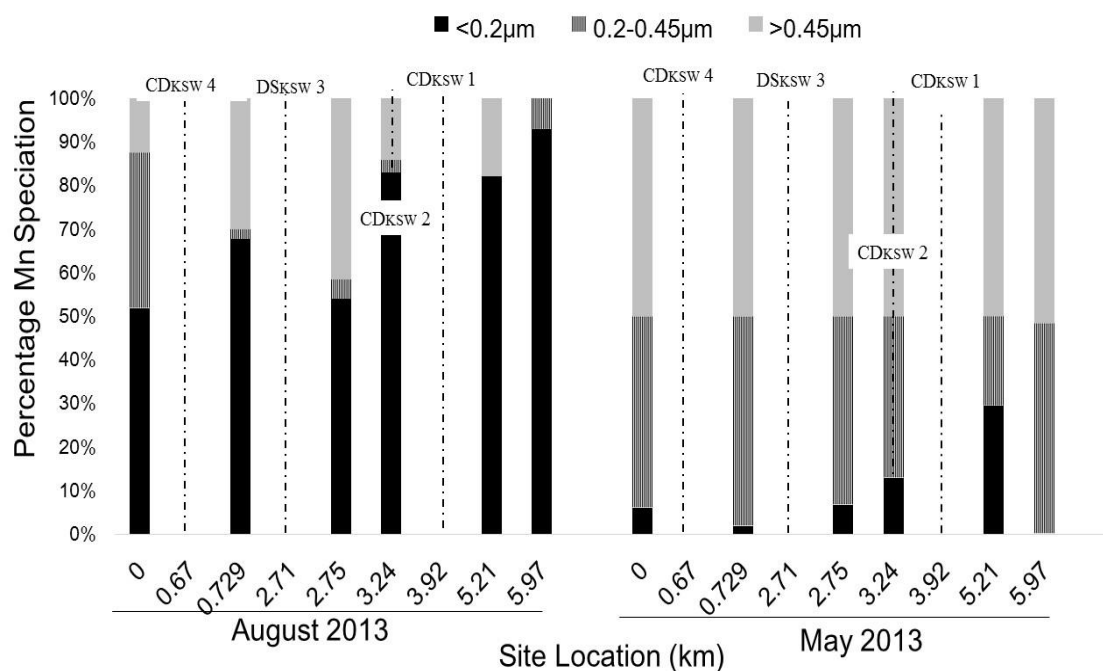
Figure 2-5 Composition of Mn forms depending on size. X-axis shows the distance of each sampling station and dams from st.1 along KSW.

Mn speciation plays a key role in Mn oxidation and is central to overall environmental Mn cycling. Figure 2-5 shows the observed Mn speciation at the study site in August and May 2013. Mn_{Diss} (<0.2um) was high in August at all of the sampling sites at KSW. May 2013 has very low <0.2um Mn_{Diss} composition, all the sampled sites had more than 50% particulate form of Mn (>0.45um). According to Morgan (2000), Mn transformation by oxidation in natural waters depends on speciation. Gardner and Apul (2002) noted that 99.9% of heavy metals in riverine systems are associated with colloidal material, with only 0.1% adsorbed to particles <0.2 µm. Contrary to our observations (Figure 2-5) the average <0.2 µm along KSW was 86% in August a season characterized by basal flows. Furthermore Canfield et al., (1993) suggested that organic matter decomposition plays an important role in iron and Mn reduction, as revealed by the presence of high fractions of Mn (II) and Fe (II) in shallow estuarine sediment. Similarly, copious sink of organic matters in the sediment inside sabo dams could have contribute to Mn forms observed in Figure 2-5.

2.5.2   Mn$_{Diss}$ along Kanosawa

The process of Mn oxidation to stable forms after reduction (Figure 2-6) rapidly follows once reduced Mn form reaches the downstream. Redox cycling of Mn is prevalent in the environment depending on the available conditions. Through reactive oxygen species diverse microorganisms in the environment accelerated the oxidation of Mn (II) to Mn (III/IV) higher than abiotic catalysis (Wang and Giammar, 2015).
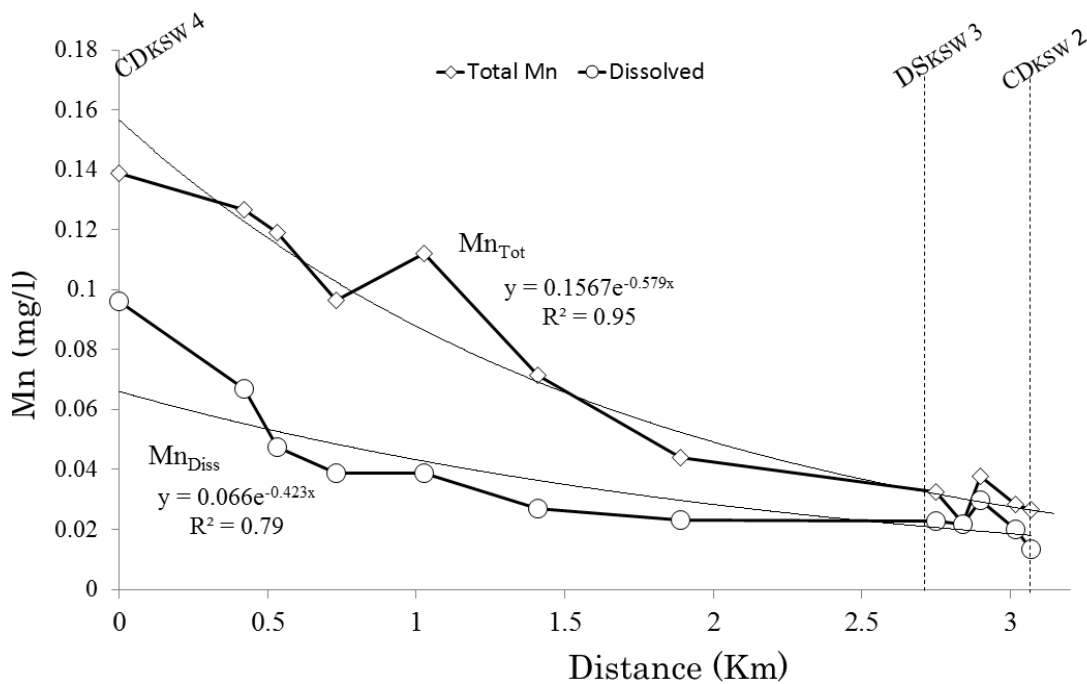
Figure 2-6 Reduction of Mn concentration in the stream from CDKSW 4 to CDKSW 2 in August 2012. The x-axis represents the distance from CDKSW 4.

The oxidized forms are passivated and settle out from the solution as observed in Figure 2-6 as the distance increases from the dam.   According to Gardner & Apul, (2002), availability of Mn (II) to oxidizing agents both biotic and abiotic is invoked by the 'free' forms, as opposed to the complexed or solid-bound Mn forms in solution. The dissolved form of Mn is central to the oxidation and removal process through oxidation, flocculation, and precipitation; hence, the observed removal rate (Figure 2-6). According to Tebo et al., (2004); Burdige (1993), in the absence of oxygen and at low pH, Mn (II) is thermodynamically favored whereas Mn(III) and Mn(IV) are favored in the presence of oxygen and at high pH. With the exception of KSW in Table 2-2, pH inside the dam was below 7, favoring Mn reduced form. pH was seen to rise slightly above 7 in downstream area enhancing Mn (III) oxidation in the oxygen rich

22

environment. We did not measure vertical dissolved oxygen (Table.1), but dissolved oxygen profile is expected to decrease with depth in sediments (Wang et al., 2015). Oxidation of Mn (II) to Mn(IV) is largely catalyzed by microorganisms in presence of oxygen, Figure 2-6 shows a decrease in both total and dissolved Mn from surface water along the stream. Once oxidized, the oxidized form of Mn (IV) precipitates and deposits onto the riverbed surface.

The deposition of Mn after the dam could be roughly described by considering pseudo-equilibrium state between reduced (Mn_{red}) and oxidized (Mn_{ox}) forms of Mn (eq.2-2) and deposition of Mn_{ox} (eq.2-4).

$$Mn_{red} + ox \leftrightarrow Mn_{ox} + red \quad , \quad K = \frac{[Mn_{ox}][red]}{[Mn_{red}][ox]}$$
(2-2)
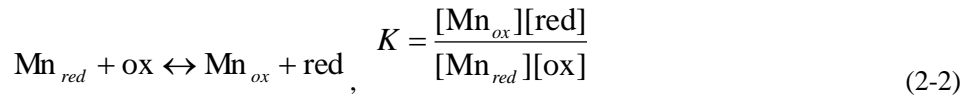
$$[Mn_{Tot}] = [Mn_{red}] + [Mn_{ox}]$$
(2-3)

$$Mn_{ox} \rightarrow \text{depositon of } Mn \quad , k$$
(2-4)

where, *ox* and *red* denote oxidant and reductant for Mn species such as biologically produced agents. *K* is conditional stability constant for the redox reaction of Mn. *k* is the rate constant for the deposition of Mn_{ox}. As described above, Mn_{Diss} is assumed to be approximately equal to Mn_{red}.

$$[Mn_{red}] \approx [Mn_{Diss}]$$
(2-5)

Assuming that the concentrations of oxidant and reductant are stable, or highly rich compared to Mn species, equations 2-2 and 2-3 indicate that Mn_{ox} and Mn_{red} will be proportional to Mn_{Tot}

$$K = \frac{[\mathrm{Mn}_{ox}][\mathrm{red}]}{[\mathrm{Mn}_{red}][\mathrm{ox}]}$$

$$[\mathrm{Mn}_{ox}] = K[\mathrm{Mn}_{red}][\mathrm{ox}]/[\mathrm{red}]$$

$$[\mathrm{Mn}_{ox}] = K([\mathrm{Mn}_{Tot}] - [\mathrm{Mn}_{ox}])[\mathrm{ox}]/[\mathrm{red}]$$

$$[\mathrm{Mn}_{ox}](1 + K[\mathrm{ox}]/[\mathrm{red}]) = K[\mathrm{Mn}_{Tot}][\mathrm{ox}]/[\mathrm{red}]$$

$$[\mathrm{Mn}_{ox}] = \frac{K[\mathrm{ox}]/[\mathrm{red}]}{1 + K[\mathrm{ox}]/[\mathrm{red}]}[\mathrm{Mn}_{Tot}]$$

$$[\mathrm{Mn}_{ox}] = K'[\mathrm{Mn}_{Tot}] \tag{2-6}$$

Equation 4 will lead to the time course change of Mn_{Tot}

$$\text{deposition rate of } \mathrm{Mn} = -\frac{d[\mathrm{Mn}_{Tot}]}{dt} = k[\mathrm{Mn}_{ox}] = kK'[\mathrm{Mn}_{Tot}] = k'[\mathrm{Mn}_{Tot}]$$

$$[\mathrm{Mn}_{Tot}] = [\mathrm{Mn}_{Tot}]_0 \exp(-k't) \tag{2-7}$$

Since the flow rate of the river does not change rapidly without rainfall, the reaction time will be proportional to the distance from the point where $[\mathrm{Mn}_{Tot}]=[\mathrm{Mn}_{Tot}]_0$. Thus, finally relationship between Mn concentration and distance between sabo dams could be described as below

$$[\mathrm{Mn}_{Tot}] = [\mathrm{Mn}_{Tot}]_0 \exp(-k''x) \tag{2-8}$$

$$[\mathrm{Mn}_{Diss}] = [Mn_{Tot}] - [\mathrm{Mn}_{ox}] = (1 - K')[\mathrm{Mn}_{Tot}] \tag{9}$$

The increase in Mn around *sabo* dams followed by rapid oxidation (k''=0.696) and deposition indicates the importance of Mn_{Diss} in Mn cycling. Studies such as that by (Nealson and Saffarini, 1994; Schamphelaire et al., 2007) argue that, in addition to the biotic environment, newly formed biogenic Mn oxides contribute to Mn oxidation. The newly formed biogenic Mn oxides of Mn (III) and Mn(IV) are poorly crystalline and have hexagonal structures that can easily adsorb Mn(II) and participate in the oxidation of Mn itself (Tebo et al., 2004). Canfield et al. (1993), in their study of anaerobic degradation of organic matter in coastal sediments suggested that on average Mn cycles between the oxidized and reduced forms about 100–300 times before finally being deposited in the sediments. This kind of reactivity affects Mn residence time and availability, which may vary with location and stream characteristics. Therefore, the impact of Mn on water quality and aquatic ecosystems may be compounded by

sabo dams through longer retention periods, oxygen depletion, and environmental modification. Understanding Mn cycling in such environments is important for ecosystem management.

2.6   Summary

We observed an increase in Mn concentration in all closed-type dams, along with resultant impacts on water quality. Specific to the study site, we found more than 200% increase in Mn_{Tot} during summer 2012. Seasonal changes characterized by flow discharge changes are important in controlling conditions in the dams, which in turn affect metal fluctuation. Because Mn is highly coprecipitating and affects the availability of other elements and pollutants in the environment, further studies on metal abundance and behavior within and downstream of *sabo* works are necessary.

References

Abesser, C., and Robinson, R., 2010. Mobilisation of iron and manganese from sediments of a Scottish Upland reservoir. J.Limnol., 69(1),42-53, DOI: 10.3274/JL10-69-1-04

Astel, A., Małek, S., Makowska, S., 2008. Effect of environmental conditions on chemical profile of stream water in sanctuary forest area. Water, Air and Soil Pollution, 195,137–149

Bilby, ER, Likens, E.G, 1980. Importance of organic debris dams in the structure and functon of stream ecosystems. Ecology 61(5), 1107-1113.

Brewer, P.G., and Spencer, D.W., 1971. Colorimetric determination of manganese in anoxic water. Limnology Oceanography, 16,107-110.

Buamah, R., 2009. Adsorptive removal of managanese, asernic and iron from ground water. Tylor and Francis Group CRC press, Netherlands.

Burdige, J.D., 1993. The biogeochemistry of manganese and iron reduction in marine sediments. Earth Science Reviews, 35, 249-284.

Burle, E., William, W. and Kirby S., 1979. Application of formaldoxime colorimetric method for the determination of manganese in the pore water of anoxic estuarine sediments, Estuaries, 2(3), 198-201

Canfield, D.E., Thandrup, B. and Hansen, J.W., 1993. The anaerobic degradation of organic matter in Danish coastal sediments: iron reduction, manganese reduction and sulphate reduction. Geochemica et cosmochemica Acta, 57, 3867-3883.

Fones, G. R., W. Davison and J. Hamilton-Taylor., 2004. The fine-scale remobilization of metals in the surface sediment of the North-East Atlantic. Continental Shelf Research 24(13-14): 1485-1504.

Gardner, K.H.., Apul, D.S., 2002. Influence of colloids and sediments on water quality. Environmental and Ecological Chemistry, 2, 264-277

Gordon, D.N., et al., 2004. Stream hydrology, An introduction for ecologists. 2nd Edition. John Wiley & sons, West Sussex England

Chuan, M.C., Shu, G.Y. and Liu, J. C., 1996. Solubility of heavy metals in contaminated soil; Effects of redox potential and pH. Water, Air and Soil Pollution,90, 543-556.

Harvey, J.W., Fuller, C.C., 1998. Effect of enhanced manganese oxidation in the hyporheic zone on basin scale geochemica balance. Water Resources Research, 34(4), 623-636

Heal, K.V., Kneale, P.E. and McDonald, A.T., 2002. Manganese in runoff from upland catchments: temporal patterns and controls on mobilization. Hydrological Sciences -Journal-des Sceiences Hydrologques, 47, 769-780.

Hem J.D., 1985. Study and interpretation of the chemical characteristics of natural water (3rd Ed.). US Geological Survey Water-Supply Paper 2254.

Howe, P.D., Malcolm, M.D. and Dobson S., 2004. Manganese and it's compounds: Environmental Aspects. Geneva: Concise International Chemical Assessment Document 63 World Health Organisation. ISSN 1020-6167; 63

ICH Guidelines Document Q2(R1)., 2005. Validation of analytical procedures: text and methodology. http://www.ich.org/fileadmin/Public_Web_Site/ICH_Products/Guidelines/Quality/Q2_R1/Step4/Q2_R1__Guideline.pdf accessed 28th January 2016

Ingri, L.J., et al., 2011. Manganese redox cycling in Lake Imandra: Impact on nitrogen and the trace metal sediment record. Biogeosciences Discuss, 8,273-321. DOI 10.5194/bgd-8-273-2011

Kajiwara, M., Goto, K., 1964. Successive Spectrophotometric determinations of manganese and iron in water with formaldoxime. Bunseki kagaku, 13(6) 529-532

Li, P., et al., 2014. Anthropogenic pollution and variability of manganese in alluvial sediments of the Yellow River, Ningxia, northwest China. Environmental Monitoring and Assessment, 186(3), 1385−1398. doi:10.1007/s10661-013-3461-3

Ministry of Land, Infrastructure, Transport and Tourism (MLIT)., 2015. Water Information System database. http://www1.river.go.jp/cgibin/SelectMap.do?cntX=140.14212009919584&cntY=38.67504341689829&scaleCd=5&systemVer=1459136102302. Accessed 28th January 2016

Morgan, J.J., 2000, August. Manganese speciation and redox reaction kinetics in natural waters. In abstracts of papers of the american chemical society (vol. 220, pp. u331-u331). 1155 16th st, nw, washington, dc 20036 usa: amer chemical soc.

Nadaska, G., Lesny, J. and Michalik, I., 2010. Environmental aspect of manganese chemistry. Hungarian Journal of Sciences, ENV-100702-A, pp.1-16. http://heja.szif.hu/ENV/ENV-100702-A/env100702a.pdf Accessed 25th September 2013

Nealson, K.H. and Saffarini, D., 1994. Iron and manganese in anaerobic respiration: environmental significance, physiology, and regulation. Annual Reviews in Microbiology, 48(1), pp.311-343.

Pinsino, A., Roccheri, M.C. and Matranga, V., 2012. Manganese: a new emerging contaminant in the environment. Dr. Jatin Srivastava (Ed.),ISBN: 978-953-51-0120-8, INTECH Open Access Publisher., http://www.intechopen.com/books/environmental-contamination/Mna-new-emerging-contaminant-in-the-environment

Raikow, D.F., Grubbs, S.A. and Cummins, K.W., 1995. Debris dam dynamics and coarse particulate organic matter retention in an Appalachian Mountain stream. Journal of the North American Benthological Society, pp.535-546.

Sabo Publicity Center. 2001. Sabo in Japan. Creating safe and rich green communities. Present state ed. Japan Sabo Association, Tokyo: Japan Sabo Association.

De Schamphelaire, L., et al., 2007. Minireview: The potential of enhanced manganese redox cycling for sediment oxidation. Geomicrobiology journal, 24(7-8), pp.547-558.

Scott, D.T., et al., 2002. Redox processes controlling manganese fate and transport in a mountain stream. Environmental science & technology, 36(3), pp.453-459..

Soja, R. and Wiejaczka, Ł., 2014. The impact of a reservoir on the physicochemical properties of water in a mountain river. Water and Environment Journal, 28(4), pp.473-482.

Tebo, B.M., et al., 2004. Biogenic manganese oxides: properties and mechanisms of formation. Annu. Rev. Earth Planet. Sci., 32, pp.287-328.

Wang, C., et al., 2015. The limiting role of oxygen penetration in sediment nitrification. Environmental Science and Pollution Research, 22(14), pp.10910-10918..

Wang, Z. and D. E. Giammar., 2015. Metal contaminant oxidation mediated by manganese redox cycling in subsurface environment. In advances in the environmental biogeochemistry of manganese oxides; Sparks, et al.; ACS Symposium Series; American Chemical Society: Washington, DC, 1197: 29-50.

Wilde, F.D., et al., 1998. Cleaning of water equipment for water sampling. In National Field Manual for the Collection of Water-Quality Data. U.S.Geological Survey, Denver, 9,15-25

Zhang, H., et al., 2002. Localised remobilization of metals in a marine sediment. Science of the Total Environment, 296(1), pp.175-187.

3   Metal behavior in mountainous streams with sabo dam structures

3.1   Introduction

Metals are abundant in the environment and the major source of major trace metals (Fe, Mn, and Al) is weathering, mineralization and desorption from soil and sediment surfaces. These metals are important in forest and aquatic ecosystems. Most importantly, many trace metals like Cu, Zn, and Mn are required micronutrients for both plant and animal life (Driscoll et al., 1994, Warren and Haack, 2001). Trace metals such as iron (Fe), manganese (Mn), nickel (Ni), zinc (Zn) and cadmium (Cd) are involved in numerous processes in the metabolisms of phytoplankton and can be toxic at high concentration (Kondo et al., 2013). Although nutritional requirement of trace elements differs between species (Mohiuddin et al., 2012), at very low concentrations organisms and plants may show deficiencies related to the missing nutrients, while in high amounts, some of these metals are toxic (Warren and Haack, 2001). Various activities have an impact on the availability of these metals especially anthropogenic activities which greatly alter their biogeochemical cycles and trace elements that may also be concentrated through the redox cycling of Mn and Fe (Tribovillard et al., 2006). Many metals like Cadmium (Cd), Nickel (Ni) and Lead (Pb) which exhibit extreme toxicity (Mohiuddin et al., 2012) are incorporated within manganese or iron oxides. Therefore dissolution of these oxides brought about by organic matter degradation and change in redox potential results in liberation of trace metals linking Mn and Fe to other trace metal.

Besides major anthropogenic activities such as mining, industrial and agricultural processes, changes in Fe and Mn along the river continuum are influenced by stream modifying activities. Damming of rivers not only traps materials being transported but also leads to dissolution of stable hydro/oxides concomitantly releasing the sorbed elements (Ingri et al., 2011). Worldwide, 30-40% of suspended material does not reach the sea or ocean, it is retained in manmade reservoirs (McClain et al., 2005). Furthermore, environmental problems such as reservoir flushing, water division, interruption of fish migration and interruption of bio-geochemical cycles are associated with dam operation (Wildi, 2010). River dams and reservoirs slow down runoff, reduce sediment delivery in the downstream and cause major changes in the upstream and downstream (Wildi, 2010). The material trapped in reservoirs undergoes several processes which result into remobilization of nutrients, metals and organic

contaminants from the sediments. Metal accumulation in reservoirs has been reported by many researchers (Fremion et al., 2016, Wildi, 2010). Reduction of metal oxides (Fe and Mn) occurs in the reduction zone in the anoxic layer and the reduced metal dissolves in pore water which may be re-oxidized after diffusion in anoxic layer. The dissolution of stable Mn and Fe oxyhydroxides together with Aluminium (Al) affects other metals such as Nickel (Ni), lead (Pb), Chromium (Cr), Copper (Cu) and Zinc (Zn) (Fremion et al., 2016; Harvey and Fuller, 1998). The fate of these metals relies on events like bioturbation, mixing with the newly formed particulate metal oxide and into the reducing layer or discharged downstream where the metal can be re-used.

Metal contamination has been linked to the lithology although, in some cases, parental material may be poorly altered (Fremion et al., 2016). For example In Fremion et al., 2016, the main source of metals (Cr, Ni and Zn) in the Rhue reservoirs was upstream tributaries. From their source, metals make their way to aquatic environment and, metal transportation along the streams and rivers majorly relies on particulate transport. Therefore, once trace metals have been eroded and discharged in aquatic environment, they participate in a range of reactions and are sorbed to suspended particles, and are subsequently deposited on the river bed, while some are suspended and exported to downstream and marine environments.

The importance of Mn in the environment relies on its forms. Mn exists in the aquatic environments in two major forms Mn^{2+} and Mn^{4+} (Pinsino et al., 2012), oscillating between these two forms vai oxidation and reduction. Mn^{2+} forms are majorly soluble whereas Mn^{4+} consists of the insoluble oxides, making the interconversion between different forms important aspect in Mn aquatic chemistry (Section 2.1). Although toxicity of most metals in water depends on speciation not on total or dissolved metals, dissolved metals play an important part in speciation (Han et al., 2013). In regards to Mn, Japanese Environmental quality standards for aquatic life were amended in 2003 to a total concentration of 0.2 mg/L for industrial water, agricultural water and environmental conservation (http://www.env.go.jp/en/water/wq/wp.pdf).

Most studies on metals in Japanese rivers have focused on urban rivers, however, water chemistry varies among rivers (Han et al., 2013), and subsequently affecting metal speciation. Sabo dams create reservoirs which result in changes in physico-chemical properties enhancing redox conditions creating hot spots around and in sabo dams does not only enhance Mn dissolution but also affect the behavior of other trace metals. Moreover, changes in sediment

redox conditions affects mobility and bioavailability of trace metals. Metal accumulation in stream sediments may be relatively harmless but release of the accumulated metals by various processes may result in hazardous effects on both aquatic ecosystem.

The objective of this study was to investigate the impact of sabo dams on manganese and iron behavior in mountainous streams with sabo dams and assess their association with other trace metals in mountainous streams

3.2   Materials and methods

3.2.1   Study area

This study was carried out in mountainous streams located in Yamagata Prefecture Japan (Figure 2-1). Two sites namely Mizunashigawa (MIZ) and Higashiwamotogawa (HIG) were selected as main study sites (Figure 2-2), and three sites Kanosawa (KSW), Maenokawasawagawa (MNK) and Imogawa (IMO) were added for monitoring to compare the observations. All the studies sites lie in elevation range of 50-1098 m, and KSW, MNK have high landslide occurrences.

MIZ, HIG and IMO are located with the same area and according to the Ministry of Land, infrastructure, transport and tourism Japan website, in 2014, this area received an average rainfall of 3435mm with 776mm/month. MNK and KSW are sub basins of Mogami River and KSW receives an average annual precipitation of 2,946 mm/year (MLIT, 2015). All the studies sites are either first order or second order mountainous streams whose surrounding environment varies along the continuum. The upper sections of the five streams are within forested environment while the downstream areas have various activities such as Agriculture and farming characterized by a number of paddy field, residential and commercial housing and transporting activities. MIZ, HIG and IMO are located within the Akagawa basin, MIZ covers an area of 15.1 km^2, while HIG watershed area is 6.2 km^2. KSW and MNK are sub basins of Mogami River covering 16.08 km^2 and 5.17 km^2 respectively (KSW details in Section 2.4.1). At each stream, four sampling stations namely; St.1, St.2, St.3, and St.4 as indicated in Figure 3-2 were selected. St.1 located upstream is at a readily accessible point in the mountainous part of the stream while St.2 and St.3 located around the closed sabo dams are in the dam reservoir and dam outflow, respectively. St.4 was selected as the last point downstream before the stream confluences with a larger river.
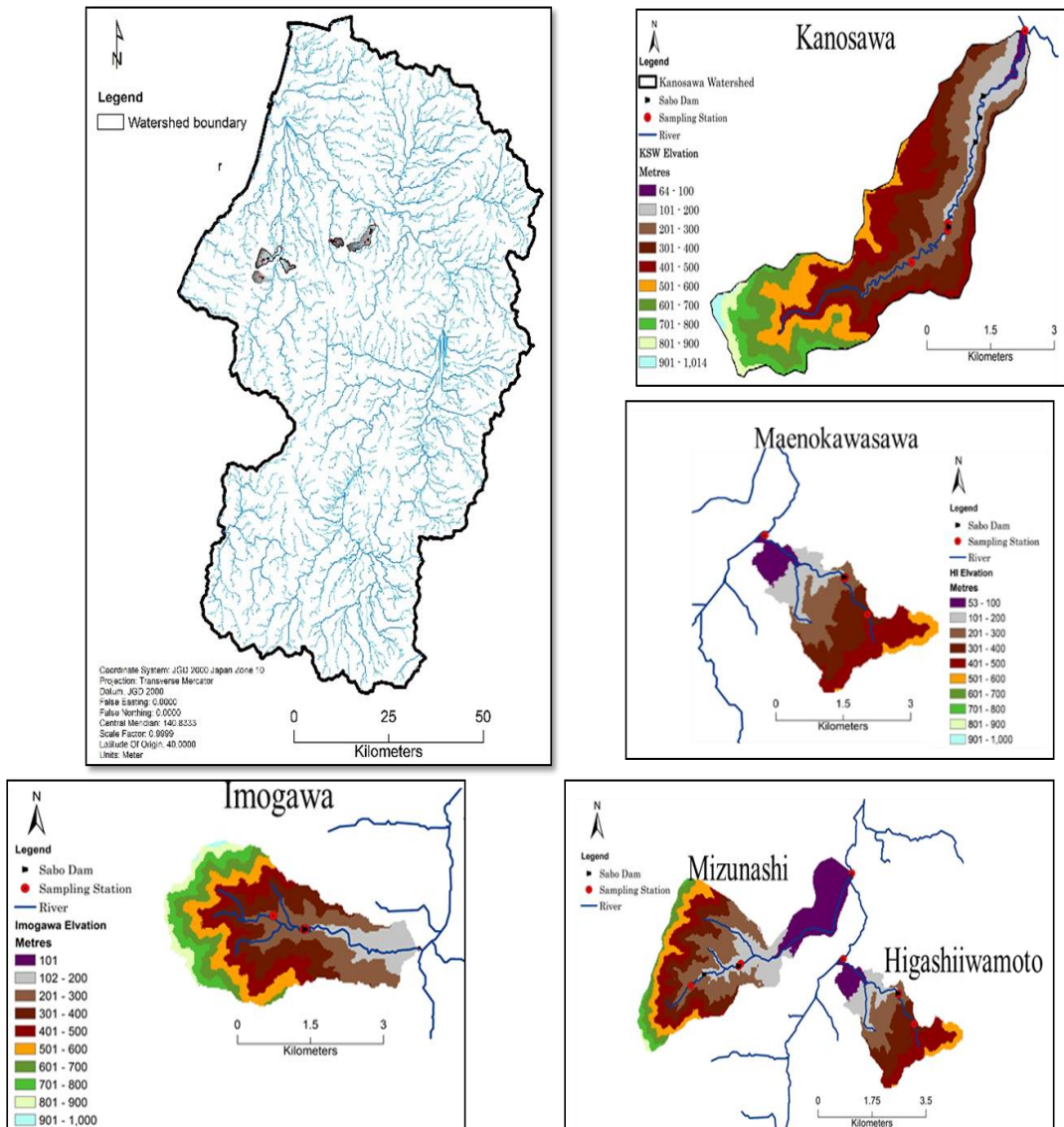
Figure 3-1   Location and details of the study sites showing elevation, sampling stations and dam location
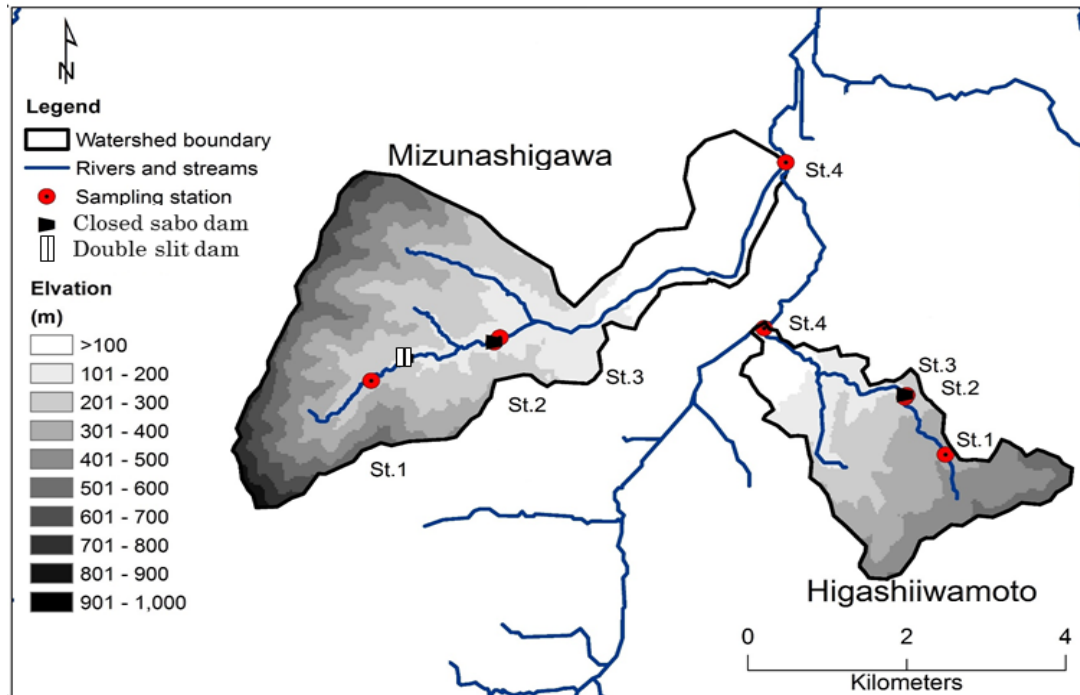
Figure 3-2 Main study sites Higashiiwamotogawa (HIG) and Mizunashi (MIZ) and location of sampling stations and sabo dams

3.2.2 Sample collection

Water sampling was done monthly from June-November 2015 at the main study sites, during August and November, water samples were collected twice as indicated in the Table A-1. A total of sixty two (62) samples was collected during the sampling period. Samples were collected from sampling stations (St.1-St.4) in 250 polyethylene sampling bottles which had been previous cleaned and soaked in 30% Nitric acid as described in Waide (1998) and rinsed with the sample before collection. At the same time, physico-chemical properties pH, temperature, dissolved oxygen (DO), electric conductivity (EC), oxidation reductive potential (ORP), and turbidity were measured at using the hand-held multi-parameter water quality checker (WQ-24, TOA-DKK). The samples were transported to the laboratory in a cooler box and analyzed for manganese Mn and other eight metals namely; Fe, Cu, Cr, Ni, Zn, Pb, Cd and Al for both total and dissolved concentration after acid treatment using ICP-MS.

3.2.3 Treatment for metal analysis

In the laboratory, samples were pre-concentrated using nitric acid (HNO_3) according to

EPA 3030B and trace metals Fe, Cu, Mn, Cr, Pb, Cd, Ni, Zn and Al were analyzed using ICP MS spectroscopy. Pre-concentration procedure was as follows; 5 ml of HNO_3 (EL) was added to 100 ml of the water sample in acid washed and well rinsed beaker. The mixture was heated on a hot plate at 170°C in a fume hood chamber to 25 ml and allowed to cool off the hot plate. After cooling, the remaining mixture was transferred to a volumetric flask and diluted to 100 ml using MilliQ water. The solution was shaken vigorously to mix the contents and then filtered into clean bottles, and stored at room temperature untill analysis. ICP-MS measurement was done following the standard procedure, and quantification limit for analyzed metals was 0.1 µg/L for Fe, Cu, Cr, Mn, Zn, Pb and Cd, and 0.5 µg/L for Ni and 0.2 µg/L for Al

3.3   Statistical analysis

Metal concentrations were log transformed to attain normality. Analysis of variance (ANOVA) and Tukey tests were used to compare metal concentrations between sites and stations respectively. In addition student t-test analysis was performed to compare significant differences between two stations. While Pearson correlation coefficients were used to assess the relationship between metals. Statistical significance is reported based on p-values as significant at P-value < 0.05 and non-significant at P-value >0.05. Kaiser Meyer Olkin (KMO) and bartlett's sphericity tests were performed on all variables (trace metals, DOC, C:N ratio and DON) to examine suitability for principal components analysis (PCA). KMO measures sampling adequacy indicating proportion of variance that may be caused by underlying factors while Bartlett's sphericity test identifies the identity of the correlation matrix that shows if variables are related (Varol et al., 2012, Shrestha and Kazama, 2007). During analysis, KMO value of was 0.63 and Bartlett's test significant at p<0.001 indicating the data was suitable for PCA. Furthermore using the variables sites we classified using cluster analysis. Statistical analysis was performed by IBM SPSS 22.

3.4   Results and discussions

3.4.1   Physicochemical properties

Table 3-1 Average physicochemical properties observed at each station per site

		pH	Temp (°C)	Turbidity (NTU)	DO (mg/L)	ORP (Mv)	EC (μS/cm)
HIG	St 1	7.3±0.3	14.2±4.3	2.5±2.0	7.7±1.5	236±100	5.70±2.7
	St 2	6.4±0.3	13.6±4.8	3.8±4.9	7.0±0.5	215±62	5.98±0.9
	St 3	6.6±0.3	14.6±5.3	3.2±3.6	6.7±0.8	205±99	6.05±1.0
	St 4	7.3±0.3	17.6±5.7	3.7±3.3	7.4±1.4	226±84	8.25±2.0
MIZ	St 1	6.9±0.1	14.9±4.9	1.8±2.3	6.8±2.3	231±69	4.97±0.9
	St 2	6.8±0.2	15.8±4.7	3.0±3.2	6.4±2.1	165±79	5.98±1.1
	St 3	7.0±0.2	15.4±4.2	3.0±2.8	7.8±2.7	150±45	5.90±0.9
	St 4	7.8±0.5	17.6±5.7	39.6±107.4	7.6±2.8	217±53	22.96±10.0
KSW	St 1	7.8±0.4	15.2±5.9	81.8±108.3	8.3±3.2	290±130	3.98±0.8
	St 2	7.3±0.2	15.6±6.2	5.7±6.1	8.1±3.5	239±109	4.05±0.7
	St 3	7.5±0.2	14.2±5.0	5.5±5.6	8.6±4.0	184±85	4.65±0.5
	St 4	7.9±0.5	16.0±5.0	6.6±4.7	8.1±4.1	228±98	5.12±0.8
MNK	St 1	7.7±0.3	12.8±2.8	15.8±23.6	7.3±2.1	284±64	5.86±0.6
	St 2	7.3±0.3	13.1±2.8	13.8±6.8	7.8±2.4	226±70	5.60±1.2
	St 3	7.3±0.1	14.1±3.9	2.1±0.5	8.3±3.3	230±40	5.87±1.1
	St 4	8.2±0.6	17.3±5.8	5.7±3.9	7.7±2.0	279±36	6.22±1.3
IMO	St 1	7.5±0.3	15.5±4.7	2.6±1.2	7.8±4.0	327±48	3.52±1.6
	St 2	7.1±0.0	16.7±3.7	0.9±1.3	7.4±3.6	294±7	3.37±0.8
	St 3	6.8±0.2	16.3±3.5	4.6±0.9	7.6±3.9	172±12	4.82±1.4

EC and temperature increased from upstream to downstream throughout the sampling at all sites while ORP was low at St.3. Except at MNK. pH changes were also low around the dam (St.2 and St.3) and high at St.4 with in all the studied sites. Despite the observed pH changes, all the values were in the range for river water 4.5-8.5 (McCutchean, 1992 cited in Bahar et al., 2008). The increase in EC from head water downstream to the river mouth is typical of EC behavior since number of tributaries and the intensity of anthropogenic activity increase in the downstream direction (Bahar et al., 2008).

3.4.2 Total metals along the stream

3.4.2.1 Mn and Fe distribution in the studied sites.

Total and dissolved metals measured varied between the sites and stations. Fe concentration was relatively higher than other metals in all station followed by Al and Mn. Mn concentration range from 0.60 µg/L at IMO to 381 µg/L at MIZ as shown in Figure 3-3. The extremely high Mn concentration was observed at St.3 in autumn (November 11th 2015) following heavy rains, besides the two extremely high concentration observed at MIZ and KSW, Mn concentration recorded for other sampling dates was less than 106.66 µg/L. From average concentrations (Table 3-2), the least Total Mn concentration was observed at St.1 (1.02±0.92 µg/L at MIZ, 6.60±4.68 µg/L at HIG, 26.15±27.30 µg/L at KSW, 1.14±0.66 µg/L at IMO and 3.64±2.24 µg/L at MNK) while the highest was observed at St.3.
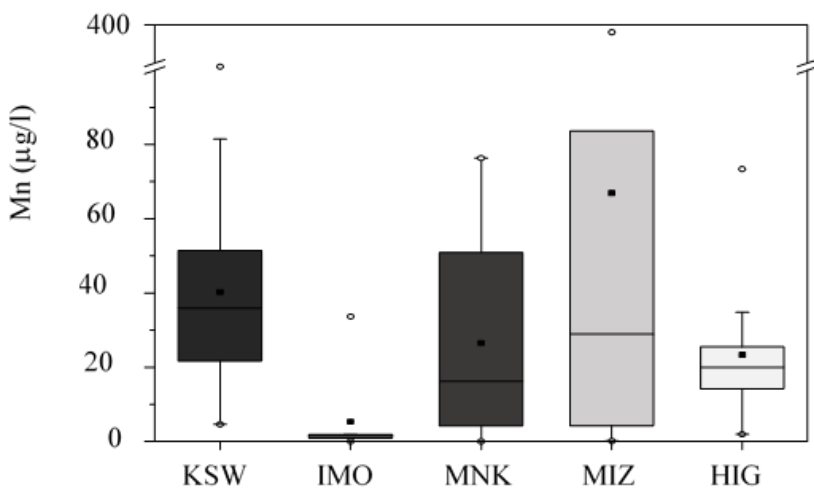
Figure 3-3 Boxplot showing Mn concentration range between the sites.

Mn_{Tot} did not vary significant between sites, $F_{(4,87)}=2.00$, p=0.101, however, significantly differences were noted between stations; $F_{(3,88)}=35.98$, p<0.001. Mn was significantly higher around the dams compared to other stations upstream and downstream. Post Hoc test (Tukey HSD), showed significance between IMO and other sites (p≤ 0.001), and KSW and MIZ (p=0.35), while Mn concentration did not vary significant among the other different sites. From ANOVA results, both site and station played a significant role in Mn_{Tot} concentration along the stream, accounting for 79.6% variance in observed Mn_{Tot} (F (11) =8.42, p≤ 0.001). The high

Fe concentration observed was expected due to the abundance of Fe the environment (Figure 3-4). The highest Fe concentration was observed at KSW in early summer (June 2015) and this corresponded to high turbid at the time of sampling (Tables 3-2 and 3-1). Compared to other sites, all metals monitored were in high concentrations at KSW in Early summer (June) (Table 3-2 and A-2). ANOVA results revealed significant variations between sites, $F_{(4, 87)} = 3.01$, $p = 0.022$, KSW had significantly higher Fe (M = 2.6, SD = 0.45), while the least was at IMO (M = 1.89, SD = 0.5). From post Hoc tests, sites that did not vary significantly in observed iron concentration were HIG, MIZ and MNK ($p \geq 0.05$), whereas, KSW and IMO varied significantly from the other sites. From ANOVA analysis, both site and station accounted for 57% variance in Fe concentration, and were significant factors for Fe observations $f_{(11)} = 3.75$, $p < 0.001$.
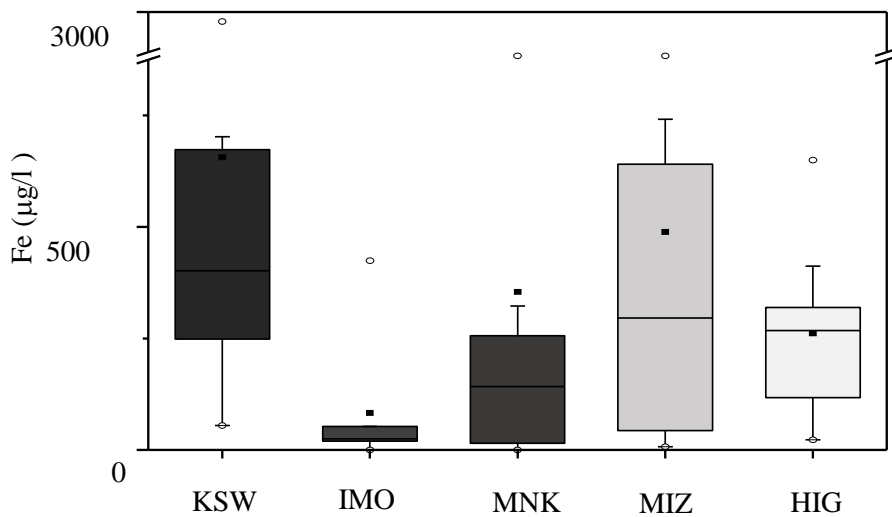
Figure 3-4 Box plot showing Fe distribution between the studied sites.

Test results for Fe and Mn between the sites shows that Fe concentrations were largely dependent on site location and stream process while Mn concentration seemed independent of the site but was controlled by stream conditions and processes. The two major study sites (MIZ and HIG) did not show any significant difference in both Mn and Fe, while very low observations at IMO may be attributed absence data at St.4.

Table 3-2 Average trace metal concentration per station per site for 2015

	HIG				MIZ				KSW				IMO			MNK			
	St 1	St 2	St 3	St 4	St 1	St 2	St 3	St 4	St.1	St.2	St.3	St.4	St.1	St.2	St.3	St.1	St.2	St.3	St.4
Fe	123.92	165.78	275.72	306.78	33.68	433.29	528.17	229.31	1102.54	394.87	453.01	675.24	30.74	29.81	281.73	166.57	145.34	578.90	160.58
	±104.39	±75.38	±49.55	±165.76	±27.48	±183.82	±182.72	±86.21	±1571.94	±287.57	±191.79	±566.90	±19.42	±10.28	±201.98	±126.35	±109.04	±568.14	±10.51
Cu	0.83	0.71	0.65	0.87	0.45	0.52	6.19	1.02	3.73	1.90	1.57	4.31	0.51	0.47	0.57	1.38	1.23	2.68	0.99
	±0.53	±0.39	±0.19	±0.46	±0.38	±0.10	±15.96	±0.24	±4.07	±1.29	±0.63	±5.35	±0.15	±0.17	±0.06	±0.82	±0.73	±3.05	±0.43
Cr	3.22	1.58	1.81	0.94	3.01	0.45	0.69	0.79	1.80	2.92	0.56	56.95	1.19	0.45	0.22	5.31	0.33	1.27	0.33
	±3.64	±0.37	±1.05	±0.85	±7.53	±0.51	±0.67	±1.38	±2.19	±3.32	±0.42	±97.88	±1.46	±0.42	±0.04	±8.36	±0.20	±1.28	±0.16
Mn	6.60	18.44	25.65	31.40	1.02	65.52	114.48	18.35	26.15	48.26	62.20	24.40	1.14	1.54	22.74	3.64	18.97	60.74	21.74
	±4.68	±5.32	±7.23	±18.73	±0.92	±26.42	±109.50	±7.19	±27.30	±28.88	±36.05	±15.67	±0.66	±0.55	±15.46	±2.42	±8.61	±21.62	±9.64
Ni	2.97	0.79	4.13	0.59	2.20	0.22	2.99	0.57	2.25	2.72	1.37	31.17	0.46	0.25	0.28	0.96	0.45	1.07	0.29
	±3.35	±0.59	±8.37	±0.37	±3.96	±0.17	±7.04	±0.54	±1.85	±2.27	±0.38	±51.98	±0.27	±0.11	±0.34	±0.91	±0.29	±1.24	±0.28
Zn	7.71	7.45	7.77	7.38	4.31	6.29	11.34	13.81	21.99	15.12	9.51	7.44	5.06	3.90	8.18	12.61	9.55	9.01	14.91
	±7.24	±5.01	±5.56	±3.51	±1.45	±6.98	±10.77	±16.53	±26.20	±9.31	±8.00	±6.68	±2.38	±2.75	±6.15	±14.08	±10.10	±8.11	±15.84
Pb	0.36	0.44	0.19	0.41	0.17	0.34	1.80	0.32	0.72	0.76	0.29	0.54	0.28	0.18	0.18	1.91	0.27	0.42	0.56
	±0.33	±0.38	±0.05	±0.18	±0.09	±0.16	±3.93	±0.08	±0.88	±0.93	±0.20	±0.54	±0.19	±0.00	±0.01	±3.02	±0.18	±0.27	±0.44
Cd	0.03	0.01	0.01	0.03	0.01	0.01	0.02	0.06	0.04	0.19	0.02	0.05	0.01	0.01	0.01	0.01	0.03	0.02	0.05
	±0.05	±0.01	±0.02	±0.02	±0.00	±0.00	±0.01	±0.09	±0.03	±0.24	±0.02	±0.05	±0.00	±0.00	±0.00	±0.00	±0.02	±0.01	±0.04
Al	72.59	87.66	70.05	127.21	17.60	44.89	153.54	87.78	828.33	224.67	194.96	217.53	34.34	26.80	35.81	114.85	93.54	239.51	47.24
	±48.09	±110.80	±27.69	±154.45	±8.44	±19.43	±274.69	±47.03	±1269.80	±228.33	±196.50	±192.53	±20.86	±19.30	±20.99	±106.46	±96.81	±273.25	±23.02

Other metals studied did not show a trend as Mn and Fe, their abundance varied between sites, stations and time of sampling. KSW had higher concentrations from the other sites especially in early summer (June 2015) as shown in Table 3-2 and A-2. Mean total concentrations per station Table 3-3 indicate metal concentration in order Fe>Al>Zn>Mn>Cr>Ni>Cu>Pb>Cd at St.1, Fe>Al> Mn>Zn>Cr>Ni>Cu>Pb>Cd at St.2, and, Fe>Al>Mn>Zn>Cu>Ni>Cr>Pb>Cd at St.3 and Fe>Al>Mn>Zn>Cr>Ni>Cu>Pb>Cd at St.4.

Table 3-3 Average concentration of all metals from all sites grouped by station

		Fe	Cu	Cr	Mn	Ni	Zn	Pb	Cd*	Al
St.1*	Average	96.98	0.80	3.01	4.19	1.99	6.95	0.56	0.02	58.27
	Max	343.00	2.13	20.08	17.00	8.40	28.70	5.40	0.11	231.86
	Min	7.25	0.20	0.09	0.12	0.15	2.54	0.11	0.01	6.72
	S.D	572.41	1.63	5.20	11.50	2.73	11.15	1.23	0.03	451.05
St 2	Average	274.51	0.85	1.10	37.33	0.89	8.11	0.42	0.04	86.55
	Max	701.85	3.34	6.60	86.79	5.23	24.85	1.82	0.36	481.46
	Min	24.80	0.34	0.15	1.85	0.11	1.94	0.14	0.01	14.38
	S.D	211.26	0.69	1.38	30.18	1.21	7.04	0.42	0.09	111.20
St 3	Average	527.29	2.96	1.05	65.64	2.50	9.44	0.83	0.02	134.51
	Max	2570.00	45.70	4.13	381.00	20.40	36.90	10.70	0.04	831.00
	Min	138.91	0.38	0.13	11.81	0.04	2.48	0.09	0.01	20.97
	S.D	509.16	9.21	0.97	74.08	5.66	7.89	2.34	0.01	194.78
St 4	Average	308.92	1.41	8.44	24.38	6.68	10.76	0.42	0.05	114.28
	Max	1315.31	10.47	169.97	73.37	91.18	53.72	1.16	0.20	499.27
	Min	97.99	0.40	0.16	7.30	0.18	2.32	0.16	0.01	21.06
	S.D	260.94	2.03	35.31	14.72	22.65	11.58	0.28	0.06	121.09

St.1* does not include KSW June results since the values were extremely higher than other sites, Cd* includes concentration measurement below quantification limit.

Out of the nine trace metals analyzed, significant difference regarding the sites were noted for Fe_{Tot}, Cu_{Tot}, Cr_{Tot}, Ni_{Tot}, Cd_{Tot} and Al_{Tot} while Mn_{Tot}, Zn_{Tot} and Pb_{Tot} did not show significant differences across sites as shown in the Table 3-4. Fe_{Tot} and Al_{Tot} were the most abundant metals, Cu_{Tot}, Cr_{Tot}, Mn_{Tot}, and Zn_{Tot} were in intermediate concentrations while Cd, Ni and Pb were in medium to very low concentrations below quantification limits.

Table 3-4 Summary for ANOVA and Post Hoc test results for metals between sites and station

	Significant						Non-significant		
Total	Fe	Cu	Cr	Ni	Cd	Al	Mn	Zn	Pb
df	4,87	4,87	4,87	4,67	4,49	4,87	4,87	4,87	4,70
F	3.01	6.73	5.41	4.62	2.851	4.88	2.00	0.72	0.70
P value	.022	.001	.01	0.02	0.033	0.01	0.1	0.53	0.59

df-Between sites and stations respectively

Regardless of such variation in concentration, after combining the stations, most total metals were found to be significantly correlated with one another (Table A-3). Strong positive correlations were found between Fe and Mn, and Al and Cu, and total Mn was significantly correlated with other metals except total Ni and Cr. Amorphous Fe and Mn hydroxides are good heavy metal scavengers, along with organic matter are predominant trace metal sorbents in aquatic systems (Shikazono et al., 2010)

3.4.3   Mn, Fe and other trace metals behaviour in along sabo dammed streams

3.4.3.1   Fe and Mn trend along sabo dammed stream
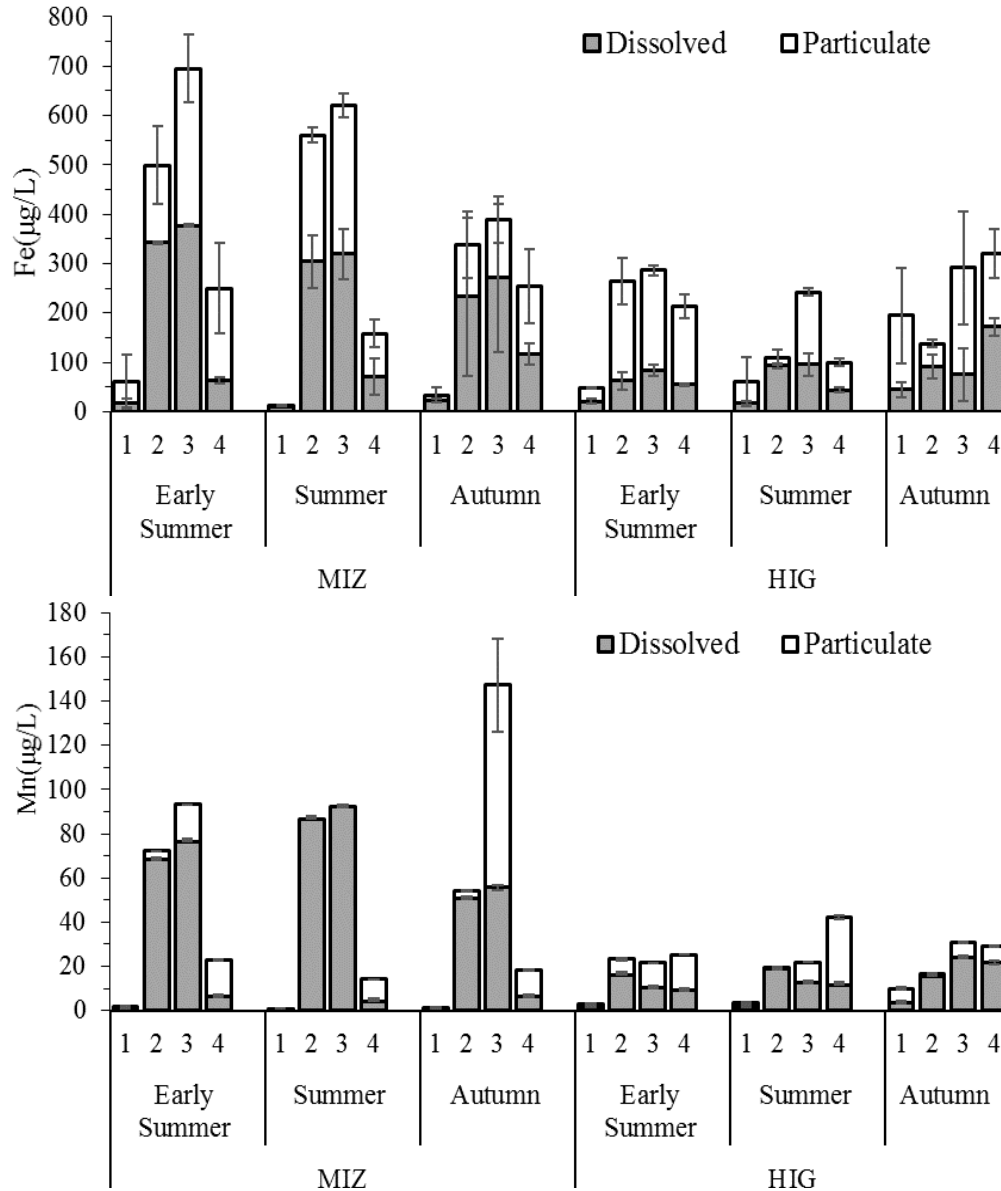
Figure 3-5 Fe and Mn trend along the stream for MIZ and HIG. Sampling months were grouped for seasonal comparison as; Early summer (June and July), summer (August) and autumn (September, October and November).

Both Mn_{Tot} and Fe_{Tot} were observed to increase around the stream (St 2 and St 3), this trend was observed throughout the sampling period except in autumn and early summer at HIG. Both Fe and Mn are redox sensitive element whose cycling between the various forms depends on the redox potential. The drastic increase in concentration from St.1 to St.2 (>70times) was

observed for both Mn and Fe at MIZ, St.2 and St.3 are separated by a dam wall but still showed variation in concentration. Implying both stations both reservoir creation and dam operation structure had an impact on Mn and Fe. At St.4 however, these station showed a different pattern with HIG having higher Mn concentration at St.4 while Fe decreased slightly in early summer and summer and increased slightly in autumn. Whereas MIZ concentrations for both Mn and Fe at St.4 were lower than st.3 concentration. Such a contrast observation may be contrast to a number of factors reflected in physicochemical properties Table 3-1.

3.4.3.2 Other trace metals
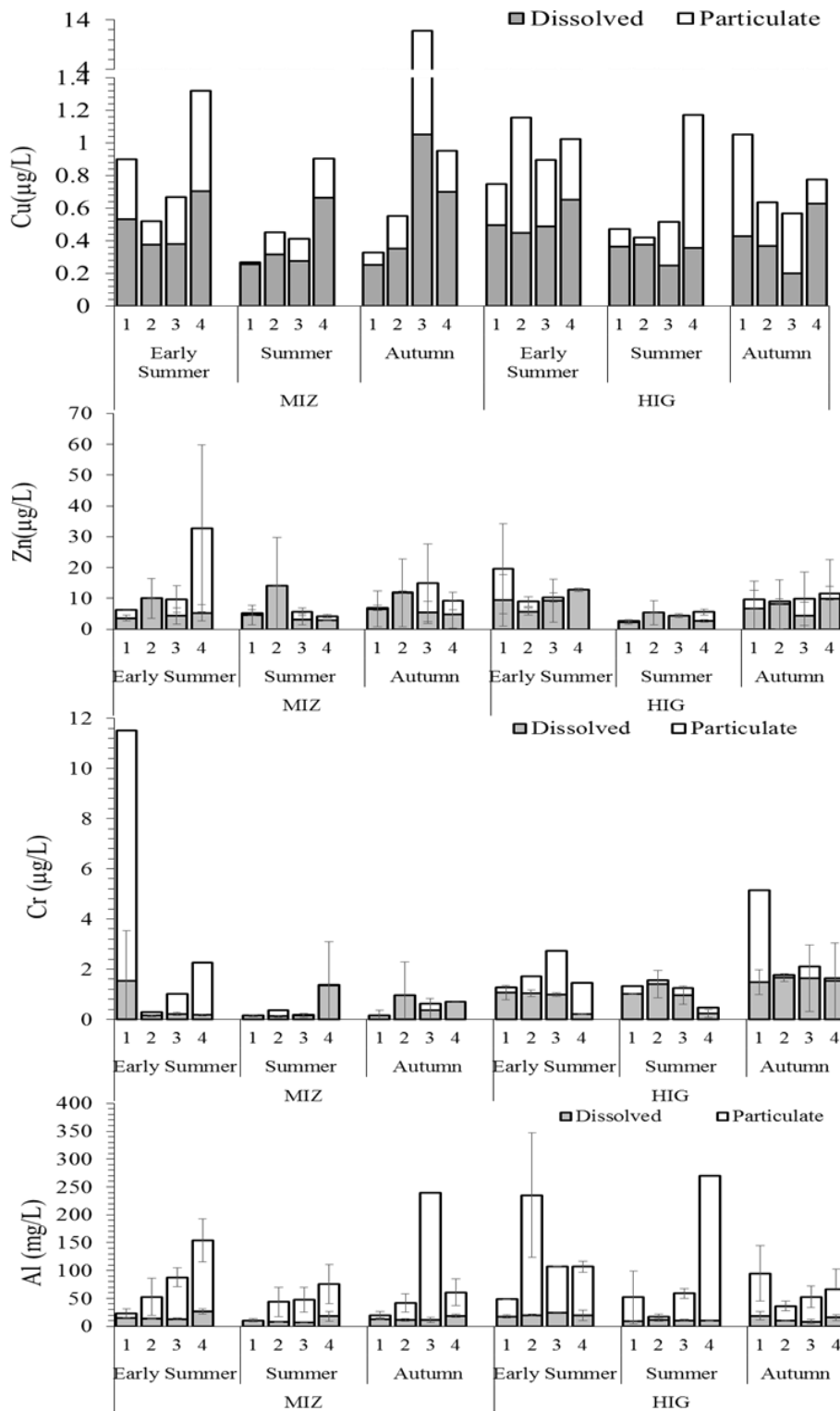
Figure 3-6 Cu, Zn, Cr and Al speciation at each sampling station for MIZ and HIG sites

Processes controlling the behavior of Fe, Mn and other trace are rather complex, in this study, Mn and Fe increase around the dams were evident Figure 3-5 as opposed to other metals Figure 3-6. In surface waters, metals are transported in suspended sediment undergoing various transformations, for example deposition and settling of the sorbed elements in suspended particles. In this study, Mn and Fe were observed to increase around the dams (Figure 3-5).

Mn and Fe remobilization from sediments has been observed in many studies such as Zhang et al., (2002), Canfield et al., (1993) in marine sediment and particularly to reservoirs, Mn remobilization from anaerobic sediments was covered by Beutel et al., (2008). The major source of trace metals in mountainous areas is weathering of rocks and atmospheric deposition. While Mn plays a significant role both biotically and abiotically in the behavior of metals, presence of other metals and prevailing environmental conditions significantly influence Mn redox kinetics (Krishnan et al., 2009). In this study, upstream site (St.1) was found to have the lowest concentration of trace metals (both dissolved and particulate for Mn, Fe, Zn, Al) for most of the sites which is reflected in the low EC observed at this station (Mohiuddin et al., 2012). Low metal concentration in upper reach of the river are consistent with results in Karbassi et al., (2008) who also observed very little variation in Cd.

Changes in water quality variables have been found to be concomitant with land use (Bahar et al., 2008).With respect to Fe, Mn and other trace metals, these exhibit complex behavior both spatially and temporal as observed from concentration changed in Fisher Creek (Gammons et al., 2004). The behavior of Mn and Fe around the dam (Figure 3-5) in which high increase in Mn concentration both total and dissolved is related to the observed ORP and pH. In the all the studied sites, average ORP around the dams (St.1 and St 2) ranged from 165$\pm$75 to 294$\pm$7 mV whereas average pH varied from 6.4$\pm$0.3 to 7.3$\pm$0.3. Notable changes in both Fe and Mn concentrations were evident around the dams while MIZ showed relatively higher concentration of both metals. Although all the studied sites have sabo dams with similar operation process, the status in the dam reservoir around MIZ can be described as more of hydric soils and a large section has transformed to a wetland. Such conditions around the dam boost the occurrence of an organic rich zone around the dams which leads to greater redox reactivity (Kedioreka et al., 2008).

The impact of sabo dams on both Mn and Fe is evident with increased concentrations mid-stream at St.2 and St.3, as opposed to observation in streams without sabo dams such as the fisher creek where total Fe load decreased with distance as Fe was precipitated and lost to the streambed (Gammons et al., 2004). Presence of dams on river not only affect biogeochemical cycle but also influence ecosystem communities for example the reach below the dam was found to have high amounts of zooplankton and benthic fine particulate organic matter, while the tributaries had more sandy material and the reach below the confluence exhibited physical characteristics that resembled both reaches of tributary and below the dam (Takao et al., 2008).

Zhang et al., (2002) and Fones et al., (2004) using diffusive gradient in thin films technique elaborated on Mn diffusion from anaerobic regions to oxic regions as the main reason for increased Mn in the surface water. It was found that Mn in anaerobic environment was coupled with other trace metals Co and Zn. However, the vertical profiles for both Mn and Fe accumulation below the sediments varied showing concentration fluctuation for these two metals at different depths. Mn and Fe transformation within anoxic region and in oxidizing environments rely on process factors like redox, sorption, precipitation and dissolution reactions (Tebo et al., 2005). An important factor in the trace metal behavior is redox potential (ORP) which determines the extent of oxidation reduction reactions that regulate the behavior of biogeochemical reactions in surface water. Environments with ORP below 300 mV have been characterized as anaerobic (Delaune and Reddy, 2005, Gancharuk et al., 2010), reduction of Mn oxhydroxides takes place within redox potential between 100 and 200 mV at pH 7 (Delaune and Reddy, 2005). Furthermore, re-precipitation of the mobilized iron at redox interfaces results into enrichment of reactive iron phases at the surface (Riedel et al., 2013).

In addition, lower velocity and water retention in the dams influences contact time and reductive dissolution. According to Kediorek et al., (2008) a lower water velocity will favor manganese dissolution especially in reservoirs however, stream flow changes may have negligible impact on iron concentrations (Gammons et al., 2003). In a study on diel changes of trace metals in Fisher creek, fivefold increase in stream flow only accounted for less than a quarter of the concentration decrease implying Fe fluctuation were independent of the stream flow. However, transportation of other trace metals may be affected especially during storms due to heavy sediment loads.

3.4.4 Principal component analysis results

In order to understand how the studied stations were related and which metals influenced the characteristics of each station, PCA analysis and hierarchical analysis were used to classify and the stations. PCA performed on log transformed data revealed four principal components (PCs) (Table 3-5) which explained 74.7% of the total variance. Correlations with the first PCs accounting for 32.3% of the total variance were strong with Fe, Al and Mn (loading >0.7) while Cr and Ni were correlated with the second PC accounting for 17.3%. Cu was moderately correlated to 2nd PC and the remaining two metals Pb and Cd correlated well with the fourth component. On the other hand, DOC and C:N ratio were correlated with PC 3 which accounted for 14.7%.

Table 3-5 PCA loading with varimax rotation

	1	2	3	4
Cu	.584	.606	.261	.017
Fe	.937	.045	.024	.093
Cr	.111	.841	-.188	.052
Mn	.897	-.116	.055	.017
Ni	-.010	.736	.154	.433
Zn	.412	.354	.048	.356
Pb	.093	.073	-.252	.833
Cd	.031	.110	.134	.899
Al	.743	.496	.094	.043
DOC	.147	-.178	.835	-.041
C:N	.069	.122	.930	.004
DON	.039	-.466	-.515	.035
Total	3.874	2.076	1.768	1.248
% of Variance	**32.285**	**17.301**	**14.730**	10.403
Cumulative %	32.285	49.587	64.317	74.720

Extraction Method: Principal Component Analysis.   Rotation Method: Varimax with Kaiser normalization.

Since some metals had dissolved metals concentration below quantification limit, total metals were used in both PCA and classical analysis.

Classification of the station using hierarchical cluster analysis portioned the stations into three clusters (Figure 3-7) although such an observation was not evident from PCA loadings (Figure A-1). The first cluster comprised mainly of St.2 and St.1 except for MIZ st.2 and HIG St.1 and 9 of the studied stations belonged to this cluster. Cluster two was only made up of two stations HIG St.1 and MNK St.3. Five sites in cluster three included HIG St.3, MNK St.4, MIZ St.2, MIZ St.3 and HIG St.4. Of all the studies sites, KSW concentrations were relatively high considered to other sites (Anova results for Fe 0) while concentrations at IMO were very low compared to other site (Post Hoc Figure 3-3). IMO site was excluded from cluster analysis, may have been influenced by sites and seasons. All stations from KSW were classified in cluster one together with MNK St 2 and 1, HIG St.2 and MIZ St.2 and St.4. No portioning on these station showed clusters based on station location implying either total metal concentrations DOC and DON alone could not be explain the differences between the stations. Other underlying factors such as land use characteristics, erosion rates and geographical locations may play a role in identification and linking of sampling sites. Metals affect water quality, combined with other environmental factors may be used to relate and discern sites from each other. From Figure 3-7, the observed clusters are
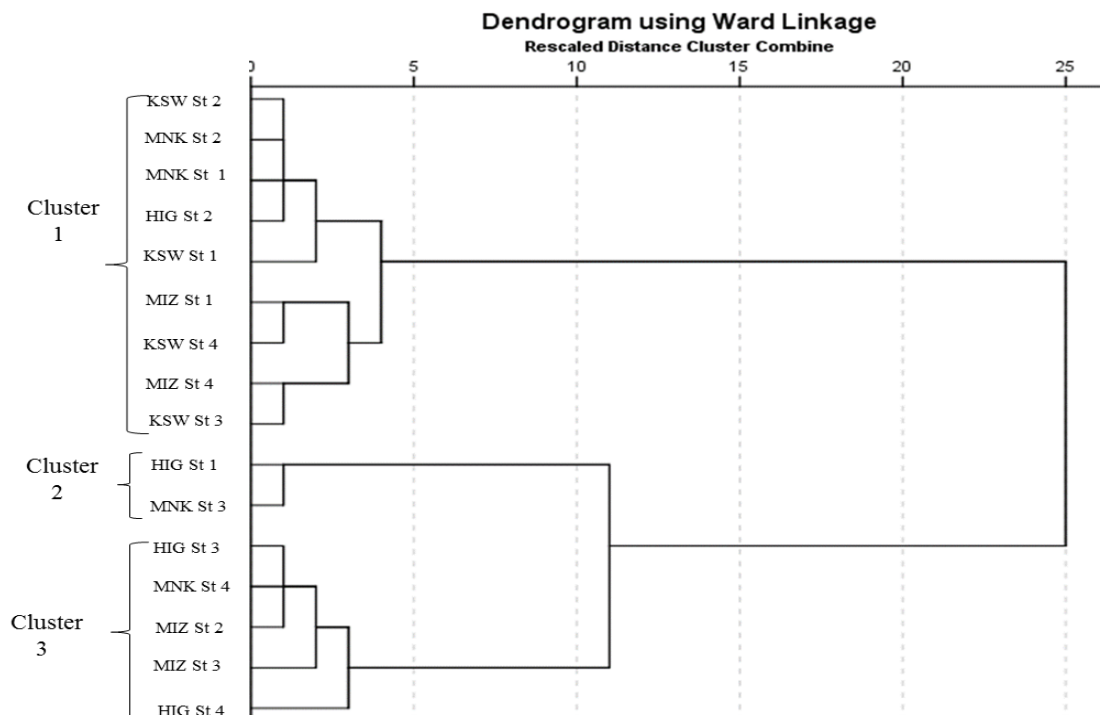
Figure 3-7 Clusters tree of sites from hierarchical clustering using wards method based on total metal concentrations

related to Figure 3-5 and Figure 3-6. Cluster 3 which comprises mainly of sites with high Fe and Mn concentrations ie HIG St.3 and St.4, MNK St.4, and MIZ St.2 and St.3.

3.5　　　Summary of study results.

In the sections dam were found to impact on redox sensitive metals (Fe and Mn) as expected. However, the extended to impact varied with location, with respect to Mn and Fe concentrations, MIZ was found to be largely impacted by the dams as opposed to HIG. At HIG, high concentrations were observed downstream at St.4. KSW site had significantly higher metal concentration as opposed to others studies, however, using hierarchical clustering, characteristics downstream and upstream had resemblance with other station. Three cluster linking stations in all the sites were independent of sites.

References

Bahar MM, Ohmori H, Yamamuro M (2008) Relationship between river water quality and land use in a small river basin running through the urbanizing area of Central Japan Limnology 9:19-26 doi:10.1007/s10201-007-0227-z

Canfield, D.E., Thandrup, B. and Hansen, J.W., 1993. The anaerobic degradation of organic matter in Danish coastal sediments: iron reduction, manganese reduction and sulphate reduction. Geochemica et cosmochemica Acta, 57, 3867-3883.

Driscoll TC, Otton KJ, Iverfeldt Ake (1994) Biogeochemistry of small catchments;　A tool for environmental research. B.Moldan and J.Cerny In eds John Wiley and Sons Ltd

Delaune RD and Reddy KR (2005). Redox potential. Encylopedia of soils in the environment, elsevier science, Oxford, Uk.

Fremion F, Bordas F, Mourier B, Lenain JF, Kestens T, Courtin-Nomade A (2016) Influence of dams on sediment continuity: A study case of a natural metallic contamination The Science of the total environment 547:282-294 doi:10.1016/j.scitotenv.2016.01.023

Gammons CH, Nimick DA, Parker SR, Cleasby TE, McCleskey RB (2005) Diel behavior of iron and other heavy metals in a mountain stream with acidic to neutral pH: Fisher Creek, Montana, USA Geochimica et Cosmochimica Acta 69:2505-2516 doi:10.1016/j.gca.2004.11.020

Han S, Naito W, Hanai Y, Masunaga S (2013) Evaluation of trace metals bioavailability in Japanese river waters using DGT and a chemical equilibrium model Water research 47:4880-4892 doi:10.1016/j.watres.2013.05.025

Karbassi AR, Monavari SM, Nabi Bidhendi GR, Nouri J, Nematpour K (2008) Metal pollution assessment of sediment and water in the Shur River Environmental monitoring and assessment 147:107-116 doi:10.1007/s10661-007-0102-8

Kondo Y, Obata H, Hioki N, Ooki A, Nishino S, Kikuchi T, Kuma K (2016) Transport of trace metals (Mn, Fe, Ni, Zn and Cd) in the western Arctic Ocean (Chukchi Sea and Canada Basin) in late summer 2012 Deep Sea Research Part I: Oceanographic Research Papers 116:236-252 doi:10.1016/j.dsr.2016.08.010

Krishnan KP, Sinha RK, Krishna K, Nair S, Singh SM (2009) Microbially mediated redox transformations of manganese (II) along with some other trace elements: a study from Antarctic lakes Polar Biology 32:1765-1778 doi:10.1007/s00300-009-0676-4

McClain ME et al. (2003) Biogeochemical Hot Spots and Hot Moments at the Interface of Terrestrial and Aquatic Ecosystems Ecosystems 6:301-312 doi:10.1007/s10021-003-0161-9

Mohiuddin KM, Otomo K, Ogawa Y, Shikazono N (2012) Seasonal and spatial distribution of trace elements in the water and sediments of the Tsurumi river in Japan Environmental monitoring and assessment 184:265-279 doi:10.1007/s10661-011-1966-1

Riedel T, Zak D, Biester H, Dittmar T (2013) Iron traps terrestrially derived dissolved organic matter at redox interfaces Proceedings of the National Academy of Sciences of the United States of America 110:10101-10105 doi:10.1073/pnas.1221487110

Shikazono N, Tatewaki K, Mohiuddin KM, Nakano T, Zakir HM (2012) Sources, spatial variation, and speciation of heavy metals in sediments of the Tamagawa River in Central Japan Environmental geochemistry and health 34 Suppl 1:13-26 doi:10.1007/s10653-011-9409-z

Shrestha S, Kazama F (2007) Assessment of surface water quality using multivariate statistical techniques: A case study of the Fuji river basin, Japan Environmental Modelling & Software 22:464-475 doi:10.1016/j.envsoft.2006.02.001

Takao A, Kawaguchi Y, Minagawa T, Kayaba Y, Morimoto Y (2008) The relationships between benthic macroinvertebrates and biotic and abiotic environmental characteristics downstream of the Yahagi Dam, Central Japan, and the State Change Caused by inflow from a Tributary River Research and Applications 24:580-597 doi:10.1002/rra.1135

Tebo BM, Johnson HA, McCarthy JK, Templeton AS (2005) Geomicrobiology of manganese(II) oxidation Trends Microbiol 13:421-428 doi:10.1016/j.tim.2005.07.009

Tribovillard N, Algeo TJ, Lyons T, Riboulleau A (2006) Trace metals as paleoredox and paleoproductivity proxies: An update Chemical Geology 232:12-32 doi:10.1016/j.chemgeo.2006.02.012

Varol M, Gökot B, Bekleyen A, Şen B (2012) Spatial and temporal variations in surface water quality of the dam reservoirs in the Tigris River basin, Turkey Catena 92:11-21 doi:10.1016/j.catena.2011.11.013

Warren LA, Haack EA (2001) Biogeochemical controls on metal behaviour in freshwater environments Earth-Science Reviews 54:261-320 doi:10.1016/s0012-8252(01)00032-0

Wildi W (2010) Environmental hazards of dams and reservoirs. NEAR Curriculum in Natural Environmental Science, Terre et Environnement, 88, 187–197Fones GR, Davison W, Hamilton-Taylor J (2004) The fine-scale remobilization of metals in the surface sediment of the North-East Atlantic Continental Shelf Research 24:1485-1504 doi:10.1016/j.csr.2004.05.007

Zhang, H., et al., 2002. Localised remobilization of metals in a marine sediment. Science of the Total Environment, 296(1), pp.175-187.

4   Dissolved organic matter composition along sabo dammed mountainous streams

4.1   Introduction

Dissolved organic matter (DOM) has been described as a heterogeneous continuum of high-to-low-molecular-weight species (Aiken et al., 2011; Sazawa et al., 2011), whose diverse properties depend on the source and digenetic state. DOM is present in all natural water systems originating from either terrestrial or aquatic environments (Helms et al., 2008). At any given time, dissolved organic carbon (DOC), which represents the amount and quality of DOM, is related to the nature of the watershed, seasonal variations, and inputs like runoff, influenced by hydrological pathway, sorption, and microbial processes (Leenher and Croué, 2003; Inamdar et al., 2011a). Organic matter (OM) in streams is a basis for the food web, serving as a primary food source for heterotrophic microbes in the form of organic carbon. However, in nutrient-rich ecosystems, organic carbon can also limit microbial-mediated heterotrophic nutrient uptake (Hotchkiss et al., 2014). DOM comprises a mixture of aromatic and aliphatic hydrocarbon structure attached to a wide range of functional groups such as amines, carboxyls, hydroxyls, and ketones (Leenher and Croué, 2003). DOM content along the flow path includes hydrophilic and hydrophobic fractions whose composition changes along the hydrological pathway (Inamdar et al., 2011a). The DOM fraction that absorbs light in the ultraviolet and visible wavelength regions is referred to as chromophoric or colored dissolved organic matter (CDOM) (Twardowski et al., 2004; Coble, 2007; Leech et al., 2016; Wen et al., 2016). CDOM is responsible for the optical properties of most natural water bodies (Helms et al., 2008) and plays a key role in shielding the biota from harmful UV irradiation and in attenuation of the photosynthetically available irradiation (Wen et al., 2016; Lennon et al., 2013; Coble, 2007). Furthermore, DOM, in particular, CDOM affects the fate and transport of many organic and inorganic chemicals, nutrient cycles, and metal speciation and solubility (Leech et al., 2016; Chen et al., 2002; Tfaily, 2011). Modification of DOM occurs as its components age through adsorbing onto particles, bacterial degradation, precipitation, and photodegradation. DOM composition may differ with regard to mobility, degradability, and bioavailability (Inamdar et al., 2011a). DOM alterations due to different processes like photolysis, photobleaching, sorption, and microbial consumption (Inamdar et al., 2011a) are controlled by hydrological flow paths (Hood et al., 2006). Spatial and temporal changes in CDOM quantity and quality are important ecological and environmental features (Leech et al., 2016). Moreover, the strong catchment link between CDOM and DOM

51

suggests that CDOM can be used for DOM monitoring (Asmala et al., 2014). Therefore, understanding DOM characteristics is important for determining the reactions, processes, and mechanisms responsible for the proper functioning of the whole ecosystem (Chen et al., 2002).

In most parts of Japan, sabo dams (Chanson, 2004) have been used in mountainous areas to prevent the impact of natural disasters (Marutani et al., 2008; Mizuyama, 2008). These structures operate in various ways reported by Chanson (2004) and affect the behavior of elements such as carbon, phosphorous, and various trace metals. Creation of areas with either higher reaction rates than the surrounding environments or short periods with relatively higher reaction rates than longer time periods (McClain et al., 2003), impacts not only trace metal concentrations (Praise et al., 2016) but also the DOM behavior. Since riverine DOM export is the largest provider of the reduced carbon from terrestrial sources to oceans at a rate of 0.25 PgCyr^{-1} (Spencer et al. 2012), changes in residence time and hydrological regime, and the reduction in turbulence (Friedl and Wüest, 2002) due to impoundments influences DOM export subsequently modifying downstream areas. Previous studies reported changes in DOM reactivity in boreal rivers between upstream and pool water samples in a riverine environment with beaver impoundments (Catalán et al., 2016). DOM in upstream samples had a small percentage of compounds that disappeared quickly and a very large composition of slowly degrading compounds, while beaver pond samples had a higher proportion of biodegradable components. Globally, residence time increases three times for 16–47 days due to dams (Friedl and Wüest, 2002); water impoundments disrupt biogeochemical cycles and cause changes, which may trigger more adverse effects. Complex DOM tendencies in mountainous catchments combined with variations in flow paths during storms and dry seasons (Vidon et al., 2008) may further enhance the effect of dam on DOM behavior and the whole catchment. Using DOM quality data, catchments can be discerned to provide differences and similarities distinct to the studied area (Jaffé et al., 2012) revealing the processes that control the DOM export. Alteration of DOM is important in ecosystem functioning. Closed sabo dams create reservoirs and redox zones, and operate differently from other dams as discussed by Chanson (2004). Hence, the DOM quality and behavior in sabo-dammed streams is different from free-flowing rivers and other dams like hydropower dams.

Characteristics of DOM fractions can be determined by ultraviolet-visible (UV-vis) spectroscopy using CDOM parameters. CDOM holds a great potential for assessing the DOM

composition, features of the UV-vis spectral slope are useful in understanding the DOM composition and modifications from the flux of constituents that occur across a broad range of freshwater ecosystems (Spencer et al., 2012). Using different wavelength ratios from the absorption spectra, alterations in CDOM due to various processes such as biological production and degradation, and photobleaching can be identified (Twardowski et al., 2004). In this study, we used previously reported CDOM properties; absorption at 250 nm to 365 nm (E2:E3) (Uyguner and Bekbolet 2005; Helms et al,. 2008; Chen et al., 2002; Wen et al. ,2016), spectral slope ratio (S_R) and slope$_{275-295}$ (Helms et al., 2008), specific UV absorbance (SUVA$_{254}$ in Lmg^{-1}m^{-1}) (Weishaar et al., 2003), and absorbance coeffient at 350 (a350) (Moran et al., 2000), summarized in Table 1 together with excitation emission matrix fluorescence and parallel factor analysis (EEM-PARAFAC) to study DOM properties in mountainous streams with sabo dams. Fluorescence spectroscopy is useful in tracing and determining the dynamics of DOM (Stedmon and Bro, 2008) based on the part of CDOM that is fluorescent (FDOM) since not all CDOM is fluorescent (Coble, 2007). Excitation emission fluorescence matrix (EEM) data gives detailed information on the chemical composition based on the fluorophores present (Coble, 2007). Combined with parallel factor analysis (PARAFAC), EEMs are decomposed and characterized into underlying individual signals enabling the quantification of the changes and tracking of DOM in the environment (Stedmon and Bro, 2008).

The objective of this study was to evaluate the impact of sabo dams on DOM characteristics in headwater streams. DOM characteristics were assessed based on its optical properties (Table 4-1) and major components identified using EEM-PARAFAC at different sections of the stream to show the behavior and composition of DOM along the path flow.

Table 4-1 CDOM properties used for characterization of DOM composition

CDOM optical indicator	Definition and significance	Source
Specific UV absorbance (SUVA$_{254}$) (Lmg^{-1}m^{-1})	UV absorbance at 254 nm divided by DOC concentration in mg L^{-1}; is used as a measure of aromaticity, SUVA$_{254}$ values increase with increasing aromatic content	(Weishaar et al., 2003)
E2:E3 ratio	Absorption coefficient at 250 nm (m^{-1}) divided by absorption coefficient at 350 nm (m^{-1}); E2:E3 ratio decreases with increasing molecular size	(Chen et al., 2002)
Spectra slope ratio (S$_R$)	The ratio of spectral slopes between shorter UV wavelength region 275-295 nm to than of longer UV wavelength 350-400 nm. Is used as a proxy for molecular weight, photo-degradability and DOM source; S$_R$ decreases as molecular weight increases	(Helms et al. 2008) (Spencer et al., 2012)
Slope$_{275-295}$ (nm^{-1})	Spectral slope in the shorter wavelength region (275-295 nm). Can be used for molecular weight. A decrease in the slope indicates increase in increase in molecular weight	(Helms et al., 2008)
Absorbance at 350 (a350 (m^{-1})	Absorption coefficient at 350 nm (m^{-1}) and is used as a proxy for CDOM concentration	(Moran et al., 2000)

4.2   Materials and methods

4.2.1   Study area and sample collection

In this study, we assessed DOM along the gradient of two mountainous streams in Yamagata, Japan (Figure 3-1). These streams, namely Mizunashi (MIZ) and Higashiiwamotogawa (HIG),

are located within the Akagawa basin and cover an area of 15.1 km^2 and 6.2 km^2, respectively (Figure 4-1). The two streams are located in a mountainous area with an elevation range of 100-1,000 m. The surrounding environment changes along the gradient, the upper section of the two streams (location of St.1-St.3) is covered with forests and dominated by evergreen needle leaf trees (*Cryptomeria japonica*) while the downstream towards the confluence has some paddy fields and infrastructure including roads and commercial and residential buildings up to the confluence with Akagawa river (St.4). Water is drawn for irrigation from the downstream after St.3 during the farming season.
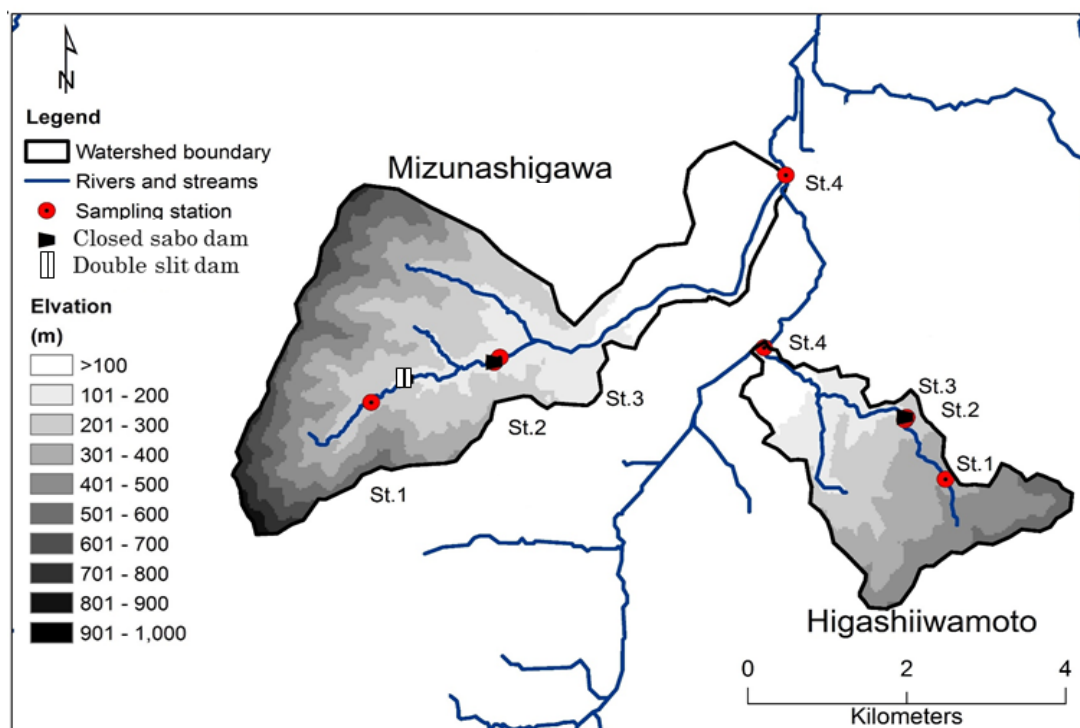
Figure 4-1 Elevation range of the two sites Higashiiwamotogawa and Mizunashi, and sampling station, and sabo dam at each site. St.2 and St.3 are located in the dam reservoir and right after the dam, respectively.

Sixty two samples collected monthly and bimonthly in August and November 2015(Table A-1) from two sites HIG and MIZ (Figure 3-1). Samples for DOC analysis were collected in 40ml glass vails that had also been previously cleaned and dried in a dissector. Syringe filtration was done on site using polycarbonate filters (0.45 µm) for metal samples while 0.45 µm polyethersulfone filters were used for DOC samples after rinsing the filters with 500ml distilled water and stream water before collection as recommended by Tanju (2003) The samples

were transported to the laboratory in a cooler box Sample analysis and data acquisition

4.2.2 Ultraviolent visible and fluorescence spectroscopy

4.2.2.1 DOC and UV-Vis parameters

In the laboratory, samples for DOM were immediately (less than 48 hours after sampling) analyzed for DOC while samples for the EEM analysis were immediately frozen at -25°C in the laboratory until the time of analysis. DOC measurement as non-purgeable organic carbon was carried out using high temperature catalytic oxidation method with TOC analyzer (TOC-L, Shimadzu). The Shimadzu TOC-L series was fitted with a TN analyzer for measurement TN and DON, TOC-L series analyzer operation is based on combustion catalytic oxidation at 680°C. During analysis, 150µl of sample injected in the analyzer was acidified with 1.5% of 1M HCl and sparged to remove dissolved inorganic carbon. The samples were then injected to the combustion chamber at 680°C packed with platinum coated beads as a catalyst. Carbon dioxide generated from the oxidation of DOC compounds was detected as non-purge able organic carbon by the non-dispersive infrared detector. Although the machine is equipped with back ground calibration for measurement, a calibration curve was prepared using TOC standard each time of analysis for concentration determination.

4.2.2.2 CDOM measurement and data acquisition

In this study, both ultraviolent visible (UV-vis) absorbance and fluorescence spectrophotometry were employed in measurement of DOM characteristics. Spectrophotometry includes any technique that uses light to measure chemical concentrations. The principle governing spectroscopy is when a molecule absorbs a photon of light, the molecule goes to an energetic excited state promoting electron transition from one molecular orbit to another with a concomitant increase or decrease in molecular energy.

4.2.2.3 Principle of UV-vis spectrophotometer

Uv-vis spectroscopy uses beer's law to measure absorbance. Absorbance is important because according to beer's law, it is directly proportional to the concentration C of the light absorbing species in the sample (D.C Harris, 8th edition).

$$A = \varepsilon bc;$$

where; c is the concentration of the sample in moles per litre (molL^{-1}), b is path length commonly expressed in cm,   and ε is the molar absorptivity M^{-1}cm^{-1}. Samples contain chromophores which are described as a functional group not conjugated with another group that exhibits characteristic absorption spectrum in the ultraviolet or visible region. Molecules or ions exhibit absorption in

the visible or ultra violet region when there is electronic transition within its structure due radiation. The absorption of light in the UV-vis region promotes electron from their ground state to different orbitals. This transmission in electronic state may be to higher energy, excited state orbital or antibonding orbitals from σ (bonding) molecular, π (bonding) molecular orbitals and η (non- bonding) to either σ^* or π^* (Thermospectronic, n.d).

The significant part of DOM known as Chromophoric or coloured dissolved organic matter (CDOM) is an optical active component which control optical properties of water, initiate biochemical and photochemical processes. In this study, a shimadzu 1800 UV spectrophotometer which features a halogen lamp, a monochromotor for selection of wavelength and a photomultiplier was used for CDOM analysis. Before analysis, the spectrophotometer was warmed for 30 minutes and samples were brought to room temperature (20°C). Absorbance measurement were carried out as detailed in Section 4.2.2.4 below

4.2.2.4 CDOM optical properties data

UV-visible absorption spectra from 200 nm to 800 nm were obtained for each sample by measuring the samples by Shimadzu UV-vis 1800 scanning spectrophotometer using 1 cm quartz cuvettes. The measured spectra were corrected using ultrapure water measured as blank. All spectra were measured under the spectrum mode three times and reported here as averages. Both UV-vis measurement and DOC analysis were carried out within 48 hours of sample collection.

S_R was calculated from spectral slopes of the natural log absorbance of 275-295 nm wavelength range ($S_{275-295}$) and 350-400 nm wavelength range ($S_{350-450}$). $S_{275-295}$ and $S_{350-450}$ were determined by applying a linear fit to the natural log-transformed absorbance data for each slope (Helms et al., 2008; Leech et al., 2016). Information provided by these slopes can be related to the source, structure, and digenesis (Jaffé et al., 2008; Leech et al., 2016), and processes such as photobleaching, microbial degradation, and lateral transport (Yamashita et al. 2013). $S_{275-295}$ works as a proxy for molecular weight and a decrease in slope indicates an increase in molecular weight. Slope values are negative but were presented as absolute values (Harvey et al., 2015; Helms et al., 2008). The use of S_R is advantageous over using the whole slope since it avoids the use of spectral data near detection limit of the instrument (Cory et al., 2010), and focuses on the absorbance ranges known to shift dramatically as a function of DOM source, quality, and diagenesis (Helms et al., 2008). Spectral correction involved subtraction of the average

absorbance of the wavelength between 700-800 nm with an assumption that absorbance in this range is zero to correct for the baseline drift, temperature scattering, and refractive effects. The conversion of absorbance to absorption coefficients was based on Coble (2007) as follows:

$$a_\lambda = 2.303 A_\lambda / L$$

where a=absorption coefficient (m^{-1}), λ=wavelength, A=Absorbance, and L=path length (m).

$SUVA_{254}$ ($Lmg^{-1}m^{-1}$) was determined by dividing the absorbance at 254 nm by cuvette path length (i.e. 0.01 m in this study) and then dividing it by DOC concentration (mg L^{-1}) (Weishaar et al., 2003).

Absorbance coefficient at 350 (a350) (Moran et al., 2000; Leech et al., 2016) was used to estimate the CDOM concentration and the proxy of CDOM (Harvey et al. 2015; Rüegg et al. 2015). a350 has successfully been used by other researchers. Obernosterer and Benner (2004) studied the effects of irradiation on optical properties of DOM and attributed indirectly 50% and 17% of the loss in a350 for black swamp and riverine water samples to photo-induced precipitation during photodegradation.

4.2.3   Excitation emission fluorescence spectroscopy and PARAFAC analysis

Both fluorescence and phosphorescence are luminescence processes used to describe light emission from electronically excited states of any substances (Lokowicz, 1999). These photon emission processes occur during molecular relaxation from electronic excited states and involves transitions between electronic and vibrational states of polyatomic fluorescent molecules   (So and Dong, 2002). Fluorophores exist in a number of vibrational energy levels in singlet electronic states S0, S1 and S2. Once a fluorophore absorbs light, it is excited to a higher energy from S0 to either S1 or S2. The fluorophore may rapidly relax to lowest vibrational level of the excited state (S1) (internal conversion) and remains in this state for a period on the order of nanoseconds, which is the fluorescence life time. (Lokawicz, 1999; So and Dong, 2002). Return to the ground state occurs rapidly by emission of a photon that is; fluorescence occurs as fluorophore decays from singlet electronic excited states to higher vibrational ground state level (So and Dong, 2002). Fluorescence spectra reflect fluorophores in vibrational levels in the ground and excited electronic states respectively. On the other hand, molecules in the S1 state can undergo a spin conversion to first triplet state. Conversion from S1 to T1 is intersystem crossing

and phosphorescence is from T1 emission.

4.2.3.1   EEM and PARAFAC analysis

Using fluorescence spectroscopy, fluorescence signal recorded as excitation emission matrices (EEMs) are obtained from a combination of emission and excitation wavelength measurement (Stedmon and Bro, 2008). EEMs represent fluorescence contour maps containing highly detailed information that are analyzed based on maximum intensity identified as excitation emission pairs (Table 4-2). This method has several advantages including rapid analysis and only requiring a small volume of sample typically about 3–4 mL (Carstea, 2012)

Table 4-2 previously reported description of fluorescence bands and position of excitation emission peaks

Flourephore[a]	Flourephore[b]	Excitaion (nm)	Emission (nm)	Description
C	5	300-370	400-500	Humic-like[a,b], ubiquitously observed humic substances thought to be associated with terrestrial sources[c]
M	3	310-320	380-400	Autochthonous production, associated with biological production of humic substances in fresh water and marine systems[c]
A	1	237-260	400-500	Humic like, terrestrial humic-like
T	4	225-237	340-381	Protein like; Amino acid like[c]; Tryptophan like[a,b,c]
		275	340	
B	6	225-237	309-321	Protein like, Amino acid like[c],Tyrosine like
		275	310	

[a]Coble, 1996 cite in Hudson et al., (2007), [b]Stedmon and Markager (2005),[c]Cory and Kaplan (2012)

Although EEMs provide wealth DOM information, this information may present difficulties in its interpretation (Stedmon and bro, 2008). Because of the difficulties associated with individual fluorescent compounds identification, the groups of fluorophores are commonly named as humic like, fulvic like and protein like (Carstea, 2012). Various methods such as visual identification of peaks and ratios and multivariate analysis and sometimes a combination of both (McKnight et al., 2001). In addition, parallel factor analysis (PARAFAC), has the capacity to decompose fluorescence signals to reveal the underling fluorescent details and has been used to track DOM in various aquatic environments.

The EEMs with PARAFAC analysis has been extensively applied in characterization and monitoring of fluorophores in dissolved organic matter (DOM) of wastewater (Sheng and Yu; 2006; Wang et al., 2009; Murphy et al., 2011), freshwater and urbanized streams (Baker et al., 2003; Hua et al., 2007;Hong et al., 2009; Yao et al., 2011; Yuan et al., 2014; Zhang et al., 2011; Hosen et al., 2014; Nie et al., 2016; Cui et al., 2016; Stubbins et al., 2014), oceanic environments (Coble 1996; Yamashita et al. 2010) and in soil (Zsolnay et al., 1999; Guigue et al., 2014). During PARAFAC analysis, EEMs are modeled according to equation 4-1;

$$x_{ijk} = \sum_{f=1}^{F} a_{if} b_{jf} c_{kf} + \varepsilon_{ijk}$$

(4-1)

Where; X_{ijk} is one of the three way data array with dimensions *I,J, and K*. X_{ijk} is the fluorescence intensity of sample *i* measured at emission wavelength *j* and excitation wavelength *k* and ε_{ijk} are residuals containing noises and other un-modeled variation. a_{if} is directly proportional to the concentration of the *f*th analyte in the *i*th sample, b_{jf} is linearly related to the fluorescence quantum efficiency of *f*th analyte at emission wavelength *j*, and c_{kf} is linearly proportional to the specific absorption coefficient at wavelength *k* (Stedmon and bro, 2008; Murphy et al., 2013; Stedmon and Markarger 2005). Data treatment and PARAFAC modeling procedure included outlier analysis, model fitting and validation and interpretation (A4).

4.2.3.2   EEM acquisition

Samples were thawed at 4°C for 24 hours, then left to warm to room temperature (20°C) before EEM measurements. EEM were measured using FP-8300 spectrofluorometer (Jasco). The

excitation wavelength (λ_{Ex}) ranged from 200-500 nm at 5 nm intervals, and emission wavelength (λ_{Em}) ranged from 210-600 nm at 2 nm intervals with a scanning speed of 1,000 nm/min at integration time of 0.2 seconds. Machine-specific spectral correction using rhodamine B was applied according to the manufacturer's recommendation. The measured EEM spectra were further processed in MATLAB 8.5 using the N-way Toolbox, to correct for inner filter and Raman scattering effects using the absorbance data and by subtracting blank EEM collected using Milli-Q (18.1 MΩ at 25°C), respectively. The EEMs were then normalized to Raman units using the area under the curve of water Raman peak at 350 nm excitation wavelength for freshly collected Milli-Q water (Cory and McKnight, 2005; Cory et al., 2010; Lowaezk and Stedmon, 2009). All EEM samples were analyzed at 20°C using newly collected ultrapure water for the baseline correction at slit widths of 5 nm for both emission and excitation, and photomultiplier tube voltage at 725 V.

Index parameters of fluorescence including the fluorescence index (FIX) (McKnight et al. 2001), humification index (HIX), and biological Index (BIX) (Birdwell and Engel 2010) were calculated from the resulting data. FIX values have been used to distinguish between CDOM from terrestrial and microbial sources (Birdwell and Engel, 2010). Previously, the ratio for the emission intensity at 450:500 nm following excitation at 370 λ_{Ex} nm was used for FIX calculations (McKnight et al., 2001; Lu et al., 2014), however a shift following spectral correction for inner filter effects and the instrument bias has been reported by several researchers (Jaffé et al., 2008). Hence, the intensity ratio for 470 to 520-nm emission wavelength at 370 nm excitation wavelength was used for the FIX calculation in this study. Although the relative contribution of CDOM sources cannot be differentiated, FIX values less than 1.4 indicate allochthonous DOM while values greater than 1.9 show autochthonous DOM (Sazawa et al., 2011). BIX assesses the contribution of autochthonous DOM to the observed values. Calculated as a ratio of emission intensity at 380-430 nm at 310 nm of excitation, BIX values between 0.8 to 1 indicate the presence of freshly produced DOM of biological or microbial origin (Birdwell and Engel 2010) while values below ~0.6 suggest allochthonous DOM (Sazawa et al., 2011). The age and recalcitrance of materials in natural systems can be identified based on the HIX values (Birdwell and Engel, 2010). Fresh plant-derived DOM has lower HIX values (<5) and HIX increases with decomposition.

4.2.3.3 PARAFAC analysis

EEM-PARAFAC analysis was conducted in MATLAB 8.5 (Math works Inc, USA) using drEEM in N-way Toolbox following the procedures described by Murphy et al. (2013). For PARAFAC modeling λ_{Em} at 290-600 nm and λ_{Ex} at 240-500 nm were used. Short wavelengths (<240 nm) for λ_{Ex} were excluded from the PARAFAC modeling. The PARAFAC procedure followed the details reported by Murphy et al. (2013) as summarized in Cui et al. (2016). PARAFAC has the ability to statistically decompose the EEM fluorescence data into individual fluorescence components (Stedmon and Bro, 2008), each representing strongly co-varying fluorophores or a single fluorophore with regard to their spectral shape (Cory and Kaplan, 2012; Stedmon et al., 2003). During the initial explanatory analysis, a total of 5 samples were excluded from the model fitting after being identified as outliers Appendix A-1. Three to four components were projected from the core consistency diagnostic results and all the fitted models had an explained variance above 99.2. Finally, only three components were validated by split-half analysis (Murphy et al. 2013). As the model output, maximum fluorescence intensity (Fmax) based on modeled PARAFAC component scores was obtained for all the samples.

4.3 Statistical analysis

Data sets were tested for normality (Shapiro-Wilk test) and for variables that failed normality tests non-parametric tests were used. Statistical analysis was performed by IBM SPSS 22. Paired t-tests and Wilcoxon tests were used for the analysis of data between stations.

4.4 Results and discussion

4.4.1 Physicochemical properties

The values of pH, EC, DO, temperature, turbidity and ORP recorded at the time of sampling are presented in Table 3-1. At site HIG, the ranges of average physicochemical properties were 7.3-7.5 pH units, 2.87-5.12 NTU, 8.43-9.31 mg L^{-1}, 258-286 mV, and 5.7-8.25 mS cm^{-1} for pH, turbidity, DO, ORP, and EC, respectively. Turbidity and ORP were slightly higher at St.2 than the other stations, while conductivity increased from upstream to downstream (St.1-St.4) (Table 2-1). At site MIZ, pH ranged from 6.8-7.8 with slightly higher values at St.4. Turbidity increased gradually at St 2 from 2.04 NTU to 3.44 NTU and remained relatively constant at St 3 (3.41 NTU). pH, EC, and turbidity within the forested area (St.1, St.2, and St.3) varied slightly between the stations. However, a significant increase was observed from 7.03 at

St.3 to 7.75 pH units at St.4, 5.9 to 23 mS.cm^{-1}, and 3.41 to 4.7 NTU for pH, EC, and turbidity, respectively. Low ORP values were recorded around the dam at St.2 and St.3 (189 mV at St.2 and 150 mV at St.3), and the lowest DO was recorded at MZ St.2. The slight increase in pH around the dam is an indicator of the dam having little to no impact on the pH of the water. The slight increase in EC around the dams and downstream (St.4) suggests increasing ionization of chemical species along the stream. High standard deviation for DO is a result of lower values recorded in August (Table A-4). ORP observations around the dam at MIZ can be attributed to the reduction of metal oxides. On the contrary, data for HIG around the dam did not reveal a strong link to reduction conditions.

4.4.2   DOM quantity along the stream

4.4.2.1   DOM concentration
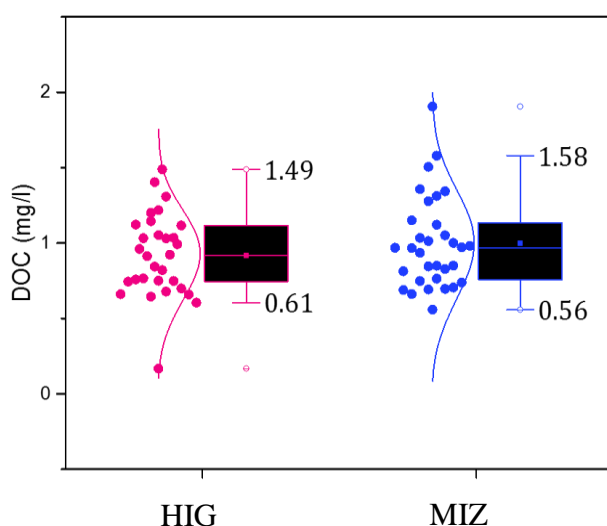
Figure 4-2 Boxplots for DOC concentration at MIZ and HIG. Open circles represent outliers while error bars show the standard deviations.

DOC concentrations ranging from 0.17 mg L^{-1} to 1.90 mg L^{-1} were recorded at two sites (Figure 4-2 and Figure 4-2a). The highest and lowest were recorded in July at MIZ St 4 and HIG St 1, respectively. At HIG, DOC ranged from 0.17-1.49 and the average recorded DOC concentration was 0.92±0.05 mg L^{-1} with the highest value observed in August (1.49 mg L^{-1} at St 1). At MIZ, DOC concentrations ranged from 0.56 mg L^{-1} to 1.9 mg L^{-1} with an average of 1.00±0.27. Average DOC observed at the two sites (MIZ and HIG) in all the samples was 0.97±0.03 mg L^{-1} with a median of 0.93 mg L^{-1}. DOC concentrations observed in this study (0.61-1.58 mg L^{-1}) are

within the range observed by Suzuki et al. (2014) and Sazawa et al. (2011) in Japanese rivers. However, this was still lower than the ranges reported by Imai et al. (2001) (1.45-3.28 mg L^{-1}) and much lower than that ranges reported by Mostofa et al. (2005). DOC concentrations did not vary significantly between the two sites (MIZ and HIG) ($p > 0.05$), but significant changes were noted between St.1 and St.4, and St.4 and St.2 ($p < 0.05$) along the stream. For St.1 and St.2, St.2 and St3, and St.1 and St.3, the differences in DOC concentrations were not statistically significant (

Table 4-3) DOC concentrations increased from upstream to downstream at both sites except in August when high DOC concentration was observed at St.1 (All August samples at HIG and August second sampling at MIZ). Around the dam at HIG (i.e. St.2 and St.3), DOC concentration variation was less than 0.17 mg L^{-1}, except in August (second sampling), where an increase of 0.19 and 0.27 mg L^{-1} was noted for HIG and MIZ, respectively (Table A-4).

Table 4-3 Paired t-test results for optical properties between the sites

Pair	S_R	E2:E3	SUVA$_{254}$	a350	Slope$_{275-295}$	DOC	C1	C2	C3
St 1-St 2	A**	A	*A	A	A**	B	B	*B	*B
St 1-St 3	A**	A**	*A	A	A**	B	B	*B	*B
St 1-St 4	B	B	*B	A	B	A	A**	*A	*A
St 2-St 3	B	B	*B	B	B	B	B	*B	*B
St 2-St 4	A**	B	*B	B	A**	A	A**	*B	*B
St 3-St 4	A**	B	*A	B	A**	A	A**	*A**	*A

"A" represents significant results at $p < 0.05$ and double asterisks (**) indicate significant results at $p \leq 0.01$. "B" shows non-significant values while single asterisk (*) before the letter shows non-parametric test.

The observed concentrations are related to the nature of the study sites and their location. The significant difference between the upstream sites (St.1, St.2, St 3) and the downstream site (St.4) ($p < 0.05$) for all samples may be related to the activities in the downstream areas such as the paddy fields (Imai et al., 2001). Mostofa et al,. (2005) reported the fluxes of effluents from paddy fields, households, and industries in the downstream location as the main contributing factor to increasing DOC levels downstream. In their study on the effect of beaver impoundments on DOM quality and biodegradability, Catalán et al., (2016) found no significant variations in DOM

concentrations between the upstream and pond sections, however; it was evident that DOM was affected by the age of the bevear and pond section.

4.4.2.2 DOM composition changes along the stream

CDOM optical properties S_R, a350, $SUVA_{254}$, E2:E3, and $S_{275-295}$ were used to assess the changes in the DOM composition. From these spectral properties, a trend showing distinct changes between the stations was evident as indicated in Figure 4-2. The distribution of optical parameters S_R, E2:E3, $SUVA_{254}$, and $S_{275-295}$ (Figure 4-2) at each station was similar between the two study sites (MIZ and HIG) (p>0.05) but varied between the stations.

At all sampling stations, average S_R values ranged from 0.68±0.06 (recorded at St.3) to 0.82±0.10 (recorded at St.4). Generally, S_R values were higher at St.1 and St.4 and lower around the dam (St.2 and St.3). At the two study sites, a contrasting pattern of S_R was observed at St.2 and St.3 around the dams, that is, a decrease was observed at MIZ while an increase was observed at HI (Figure 4-2). When all samples were grouped by stations, the values ranged from 0.72-0.95 (average of 0.81±0.05), 0.61-0.92 (average 0.70±0.09), 0.57-0.95 (average 0.69±0.1), and 0.58-0.99 (average 0.82±0.1) for St.1, St.2, St.3, and St.4 respectively. The S_R results presented in Table 3-2 clearly show a difference between the stations; St.1 and St.4 show similar characteristics (*p*>0.05), which are different from St.2 and St.3. In the upper section (St.1-St.4), the lowest S_R value was observed in early summer at each station; 0.79±0.03 (St.1), 0.63±0.04 (St.2), and 0.59±0.02 (St.3) all at MIZ, and the highest in summer at St.1 (0.84±0.05), and in Autumn at St.2 (0.76±0.12) and St .3 (0.74±0.15) (Table 4-4). Downstream at St.4, however, the lowest value was observed in summer (0.78±0.29) while the highest value was observed in early summer (0.89±0.09) at MIZ. At both sites, the lowest value was observed in early summer (0.66±0.03 at St.2) at HIG and at St.3 (0.59±0.02) for MIZ (Table 4-4).

S_R has been used to characterize the CDOM of different origin in natural waters (Helms et al. 2008; Spencer et al. 2010) and in photobleaching experiments (Obernosterer and Benner, 2004; Zhang et al., 2013). Low values indicate high molecular weight DOM with greater aromaticity and increasing vascular plant inputs (Spencer et al., 2012). In this study, lower values were observed at St.2 and St.3 as opposed to St.1 (upstream) and St.4 (downstream). These values were lower than most previously reported values in Beaver Creek (0.7) and Hess Creek (0.63) during winter by O'Donnell et al., (2012). Since sabo dams retain particulate material including

sediments and terrestrial inputs, low S_R values were expected. Low S_R values around the dam are therefore related to the processes such as the increase in vascular plant material and decomposition of material retained by the dam.

Table 4-4 Average seasonal CDOM properties per station

Site	Season	Station	DOC		$SUVA_{254}$		a350		E2:E3		S_R		$S_{275\text{-}295}$	
HIG	Early Summer	St 1	0.46	±0.41	2.96	±0.11	1.63	±0.28	4.54	±0.24	0.82	±0.07	0.0131	±0.0006
		St 2	0.94	±0.16	2.82	±0.05	1.81	±0.58	4.52	±0.60	0.66	±0.03	0.0115	±0.0022
		St 3	0.99	±0.21	2.74	±0.46	1.89	±0.32	4.38	±0.59	0.70	±0.04	0.0117	±0.0004
		St 4	0.92	±0.01	3.11	±0.30	1.94	±0.24	4.47	±0.30	0.83	±0.03	0.0136	±0.0006
	Summer	St 1	1.26	±0.32	2.25	±0.20	1.77	±0.47	5.10	±0.34	0.81	±0.04	0.0137	±0.0006
		St 2	0.71	±0.09	4.14	±0.19	2.23	±0.40	4.20	±0.03	0.69	±0.10	0.0109	±0.0006
		St 3	0.82	±0.20	3.53	±0.29	2.23	±0.41	3.94	±0.18	0.72	±0.02	0.0113	±0.0002
		St 4	0.87	±0.17	3.63	±0.80	2.34	±0.34	4.13	±0.68	0.87	±0.13	0.0124	±0.0001
	Autumn	St 1	0.89	±0.22	3.20	±0.19	1.97	±0.66	4.43	±0.19	0.81	±0.04	0.0124	±0.0002
		St 2	0.86	±0.31	3.82	±1.52	2.37	±0.87	3.92	±0.33	0.68	±0.09	0.0116	±0.0009
		St 3	0.79	±0.22	3.60	±0.88	2.11	±0.67	4.03	±0.31	0.70	±0.07	0.0118	±0.0001
		St 4	1.26	±0.12	2.93	±0.32	2.68	±0.57	4.19	±0.08	0.79	±0.08	0.0120	±0.0004
MIZ	Early Summer	St 1	0.80	±0.05	3.09	±0.20	1.53	±0.10	5.05	±0.13	0.79	±0.03	0.0136	±0.0005
		St 2	0.99	±0.19	5.28	±1.20	4.27	±0.29	3.48	±0.14	0.63	±0.04	0.0107	±0.0005
		St 3	0.93	±0.12	6.18	±0.88	5.03	±0.16	3.31	±0.04	0.59	±0.02	0.0098	±0.0002
		St 4	1.74	±0.23	2.44	±0.41	2.83	±0.14	4.47	±0.03	0.89	±0.09	0.0140	±0.0006
	Summer	St 1	0.99	±0.41	4.23	±3.29	2.27	±1.23	4.92	±0.83	0.84	±0.05	0.0140	±0.0006
		St 2	0.82	±0.17	5.45	±4.48	3.22	±2.87	4.49	±1.63	0.70	±0.06	0.0121	±0.0024
		St 3	0.91	±0.08	7.00	±0.31	5.68	±0.33	3.31	±0.05	0.60	±0.01	0.0097	±0.0001
		St 4	0.94	±0.53	6.28	±2.78	4.20	±1.24	3.76	±0.62	0.78	±0.29	0.0116	±0.0027
	Autumn	St 1	0.85	±0.17	3.17	±0.21	1.75	±0.35	4.66	±0.46	0.81	±0.10	0.0130	±0.0003
		St 2	0.90	±0.14	3.34	±0.55	2.14	±0.60	4.25	±0.29	0.76	±0.12	0.0117	±0.0012
		St 3	0.89	±0.23	3.71	±0.43	2.40	±0.58	4.11	±0.15	0.74	±0.15	0.0115	±0.0010
		St 4	1.29	±0.23	2.86	±0.52	2.55	±0.69	4.38	±0.22	0.79	±0.07	0.0129	±0.0007

The E2:E3 ratio has been linked to molecular size changes. The results (Table 4-4 and A4-1) showed differences between the two study sites and the trend between the stations was similar to S_R observations. St.1 and St.4 showed higher values than St.2 and St.3. Average values for the two sites varied at the upstream stations (St.1, St.2, and St.3) but were the same at St.4 (4.27 ±0.18 and 4.27±0.20 at HIG and MIZ, respectively). Although a similar trend was observed from St.1 to St.3, St.3 values at MIZ were lower (3.71± 0.44) than at HI (4.10±0.36). At St.2 and St.3, the highest and lowest E2:E3 ratio were recorded in summer (4.49±1.63) and in autumn 4.11±0.15 for St.2 and St.3 at MIZ, and 4.52±0.60 and 4.38±0.59 for St.2 and St.3 at HIG, respectively. Statistical analysis revealed significant differences only between pairs St.1-St.2 and St.1-St.3 indicating the abundance of low molecular weight compounds at St.1 compared to other sites for both HIG and MIZ. Since $S_{275-295}$ can be used as a proxy for molecular weight, combined with E2:E3 more details regarding the DOM character can be identified. At $p<0.01$ (Table 3-2, St.1 and St.3), significant differences in $S_{275-295,}$ difference in molecular weight was evident between the upstream (St.1) and downstream sections of the dam (St.3) (Table 4-4). Thus, both $S_{275-295}$ and E2:E3 indicate the change in molecular weight going downstream from St. 1 to St. 2 and from St. 3 to St. 4.
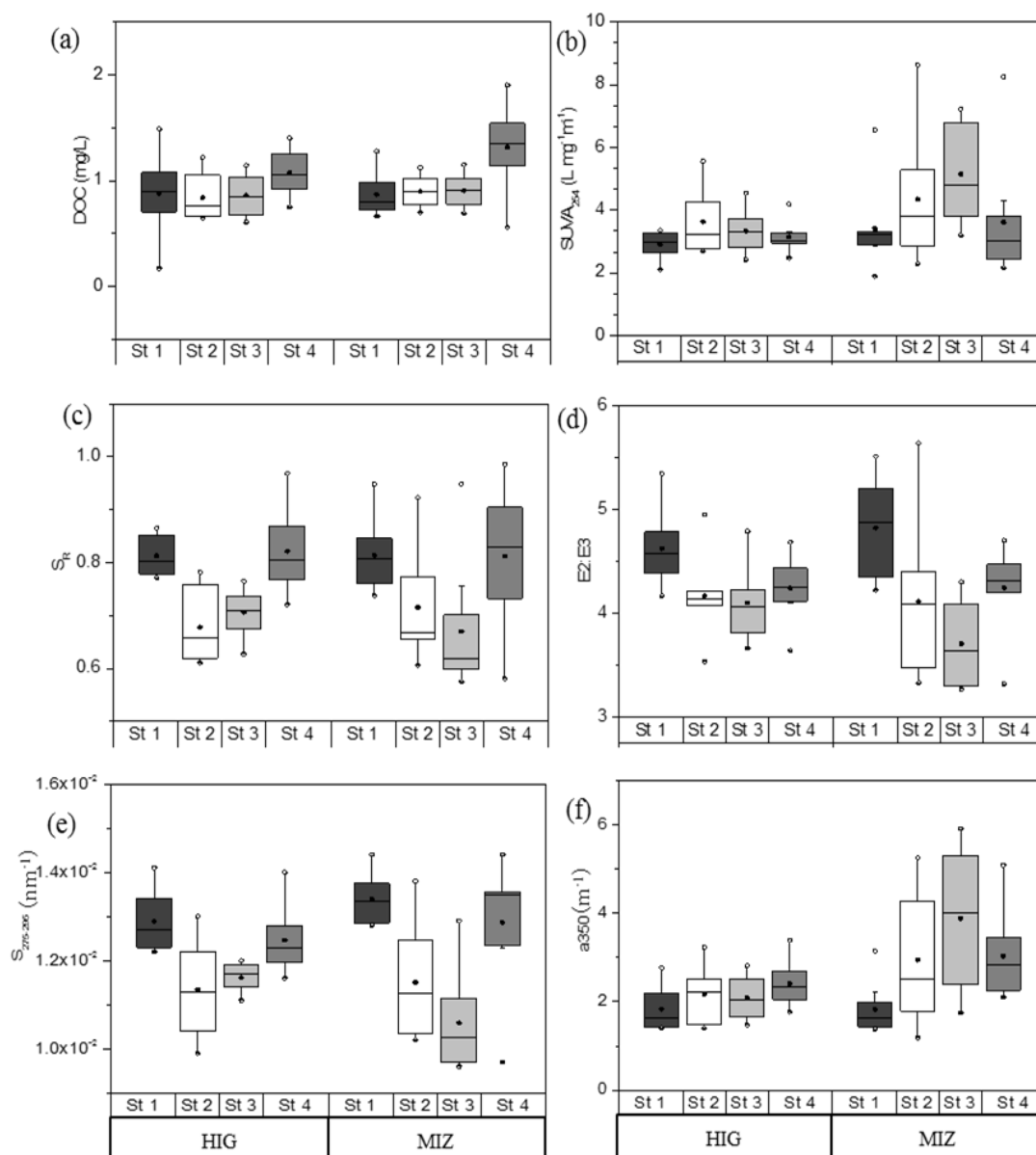
Figure 4-2 Box plots for DOM optical properties at each sampling station for the whole sampling period a) DOC concentration, b) SUVA$_{254}$, c) spectral slope ratio (S$_R$), d) E2:E3 ratio e) S275-295, f) a350. The solid black line in the box represents the median, the lower, and upper boundaries of the box represent the 25th and 75th percentile, and open circles represent the 10th and 90th percentile while the black solid circle in the box shows the average.

SUVA$_{254}$ ranged from 1.9-8.6 Lmg^{-1}m^{-1} with values higher than 6 Lmg^{-1}m^{-1} observed at MIZ around the dam in June and August and at St.4 in August. At HIG, values ranging from 2.11 to 5.55 were recorded with most of the values in 2-3.44 range. These values at MIZ were slightly

higher than at HIG. Average $SUVA_{254}$ values in Figure 4-2 indicate an increase around the dams at St.2 and St.3. Similar to all other CDOM optical indices, SUVA values changed drastically between the stations; they were higher around the dam at St.1 and St.2 and low in upstream (St.1) and downstream stations (St.4). The highest value was 4.42 ± 0.19 $Lmg^{-1}m^{-1}$ at HI and 7.00 ± 0.31 $Lmg^{-1}m^{-1}$ at MIZ and both values were around the dams (St.2 and St.3 respectively). The highest seasonal value was observed in summer at both sites; MIZ (7.00 ± 0.31 $Lmg^{-1}m^{-1}$) and HIG (4.14 ± 0.19 $Lmg^{-1}m^{-1}$). $SUVA_{254}$ correlates positively with DOM aromaticity (Weishaar et al., 2003), and typically ranges from 1 to 6 $Lmg^{-1}m^{-1}$ in fresh water, although higher values have been reported in waters with strong terrestrial DOM (Jaffé et al., 2008; Inamdar et al., 2011b). In this study, $SUVA_{254}>6$ $Lmg^{-1}m^{-1}$ was observed at MIZ and mostly at the sites around the dam. The increase in $SUVA_{254}$ at St.2 and St 3 not only shows increased aromaticity around the dam but also may be related to the increase in lignin content within the dam area since lignin carbon-normalized yields have been found to correlate positively with $SUVA_{254}$ ($r^2=0.77$, $p<0.001$) (Spencer et al., 2012). Lignin is an aromatic compound present in plants and the material observed within the reservoir of two dam sites mainly consisted of plant material; therefore, the decomposition and organic matter mineralization will cause an increase in lignin content at the sites around the dam. Moreover, the removal of debris dams increased the coarse particulate matter export by 552% (from 707 kg dry mass to 4,610 kg dry mass (Bilby 1981), and the coarse particulate organic matter became relatively high in log jams (11,562 gm^{-2}) compared to surface sites (734 gm^{-2}) in a mountainous stream (Flores et al., 2013). In relation to these studies, areas around the dam are likely to have high lignin content from the remineralization of plant material. A study on beaver impoundments on DOM quantity and quality by Catalán et al., (2016) reported a significantly high $SUVA_{254}$ around the ponds related to the release of DOM from inundated soils and the decomposition of wood at the bottom of the pond.

Around the dams (St.2 and St.3), the aromaticity ($SUVA_{254}$) and molecular weight (E2:E3, $Slope_{275-290}$, and S_R) of DOM were observed to vary from other sites. Moreover, lower S_R values around the dams showed increased allochthonous character and the presence of less photodegradable DOM. S_R, $SUVA_{254}$, and E2:E3 varied significantly in the downstream areas (St.4), which may have been influenced by the photo degradation and anthropogenic activities such as agriculture. Regardless of the variability in anthropogenic activities, DOM quality may stay the same (Hosen 2014), however, in this study, the activities in downstream areas had a

higher impact on DOM quality compared to sabo dams (Figure 4-2). The mean values of S_R, $SUVA_{254}$, and E2:E3, in this study, were in the same range reported by other researchers. S_R values at St.1 and St.4 (0.79 ± 0.03-0.89 ± 0.09) are similar to the values for Fishing Brook, Hubbard Brook, Passadumkeag, and Pike rivers in the US reported by Spencer et al., (2012) and to the S_R, $SUVA_{254}$, and E2:E3 values reported by Leech et al., (2016) for black waters of the Chowan River in the US and its tributaries. The values around the dam were slightly lower than the previously reported values for fresh water. According to Inamdar et al., (2011), groundwater sources including hyporheic water DOM have low humic and aromatic content. Therefore, the water exchange between hyporheic zone and surface water coupled with photo-degradation can alter DOM composition (Cory and Kaplan, 2012). Solar irradiation transforms high molecular weight compounds to lower molecular weight ones. Therefore riverine DOM was transformed to low molecular weight photoproducts as a result of irradiation (Obernosterer and Benner, 2004) hence the low values observed at St.4. In this study, low molecular weight compounds at St.1 increased to high molecular weight aromatic compounds around the dams (St.2 and St.3) and were degraded downstream at St.4. Such changes in DOM pool along the stream can be linked to hydrological pathways, residence time, and various processes within the dam. At the study site, there is no impact from human activities at St.1 and OM present in this section of the stream is mainly from terrestrial inputs. Similarly, OM at St.2 and St.3 is primarily of terrestrial origin, however, the presence of the dam increases the residence time in addition to anaerobic decomposition of OM. The breakdown of retained OM such as leaf litter, driftwood, and leaching soil organic matter from terrestrial sources results in high molecular, highly aromatic compounds such as lignin and phenols (Kaiser et al., 2001). The composition of these compounds changes along the stream with influx from agricultural fields and other anthropogenic activities from various processes such as solar irradiation, groundwater mixing, and inputs from anthropogenic sources (evident at St.4).

4.4.3   EEM and PARAFAC modelling

4.4.3.1   Fluorescence Indices
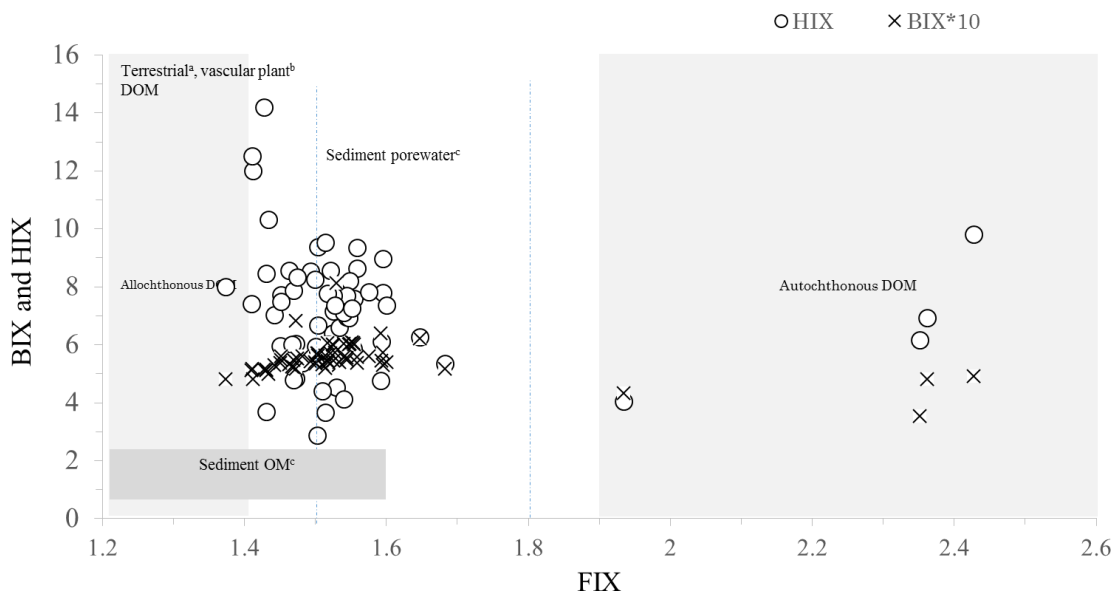
Figure 4-3 BIX and HIX values for the whole sampling period against FIX values. Vertical lines indicate DOM sources of different ranges of FIX [b]Inamdar et al., 2011, [c]Birdwell and Engel ,2010. Sediment organic matter range is 1.2-1.6 (Birdwell and Engel, 2010).

All three fluorescence indices extracted from the EEM data can be used to provide useful information regarding the DOM character as previously discussed. Average FIX values were 1.33±0.06 (HIG St 3) and 1.57±0.16 (HIG St 2 and MIZ St 3) indicating terrestrial DOM content at all stations with the strongest terrestrial DOM signature exhibited at MIZ St 3 (Table 4-5). Sazawa et al., (2011) used FIX to classify DOM characteristics in Japanese rivers and proposed that FIX values ≤1.4 indicate allochthonous DOM while values ≥1.9 show autochthonous DOM. Most BIX values were below 0.6 at all stations; the lowest mean value was recorded at MIZ St 2 (0.44±0.07) and the highest mean values were observed at St.4 (0.59±0.02 at MIZ and 0.58±0.03 for HI) (Table A-4). Except at MIZ St 1 (10.0), average HIX varied from 5.5 to 7.7 (Table 4-5) from St.2 to St.4 along the stream. High HIX value at MIZ St.1 may be linked to freshly leached soil organic matter and nature of the sampling site. Fluorescence indices in Figure 4-3 show that all BIX and HIX values lie within the range for terrestrial-derived organic matter including vascular plants, soil pore water, and sediment organic matter sources (Birdwell and Engel 2010). Although few sites had freshly produced DOM (HIX<5), most sites had decomposed organic

matter with a humification range of 5.5-10. At MIZ, HIX values were high at St.1 compared to the other stations except during the second sampling campaign in August (Table A-4). From fluorescence indices data, the stations were dominated with terrestrial DOM with only four sites showing microbial fresh DOM input (FIX>1.8). Contrary to the CDOM properties, no clear trend was observed in FIX, HIX, and BIX values between the stations.

Table 4-5 Average fluorescence-derived indices per station

Station		MIZ			HIG		
		FIX	BIX	HIX	FIX	BIX	HIX
St 1	Mean	1.55	0.51	10.02	1.50	0.56	6.72
	SD	0.36	0.02	2.97	0.07	0.06	2.03
	Max	2.43	0.55	14.20	1.60	0.68	8.96
	Min	1.37	0.48	4.78	1.41	0.51	3.67
St 2	Mean	1.50	0.54	6.59	1.57	0.44	5.56
	SD	0.03	0.02	1.11	0.39	0.07	0.66
	Max	1.54	0.57	7.89	2.36	0.54	7.36
	Min	1.45	0.52	4.41	1.45	0.36	5.35
St 3	Mean	1.57	0.54	7.67	1.33	0.51	5.68
	SD	0.15	0.04	1.93	0.06	0.10	1.93
	Max	1.93	0.56	9.53	1.59	0.81	8.65
	Min	1.47	0.43	4.05	1.43	0.51	3.69
St 4	Mean	1.54	0.59	6.13	1.52	0.58	7.21
	SD	0.05	0.02	1.82	0.03	0.03	1.13
	Max	1.65	0.62	8.34	1.55	0.61	8.56
	Min	1.47	0.55	2.87	1.47	0.52	5.37

4.4.3.2 DOM components identified by PARAFAC

Three components were successfully identified by the PARAFAC analysis (Figure 4-4). These components (C1, C2, and C3) can be described based on their peak locations and maximum intensities (Fmax (RU)) modeled as humic-like and protein-like components. Component 1 (C1) had two peaks at λEm 420 nm and λEx 320 nm and 240 nm (Yamashita et al., 2008). This component can be described as humic-like (Yamashita et al., 2011) and it consisted of peak C and M (Coble 2007). With peaks at λEm 480 nm and λEx 370 nm and 240 nm, C2 can also be described as humic-like. Humic-like components C1 and C2 can further be differentiated by their fulvic acid and humic acid fractions. The former is enriched in fulvic acid while the latter is more of humic acid-like (Ohno and Bro 2006). C2 is a mixture of peaks A and C as described by Coble

(2007). The third component (C3) was located in the wavelength region of protein-like components with another peak in Ex/Em of 270 nm/550 nm. This component may be described as tryptophan-like with a peak at λEx >250,280/λEm 338, whereas the peak at 270 nmλEx /550 nmλEm could not be described. Mainly two protein-like components (tryptophan-like and tyrosine-like) have been identified in previous studies (Yamashita et al., 2011; Stedmon and Markager, 2005; Cory and Kaplan, 2012; Birdwell and Engel, 2010).

Component	Contour plot	Loadings
C1- Humic-like fluorophore of terrestrial origin (Hosen, 2014; Cory and Kaplan, 2012; Fellman ,2010), Fulvic acid rich fraction (Ohno and Bro, 2006; Yamashita et al., 2010)		
C2 Humic-like fluorophore with high fraction of humic acid (Yamashita et al., 2011)		
C3 Tryptophan-like amino acid protein (Cory and Kaplan 2012; Yamashita et al., 2011; Coble, 2007) with an identified peak Ex 270 nm/Em 550 nm		

Figure 4-4 Contour plots for three components (C1, C2 and C3) identified by PARAFAC analysis with corresponding loadings on emission and excitation wavelength.

Both humic-like and protein-like components identified in this study resembled the three components identified by Yamashita et al., (2011) in an experimental forest located in Appalachian Mountains, North Carolina, USA and were more abundant downstream at St.4 (Figure 4-5). At MIZ, all components increased along the stream, from average values; C1 increased from St.1 to St.3, C2 fluctuated slightly between St.1 and St.3 while C3 slightly increased from St.1 to St.2 and remained constant around the dams (St.1 and St.3) (Figure 4-5). Components contrasted between the two sites with HIG showing a random abundance of components at each station while MIZ showing a clear trend (Figure 4-). Such differences may have been enhanced by hydrological processes and primary productivity variations (Jaffé et al., 2008) between the two watersheds.
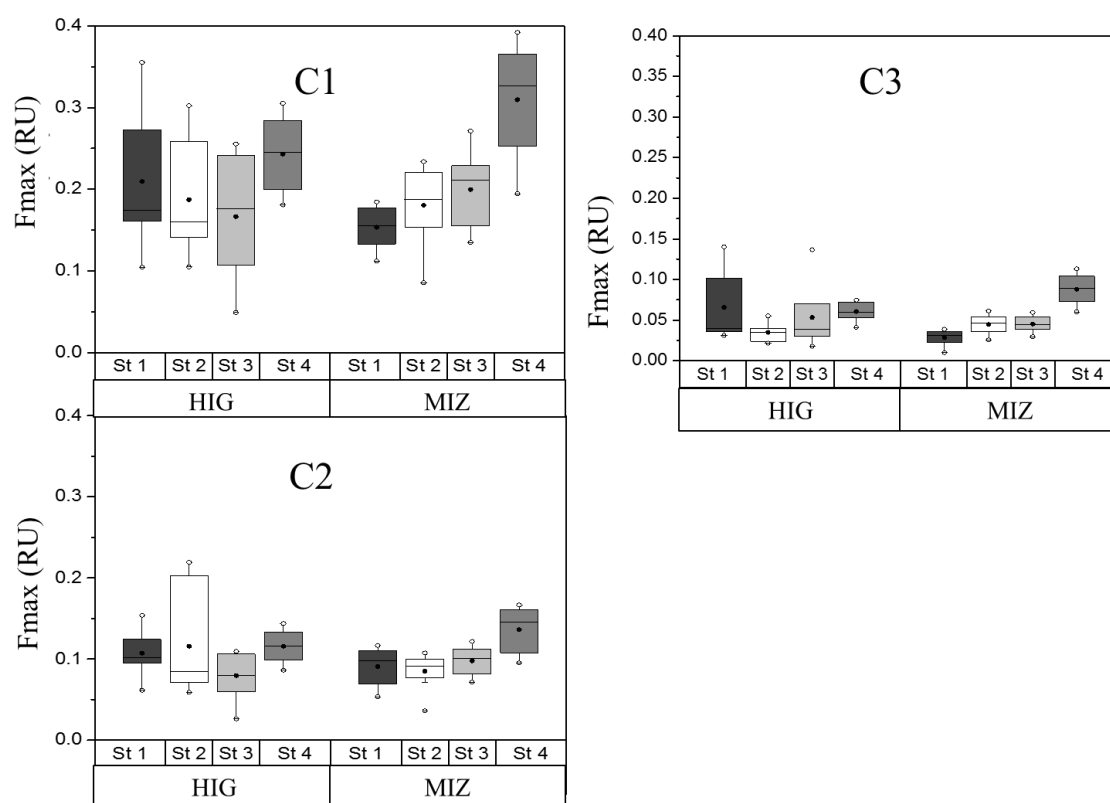
Figure 4-5 Boxplot showing maximum intensity (Fmax) for each of the components identified by PARAFAC at each sampling station. Black circles show averages awhile the solid black line in the box represents the median, the lower and upper boundaries of the box represent the 25th and 75th percentile, and open circles represent the 10th and 90th percentile, and outlier values.
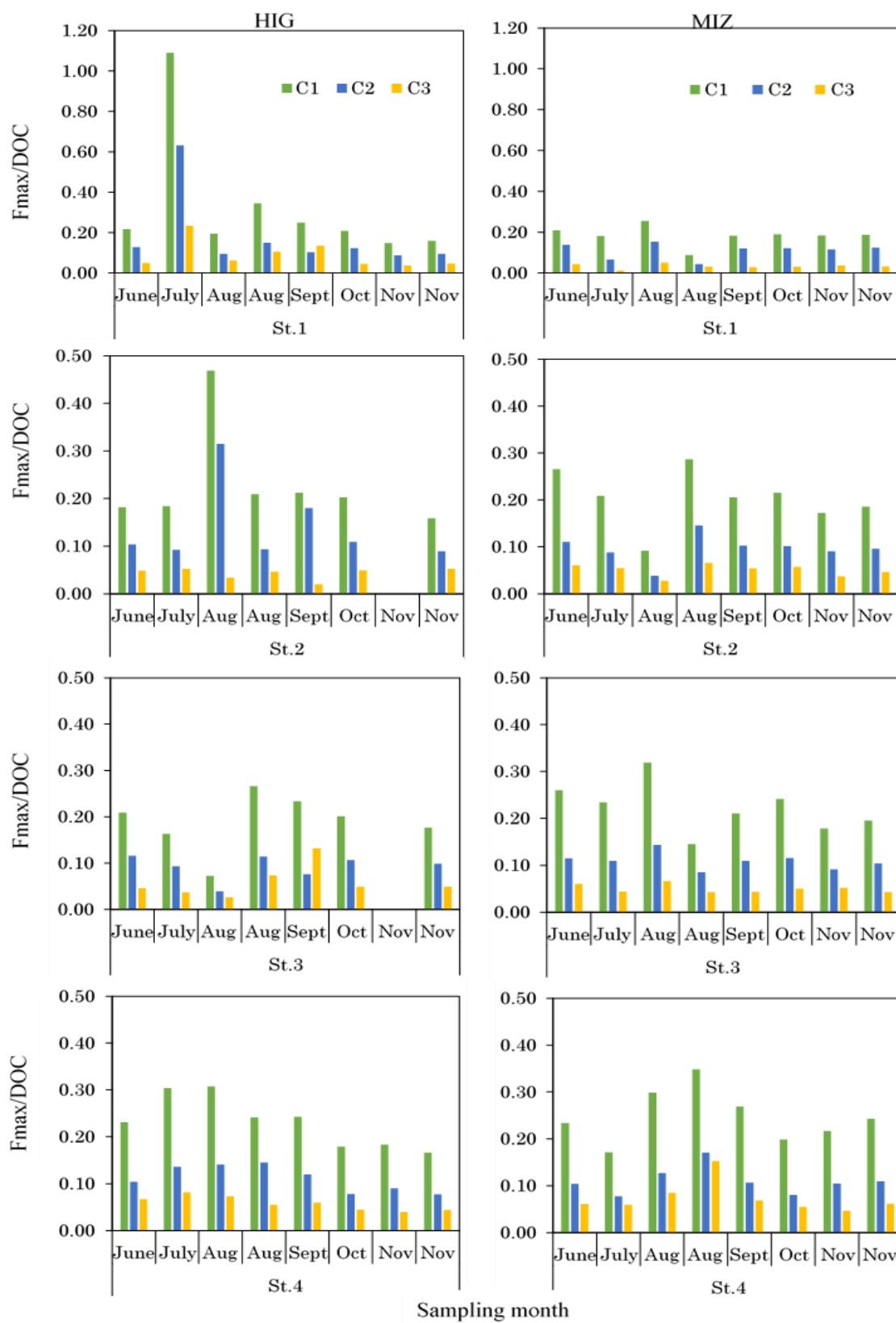
Figure 4-6 PARAFAC Components normalized to DOM concentration per station for HIG and MIZ

Out of the three components identified by the PARAFAC analysis, C1 was more abundant than the other two components at all stations. This is typical of fulvic acid-like components, which are the major constituents of DOM (Suzuki et al., 2014), four to nine times the amount of humic acid-like components (Mostofa et al., 2010). The ratio of C1 to C2 is smaller in low DOM environments and increases with increasing organic matter concentrations. In this study, the ratio of C1 to C2 was much lower ranging from 1.2 to 3.1. Although all three components varied between the upstream sites (St.1, St.2, and St.3) and the downstream site (St.4) (Figure 4-5), results from the paired t-test showed significant distinction between stations St.1 and St.4 ($p \leq 0.01$), St.2 and St.4 ($p \leq 0.01$), and St.3 and St.4 ($p \leq 0.01$) for C1. This may be attributed to land use effects since the major difference between these sites is the location, anthropogenic activities, and increase in DOM. On the other hand, results showed resemblance in DOM fluorophores at St.1, St.2, and St.3 ($p \geq 0.05$), and a high variation between the pairs of St.1 and St.4 and St.3 and St.4 for C2 and C3 (Table 4-3). Land use and seasonal patterns are important in DOM composition. For example, a study on water seepage from organic forests found high DOC concentrations with more hydrophobic, aromatic and aliphatic structures, carboxyl groups, and lignin decomposition products, which varied with seasons (Kaiser et al., 2001). These heavier molecules are more photodegradable as opposed to autochthonous microbial/algal-derived DOM (Brandão et al., 2016). The absence of autochthonous DOM at most of the stations could have been due to its low molecular weight nature and susceptibility to biodegradation. While photodegradation experiments have shown a decrease in tryptophan-like fluorescence by up to 5-59% in river water, mixing with water from the surrounding environment increases the component abundance. Specifically, water from the hyporheic region (Inamdar et al., 2011) and anthropogenic sources (Nie et al., 2016) have high abundance of tryptophan-like components.

In this study, C3 abundance increased along the stream especially at MZ and the highest was at St.4. While HIG and MIZ are located in a mountainous area with similar environmental surroundings, there is a constant overflow at HIG dam, which could have influenced the observations. However, at the MIZ dam, water seeps through the accumulated material and flows out of the dam through the vents in the dam wall. Still, DOM characteristics at St.2 and St.3 did not vary significantly (Table 4-3). On the other hand, this study showed that the quality of OM was impacted by sabo dams due to the sedimentation of organic particles dividing the stream into three sections (upstream, around the dam, and downstream). Although t-test results were not significant for S_R, $SUVA_{254}$, E2:E3, and slope$_{275-295}$, they were significant for a350, DOC, C1, C2,

and C3. This shows that while St.1 and St.4 DOM is dominated by low molecular weight compounds, CDOM composition varies and fluorescence DOM is significantly different. Since DOM is known to play a major role in the biogeochemical cycle of trace metals and colloidal mobility in aquatic environments, the changes in the DOM character affect not only the metal cycle but also the whole ecosystem (Aiken 2011). The DOM character influenced by its aromaticity, elemental composition, and major functional groups such as carboxylates, phenols, thiols, and amines carboxyl is important for metal-binding and ultimately affects the levels of bioavailable metals and nutrients for organisms. Three components identified by EEM-PARAFAC were dominated by humic-like DOM at both sites in each sampling period (Figure 4-6). During the initial stages of photo-oxidation, chromophores are rapidly lost (Sharpless and Blough 2014). In this study, however, FDOM increased along the stream. As opposed to the behavior of EEM-PARAFAC components, CDOM properties showed a clear trend between the sites differentiating between upstream, around sabo dams, and downstream. This may be due to the fact that not all CDOM is fluorescent (Coble 2007) and also influx of DOM from other sources along the flow path. Although CDOM properties summarized in Table 4-1 show similarity in DOM character between St.1 and St.4, the details of the EEM-PARAFAC analysis reveal the difference in composition of fluorophores at these sites. DOM composition has been linked to the ecosystem function (Jaffe et al., 2008); therefore, the factors that control its behavior and fate in the environment are important in ecosystem management as well.

4.5   Summary

DOM quality and quantity along the stream vary depending on the prevailing conditions. In this study, we evaluated the impact of sabo dams on DOM characteristics in headwater streams using both UV-visible optical properties and PARAFAC. Using UV-vis properties, we were able to differentiate DOM composition between the upstream, around the dam, and downstream sections. DOM in the upstream area comprised mainly of low molecular weight compounds while around the dams (the reservoir and immediate downstream), the DOM character was more aromatic with higher molecular weight compounds. Further downstream, DOM properties showed loss of highly aromatic, high-molecular-weight compounds since all optical property results indicated the existence of low molecular weight, less aromatic content downstream. On the other hand, PARAFAC results did not differentiate dam sites from the other sections of the stream. All PARAFAC components increased from the upstream to downstream areas and were more abundant in the downstream area dominated by DOM inputs from anthropogenic activities. DOM at all stations was dominated by humic-like fluorophores with a large fraction of

terrestrial-derived DOM.

References

Aiken GR, Hsu-Kim H, Ryan JN (2011) Influence of dissolved organic matter on the environmental fate of metals, nanoparticles, and colloids. Environmental Science & Technology 45:3196-3201. doi:10.1021/es103992s

Asmala E, Autio R, Kaartokallio H, Stedmon CA, Thomas DN (2014) Processing of humic-rich riverine dissolved organic matter by estuarine bacteria: effects of predegradation and inorganic nutrients. Aquatic Sciences 76:451-463. doi:10.1007/s00027-014-0346-7

Bilby RE (1981) Role of Organic Debris Dams in Regulating the Export of Dissolved and Particulate Matter from a Forested Watershed. Ecology 62:1234-1243. doi:10.2307/1937288

Birdwell JE, Engel AS (2010) Characterization of dissolved organic matter in cave and spring waters using UV–Vis absorbance and fluorescence spectroscopy. Organic Geochemistry 41:270-280. doi:10.1016/j.orggeochem.2009.11.002

Brandão LPM, Staehr PA, Bezerra-Neto JF (2016) Seasonal changes in optical properties of two contrasting tropical freshwater systems. Journal of Limnology 75(3):508-519. doi:10.4081/jlimnol.2016.1359

Catalán N et al. (2016) Effects of beaver impoundments on dissolved organic matter quality and biodegradability in boreal riverine systems. Hydrobiologia.1–14: doi:10.1007/s10750-016-2766-y

Chen J, Gu B, LeBoeuf EJ, Pan H, Dai S (2002) Spectroscopic characterization of the structural and functional properties of natural organic matter fractions. Chemosphere 48:59–68. doi.10.1016/S0045-6535(02)00041-3

Coble PG (2007) Marine Optical Biogeochemistry: The Chemistry of Ocean Color. Chemical Reviews 107:402-418. doi:10.1021/cr050350+

Cory RM, McKnight DM (2005) Fluorescence spectroscopy reveals ubiquitous presence of oxidized and reduced quinones in dissolved organic matter. Environmental Science & Technology. 39:8142–8149. doi:10.1021/es0506962

Cory RM, Kaplan LA (2012) Biological lability of streamwater fluorescent dissolved organic matter. Limnology and Oceanography 57:1347-1360. doi:10.4319/lo.2012.57.5.1347

Cory RM, Miller MP, McKnight DM, Guerard JJ, Miller PL (2010) Effect of instrument-specific response on the analysis of fulvic acid fluorescence spectra. Limnology and Oceanography: Methods 8:67-78. doi:10.4319/lom.2010.8.67

Cui H et al. (2016) Characterization of chromophoric dissolved organic matter and relationships among PARAFAC components and water quality parameters in Heilongjiang. China Environmental Science and Pollution Research International 23:10058-10071. doi:10.1007/s11356-016-6230-3

Chanson, H., 2004. Sabo check dams-mountain protective systems in Japan. International Journal of River Basin Management 2:301–307.

Flores L, Díez JR, Larrañaga A, Pascoal C, Elosegi A (2013) Effects of retention site on breakdown of organic matter in a mountain stream. Freshwater Biology 58:1267-1278. doi:10.1111/fwb.12125

Friedl G, Wüest A (2002) Disrupting Biogeochemical Cycles—Consequences of Damming. Aquatic Sciences 64:55-65. doi:10.1007/s00027-002-8054-0

Harvey ET, Kratzer S, Andersson A (2015) Relationships between colored dissolved organic matter and dissolved organic carbon in different coastal gradients of the Baltic Sea. Ambio 44 Suppl 3:392-401. doi:10.1007/s13280-015-0658-4

Helms JR, Mao J, Stubbins A, Schmidt-Rohr K, Spencer RGM, Hernes PJ, Mopper K (2014) Loss of optical and molecular indicators of terrigenous dissolved organic matter during long-term photobleaching. Aquatic Sciences 76:353-373. doi:10.1007/s00027-014-0340-0

Helms JR, Stubbins A, Ritchie JD, Minor EC, Kieber DJ, Mopper K (2008) Absorption spectral slopes and slope ratios as indicators of molecular weight, source, and photobleaching of chromophoric dissolved organic matter. Limnol Oceanogr 53: 955–969. doi: 10.4319/lo.2008.53.3.0955

Hotchkiss, E. R., R. O. Hall Jr., M. A. Baker, E. J. Rosi-Marshall, and J. L. Tank (2014), Modeling

priming effects on microbial consumption of dissolved organic carbon in rivers, Journal of Geophysical Research, Biogeosciences. 119:982–995. doi:10.1002/ 2013JG002599

Hood E, Gooseff MN, Johnson SL (2006) Changes in the character of stream water dissolved organic carbon during flushing in three small watersheds. Oregon Journal of Geophysical Research 111:G01007 doi:10.1029/2005jg000082

Hosen JD, McDonough OT, Febria CM, Palmer MA (2014) Dissolved organic matter quality and bioavailability changes across an urbanization gradient in headwater streams. Environmental Science & Technology 48:7817-7824. doi:10.1021/es501422z

Imai A, Fukushima T, Matsushige K, Hwan Kim Y (2001) Fractionation and characterization of dissolved organic matter in a shallow eutrophic lake, its inflowing rivers, and other organic matter sources. Water Research 35:4019-4028. doi:10.1016/s0043-1354(01)00139-7

Inamdar S et al. (2011a) Dissolved organic matter (DOM) concentration and quality in a forested mid-Atlantic watershed, USA. Biogeochemistry 108:55-76. doi:10.1007/s10533-011-9572-4

Inamdar S et al. (2011b) Fluorescence characteristics and sources of dissolved organic matter for stream water during storm events in a forested mid-Atlantic watershed. Journal of Geophysical Research 116:G03043: doi:10.1029/2011jg001735

Jaffé R, McKnight D, Maie N, Cory R, McDowell WH, Campbell JL (2008) Spatial and temporal variations in DOM composition in ecosystems: The importance of long-term monitoring of optical properties. Journal of Geophysical Research 113: G04032 doi:10.1029/2008jg000683

Jaffé R et al. (2012) Dissolved Organic Matter in Headwater Streams: Compositional Variability across Climatic Regions of North America. Geochimica et Cosmochimica Acta 94:95-108. doi:10.1016/j.gca.2012.06.031

Kaiser, K., Guggenberger, G., Haumaier, L. et al. (2001). Seasonal variations in the chemical composition of dissolved organic matter in organic forest floor layer leachates of old-growth Scots pine (Pinus sylvestris L.) and European beech (Fagus sylvatica L.) stands in northeastern Bavaria, Germany. Biogeochemistry 55:103–143.

doi:10.1023/A:1010694032121

Leech DM, Ensign SH, Piehler MF (2016) Spatiotemporal patterns in the export of dissolved organic carbon and chromophoric dissolved organic matter from a coastal, blackwater river. Aquatic Sciences 78(4):823-836 doi:10.1007/s00027-016-0474-3

Leenher JA, Croué J-P (2003) Organic matter characterization. Aquatic organic matter; Understanding the unknown structures is key to better treatment of drinking water. Environmental Science & Technology 37 (1), 18A–26A: doi: 10.1021/es032333c

Lennon JT, Hamilton SK, Muscarella ME, Grandy AS, Wickings K, Jones SE (2013) A source of terrestrial organic carbon to investigate the browning of aquatic ecosystems. PloS One 8:e75771. doi:10.1371/journal.pone.0075771

Lokowicz JR (1999) Principles of fluorescence spectroscopy. 3rd Edition, Kluwer Academic publishers

Lu YH, Bauer JE, Canuel EA, Chambers RM, Yamashita Y, Jaffé R, Barrett A (2014) Effects of land use on sources and ages of inorganic and organic carbon in temperate headwater streams. Biogeochemistry 119:275-292. doi:10.1007/s10533-014-9965-2

Marutani, T., et al., 2008. The light and dark of sabo-dammed streams in steepland settings in Japan. In: River futures: an integrative scientific approach to river repair. Edited by Gary J.Brierley and Kirstie A. Fryirs Washington, DC: Island Press, 220–236

McClain ME et al. (2003) Biogeochemical Hot Spots and Hot Moments at the Interface of Terrestrial and Aquatic Ecosystems. Ecosystems 6:301-312 doi:10.1007/s10021-003-0161-9

McKnight DM, Boyer EW, Westerhoff PK, Doran PT, Kulbe T, Andersen DT (2001) Spectrofluorometric characterization of dissolved organic matter for indication of precursor organic material and aromaticity. Limnology and Oceanography 46:38–48.

Mizuyama T (2008) Structural Countermeasures for Debris Flow Disasters. International Journal of Erosion Control Engineering Vol. 1:38-43

Moran AM, Sheldon WMJ, Zepp RG (2000) Carbon loss and optical property changes during long-term photochemical andbiological degradation of estuarine dissolved organic matter.

Limnology and Oceanography 45:1254–1264: DOI: 10.4319/lo.2000.45.6.1254

Mostofa KMG, Honda Y, Sakugawa H (2005) Dynamics and optical nature of fluorescent dissolved organic matter in river waters in Hiroshima Prefecture. Japan Geochemical Journal 39: 257-271. doi.10.2343/geochemj.39.257

Murphy KR, Stedmon CA, Graeber D, Bro R (2013) Fluorescence spectroscopy and multi-way techniques. PARAFAC Analytical Methods 5: 6541–6882 doi:10.1039/c3ay41160e

Nie Z et al. (2016) Tracking fluorescent dissolved organic matter in multistage rivers using EEM-PARAFAC analysis: implications of the secondary tributary remediation for watershed management. Environmental Science and Pollution Research International 23:8756-8769. doi:10.1007/s11356-016-6110-x

O'Donnell JA, Aiken GR, Walvoord MA, Butler KD (2012) Dissolved organic matter composition of winter flow in the Yukon River basin: Implications of permafrost thaw and increased groundwater discharge. Global Biogeochemical Cycles 26: GB0E06 doi:10.1029/2012gb004341

Obernosterer I, Benner R (2004) Competition between biological and photochemical processes in the mineralization of dissolved organic carbon. Limnology and Oceanography 49:117–124. doi:10.4319/lo.2004.49.1.0117

Ohno T, Bro R (2006) Dissolved Organic Matter Characterization Using Multiway Spectral Decomposition of Fluorescence Landscapes. Soil Science Society of America Journal 70:2028-2037 doi:10.2136/sssaj2006.0005

Praise S, Watanabe T, Watanabe K, Ito H, Okubo H (2016) Impact of closed sabo dams on manganese concentration change in mountainous streams. International Journal of River Basin Management:1-8. doi:10.1080/15715124.2016.1209510

Rüegg J, Eichmiller JJ, Mladenov N, Dodds WK (2015) Dissolved organic carbon concentration and flux in a grassland stream: spatial and temporal patterns and processes from long-term data. Biogeochemistry 125:393-408. doi:10.1007/s10533-015-0134-z

Sakamoto and Yamaguchi, (2009). Water Storage, transport and distribution. Encyclopedia of life support systems, chapter 2. Edited by Yutaka Takahashi. Oxford, United Kingdom

Sazawa K, Tachi M, Wakimoto T, Kawakami T, Hata N, Taguchi S, Kuramitz H (2011) The evaluation for alterations of DOM components from upstream to downstream flow of rivers in Toyama (Japan) using three-dimensional excitation-emission matrix fluorescence spectroscopy. International Journal of Environmental Research and Public Health 8:1655-1670. doi:10.3390/ijerph8051655

Sharpless CM, Blough NV (2014) The importance of charge-transfer interactions in determining chromophoric dissolved organic matter (CDOM) optical and photochemical properties. Environmental Science: Processes & Impacts 16:654-671. doi:10.1039/c3em00573a

So TCP and Dong YC (2002) Fluorescence spectrophotometry Encyclopedia of life sciences. Macmillan Publishers, Nature PG

Sobczak WV, Raymond PA (2015) Watershed hydrology and dissolved organic matter export across time scales: minute to millennium. Freshwater Science 34:392-398. doi:10.1086/679747

Spencer RGM, Butler KD, Aiken GR (2012) Dissolved organic carbon and chromophoric dissolved organic matter properties of rivers in the USA. Journal of Geophysical Research: Biogeosciences 117: G03001 doi:10.1029/2011jg001928

Spencer RGM, Hernes PJ, Ruf R, Baker A, Dyda RY, Stubbins A, Six J (2010) Temporal controls on dissolved organic matter and lignin biogeochemistry in a pristine tropical river, Democratic Republic of Congo. Journal of Geophysical Research 115 G03013 doi:10.1029/2009jg001180

Stedmon CA, Bro R (2008) Characterizing dissolved organic matter fluorescence with parallel factor analysis: a tutorial Limnology and Oceanography: Methods 6:572–579. doi: 10.4319/lom.2008.6.572b

Stedmon CA, Markager S (2005) Tracing the production and degradation of autochthonous fractions of dissolved organic matter by fluorescence analysis. Limnology and Oceanography 50:1415–1426. doi: 10.4319/lo.2005.50.5.1415

Stedmon CA, Markager S, Bro R (2003) Tracing dissolved organic matter in aquatic environments using a new approach to fluorescence spectroscopy. Marine Chemistry 82:239-254. doi:10.1016/s0304-4203(03)00072-0

Suzuki T, Nagao S, Horiuchi M, Maie N, Yamamoto M, Nakamura K (2014) Characteristics and behavior of dissolved organic matter in the Kumaki River, Noto Peninsula. Japan Limnology 16:55-68. doi:10.1007/s10201-014-0441-4

Tanju K, Ilke E, Schlautman MA (2003) Selecting filter membranes for measuring DOC and UV254. Journal American Water Works Association 95:86-100.

Tfaily MM (2011) Molecular characterization of dissolved organic matter in northern peatlands: Identifying the chemical signatures of climate change. A Dissertation submitted to the Department of Chemistry and Biochemistry in partial fulfillment of the requirements for the degree of Doctor of Philosophy.

Thermospectronic (n.d), Basic Uv-vis theory, concepts and Applications

Twardowski MS, Boss E, Sullivan JM, Donaghay PL (2004) Modeling the spectral shape of absorption by chromophoric dissolved organic matter. Marine Chemistry 89:69-88. doi:10.1016/j.marchem.2004.02.008

Uyguner CS, Bekbolet M (2005) Implementation of spectroscopic parameters for practical monitoring of natural organic matter. Desalination 176:47-55. doi:10.1016/j.desal.2004.10.027

Vidon P, Wagner LE, Soyeux E (2008) Changes in the character of DOC in streams during storms in two Midwestern watersheds with contrasting land uses. Biogeochemistry 88:257-270. doi:10.1007/s10533-008-9207-6

Weishaar LJ, Aiken RG, Bergamaschi AB, Fram SM, Fujii R, Moppers K (2003) Evaluation of Specific Ultraviolet Absorbance as an Indicator of the Chemical Composition and Reactivity of Dissolved Organic Carbon. Environmental Science & Technology 37:4702-4708. doi:10.1021/es030360x

Wen ZD, Song KS, Zhao Y, Du J, Ma JH (2016) Influence of environmental factors on spectral characteristics of chromophoric dissolved organic matter (CDOM) in Inner Mongolia Plateau, China. Hydrology and Earth System Sciences 20:787-801. doi:10.5194/hess-20-787-2016

Yamashita Y, Boyer JN, Jaffé R (2013) Evaluating the distribution of terrestrial dissolved organic

matter in a complex coastal ecosystem using fluorescence spectroscopy. Continental Shelf Research 66:136-144. doi:10.1016/j.csr.2013.06.010

Yamashita Y, Kloeppel BD, Knoepp J, Zausen GL, Jaffé R (2011) Effects of Watershed History on Dissolved Organic Matter Characteristics in Headwater Streams. Ecosystems 14:1110-1122. doi:10.1007/s10021-011-9469-z

Yamashita Y, Scinto LJ, Maie N, Jaffé R (2010) Dissolved Organic Matter Characteristics Across a Subtropical Wetland's Landscape: Application of Optical Properties in the Assessment of Environmental Dynamics. Ecosystems 13:1006-1019. doi:10.1007/s10021-010-9370-1

Zhang Y, Liu X, Osburn CL, Wang M, Qin B, Zhou Y (2013) Photobleaching Response of Different Sources of Chromophoric Dissolved Organic Matter Exposed to Natural Solar Radiation Using Absorption and Excitation–Emission Matrix Spectra. PloS One 8:e77515. doi:10.1371/journal.pone.0077515.g001

5   Linking DOM characteristics to trace metals the sabo dammed streams

5.1   **Introduction**

Metal toxicity, bioavailability, and mobility in the environment are controlled by speciation (Yamashita and Jaffe, 2008, Worms et al., 2006, Slaveykova and Wilkinson, 2005). Natural organic matter (NOM) produces diverse mixtures of functional groups which interact strongly with trace metals creating avenues for both metal immobilization and transport (ElBishlawi and Jaffe, 2015; Montoura et al., 1978). Besides DOM, trace metals in aquatic environments exist are either in soluble form or adsorbed onto particles as a function of surface runoff from terrestrial environments, groundwater mixing, sediment dissolution, deposition from the atmosphere, redox conditions and anthropogenic activities Mohiuddin et al., (2012). Biotic and abiotic process controls their removal from the water column. Under reducing conditions, abiotic processes influence metallic ion or ionic species adsorption onto organic mineral substrates to form organometallic complexes (Tribovillard et al., 2006).

Natural waters contain a variety of trace metals which tend to have the ability to exist in more than one oxidation state and have affinities for both soft and hard ligands. These tend to compete to a greater or a lesser extent, bind with soft ligands (due to their high affinity) and removes them from solution (Warren and Haack 2001). DOM interacts with trace metals in various ways; such as affecting exerting metal abundance through DOM binding and chelation. DOM components especially humic substances which account for about 60-80% have the ability to form complexes with metals (Montoura et al., 1978, Terajima and Moriizumi 2013). For example in fresh water, despite the low concentration of ligands, complexation with humic compounds was observed to be 99% for Cu and Hg, other trace metals only bound 8% regardless of the being >70% dominating free ions (Montoura et al.,1998), Biken et al. (2011) found linear relationship between metal binding activity and DOM aromaticity in natural samples. This means that trace metal affinity increases with increasing humic substances. (Biken et al. 2011). Furthermore, DOM chemistry and composition is highly variable and depends on OM source and other environmental conditions such as temperature, ionic strength, pH, surface chemistry, and system microbiology (Leenheer and Croue, 2003, Elbadshwin and Jaffe 2015, Ren et al. 2015). DOM heterogeneity affects metal binding, due to changes in functional groups, and recently, incorporating a measure of DOM quality into speciation models has been deemed feasible

Mueller et al., (2012). Highly aromatic DOM such as humic substances favours the formation of highly stable complexes, hence reducing the concentration of free/labile metal ions (Gueguen and Clarisse 2011). Moreover, DOM is also recognized as a redox controlling factor (Kedziorek et al., 2007) hence a significant factor in the environmental behavior of many metals.

In addition to trace metal-DOM complexation, Fe and Mn oxide reduction are known to be potentially important pathways for organic matter degradation (Canfield et al. 1993, Kostka et al. 2002). Fe and Mn rich materials which can sorb other trace elements were found to contain relatively large amounts of organic matter (Tessier et al., 1996). In Mn rich deposits from a fresh water lake most trace metals were significantly (Ca, Cd, Cu, Ni, and Zn) correlated to Mn as well as to Fe in clear water (Tessier et al. 1996). In Tessier et al., 1996, OM sorbed to hydroxides was thought to be mainly humic substance (HA and FA,) and bacterial deposits and over the years, many studies on metal speciation mobility and ecotoxicology have incorporated NOM in aqueous models (Dudal and Gerald, 2004). Metal speciation studies on metal speciation using models usually neglect variation in DOM quality based on functional groups (Biken et al., 2011; Ren et al., 2015) yet, DOM quantity and DOM quality were found to have almost an equal impact on trace metal mobilization. Instead, assumption is always made regarding DOM composition i.e., 65% FA of which 35% is considered inert (Biken et al., 2011). Rivers are dominant pathways for trace metal and other elements Mohiuddin et al. (2012), whose behavior heavily relies on substrate sediment composition, suspended sediment composition, and water chemistry. Along the river stretch, changes have been noted for DOM and trace metal characteristics. In rivers with sabo dams, DOM behavior was found to be substantially affected demonstrated by increased aromaticity, molecular size in Chapter 4. Discrepancies regarding how to relate metal–DOM complexation behavior with acidic moieties of DOM still exist. Prevailing environmental conditions not only affect metal and NOM behavior but also influence the interaction between these two important elements. Hence a need for studies on trace metals and DOM interaction in various environmental settings.

5.2 Objectives of the study

The purpose of this chapter was to assess how dissolved organic matter characteristics and dissolve trace metals are related in streams and to show how DOM composition characteristics affect dissolved trace metal fate and behavior along the stream gradient. We

hypothesize that fulvic acid fraction (C1) observation are dependent on observed metal concentration especially around sabo dams. Furthermore, this chapter covers the general objective of the study *i.e.,* To elucidate the impact of sabo dams on the behavior and fate of trace metals and DOM behavior in mountainous streams.

5.3   Material and method

Results from chapter 3 and 4 for the mains study sites (3.2.1) were used together with statistical analysis in this section.

Correlation analysis was used to test the hypothesis that DOM characteristic are linked to the observed dissolved trace metals around the dams. While PCA and cluster analysis were used to analyze trace metals, DOM characteristics and physicochemical properties to elucidate the overall impact of sabo dams on the behavior of trace metal and DOM. Hierarchical clustering was applied to identify linkage between the studied sites.

5.4   Results and discussion

5.4.1   UV-vis DOM spectral properties, PARAFAC components, and dissolved trace metal correlations

Both total and dissolved forms of Mn and Fe correlated differently at each station. As expected, a negative correlation between C1 was observed at St.1 and St.4. Neither total Fe nor Mn were significantly correlated with any DOM characteristic at St.1, regardless of being strongly correlated to each other (r=0.917, p<0.001). The dissolved forms, however, were negatively correlated to $S_{275-295}$ an indicator of molecular size (r=-0.843, p<0.001 for Fe Diss and -0.621, p<0.05 for MnDiss). A Strong relationship was found between trace metal (total fraction of Zn, Pb, and Cd) and PARAFAC components (C2 and C3) while dissolved Cu and Cr showed a significant positive correlation with a ratio of C1 to C3. At St 2, In addition to Fe and Mn (both forms), dissolved forms of Cr and Zn significantly correlated with C1 whereas total forms of Cu and Zn showed a moderate significant correlation with DOC (r=0.531 and 0.537, p<0.05 for Cu and Zn respectively. Also the ratio of C1 to C2 appear to be a major factor for most of the analyzed metals (Fe, Cr, Mn Ni and Cd) after moderate significant correlation were observed (Table 5A-1). At St.2, only two trace metals significantly correlated with Fe and Mn *i.e.,* CrDiss and ZnDiss. At all the four stations, both Fe and Mn were strongly correlated with each other, very strong significant relation, especially with dissolved forms, was observed at St.1 and St.3

(r=<0.9, p<0.001) (Table 5A-1).

DOC and Mn interdependence was exhibited at St.3 with the strong positive significant correlation between most of the trace metals and DOC properties (Table 5A-1). Both Mn and Fe correlated positively with C1, $SUVA_{254}$, and a350 and negatively with E2: E3 ratio, S_R, and $S_{275-295}$. Such significant correlations at St.3 reveal the association and interdependence of these elements under changing environmental conditions as observed in sediments by Zhang et al., (2002) and Canfield et al., (1993). Also, Cu, Cr, Ni, Zn, Pb and Al were also correlated to some DOM characteristics although these showed a positive relation with DOM properties for molecular size (S_R, E2: E3, and $S_{275-295}$). At St.4, only PbDiss was strongly connected to both C1 and C2. Also FeDiss had significant correlations with all the three components identified by PARAFAC. In addition Zn, CrDiss, PbDiss and AlDiss showed correspondences to molecular size CDOM property ($S_{275-295}$).

In the previous chapters (II and III), the trend of Mn, Fe and DOM in streams with Sabo dams was clearly elaborated. However, since all these elements are related, especially humic substances play a major role in trace metal abundance. The association between trace metals and DOM composition in environmental setting was investigated. At st.1 and St.4, correlation for Fe, Mn, and DOM composition were negative, showing an inverse association between these elements. Although at St.1 no significant correlations were observed between the metals and DOM while at St.4, total Fe and Mn forms were significantly correlated to C1 and C3, dissolved Fe was significantly correlated to all three components identified by PARAFAC while dissolved Mn   C1 and C3(r=<-0.5, p<0.05) (Table 5A-1).
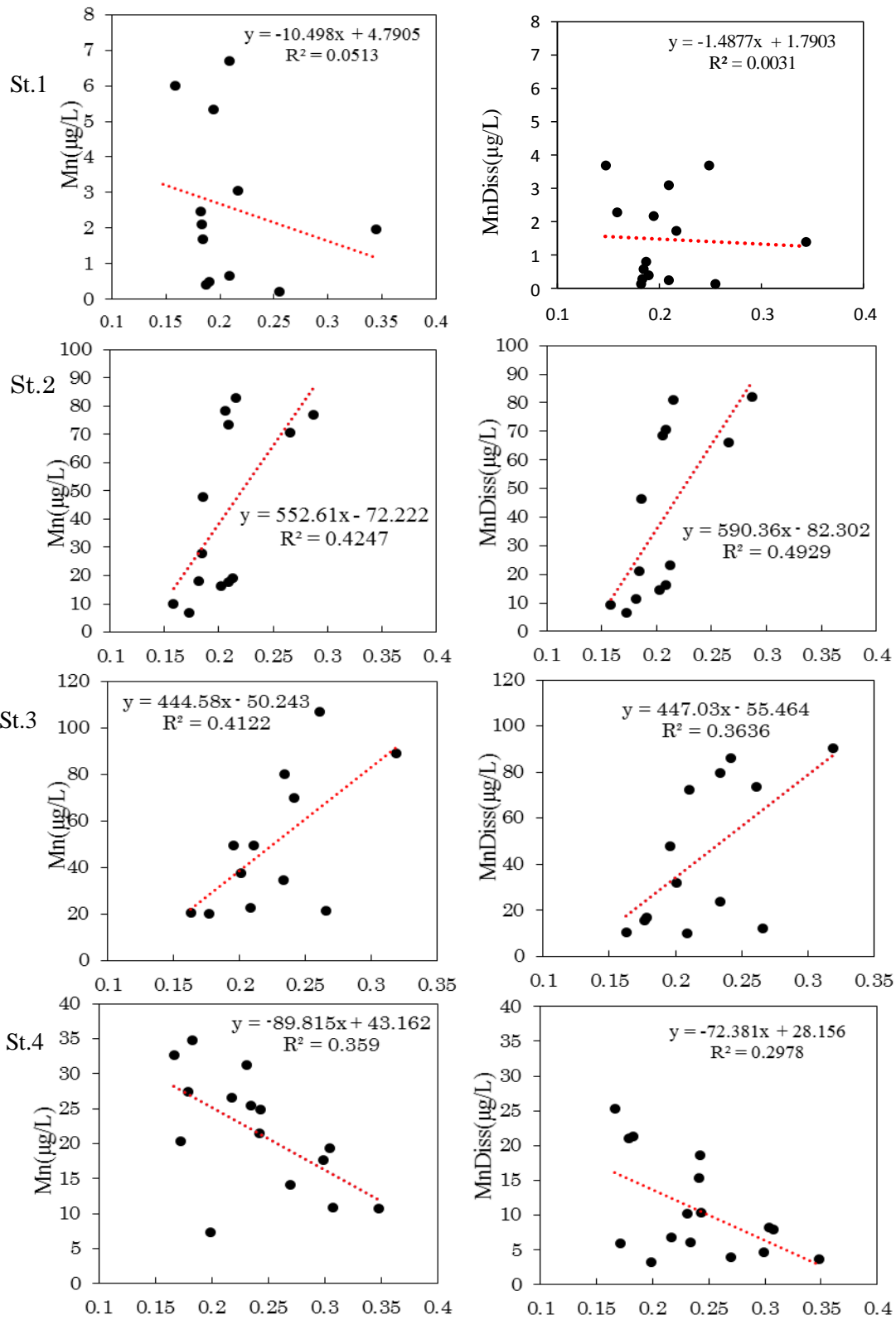
Figure. 5-1   Linear fit for total and dissolved Mn vs PARAFAC C1 per station
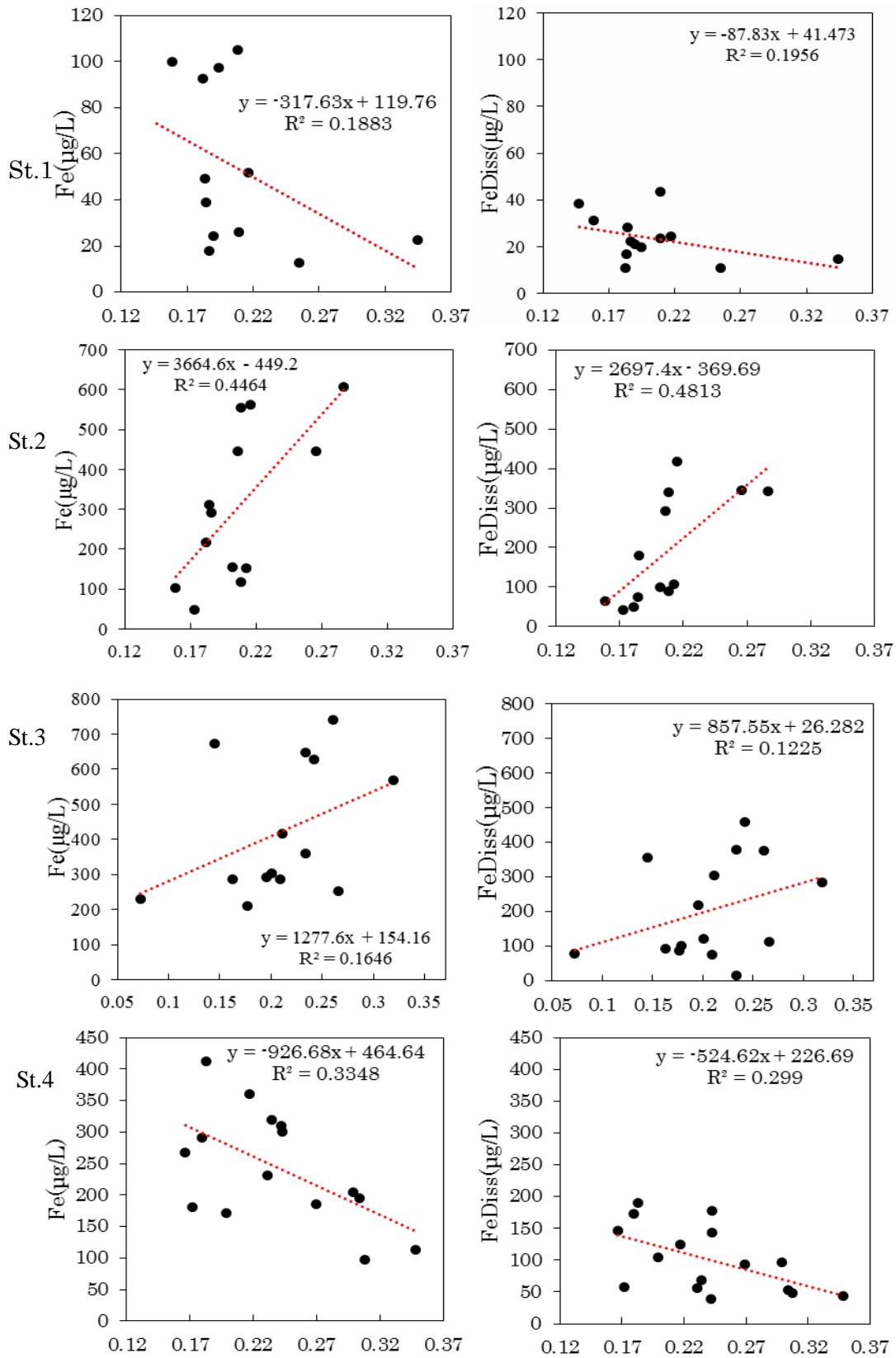
Figure. 5-2 Linear fit for total and dissolved Vs C1 Fe per station

Positive correlations with C1 at St.2 for both total and dissolved Fe and Mn, and positive correlation for total metals and C1 and to $SUVA_{254}$, a350 at St.3 St.2 and St.3 with $SUVA_{254}$, Fe and Mn (both total and dissolved forms) significant regardless of high correlations between these Fe and Mn (Figure 5-1, 5-2 and Table A-5). Mn and Fe hydroxides have been described as good scavengers for other trace metals, however, in the studied stations, total Al (St.1), dissolve Cr, Zn (St.2) and dissolved Cr (St.3) were the only metals significantly correlated with total Fe and Mn (Table A-5). Most of the trace metals lacked significant correlations with PARAFAC components (C1 or C2) at St.2 and St.3 an indication that other factors influenced the interactions between trace metals and DOM. For example, Cu has a strong affinity with organic ligands including humic substances and has been extensively studied under laboratory conditions. However, in this study, total CuDiss only showed significant correlation with a ratio of humic acid-like to fulvic acid-like (C1: C2 ratio) at St.1 and with molecular size at St.3 (Table A-5).

From correlation with CDOM properties and PARAFAC component (C1) at St.3 results at St.2, it is evident that Mn shows slightly stronger significant correlations than Fe. For example; Figure 5-2 and Table A-5, correlation between Fe_{Tot} and C1 was significant at r=0.59, p<0.05 (FeDiss at r=0.45 was not significant) while Mn at r=0.64 and 0.60 significant at p<0.05 for total and dissolved forms. Although Fe is more abundant than Mn oxides are more reactive than Fe and have a strong ability to scavenge a variety of metals (Warren and Hack, 2001). Also Mn may persist in the environment longer that Fe since in conditions prevailing in most surface water, Mn oxidation is mostly controlled by the biological process (Warren and Hack, 2001; Tebo et al., 2005).

The absence of strong and significant correlation between other metals and PARAFAC components is in line with the observation made by Montenoura et al., (1998) that trace metals are bound directly to hydroxyl groups of Fe or Mn oxyhydroxides and not to functional groups of adsorbed humic substance. Regardless significant relationship between Fe, Mn and CDOM and PARAFAC components, the processes happening within the reservoir are evident from the results at St.3. During reduction of metal hydroxides, reduced forms diffuse to both pore and surface water. At St.2, only a small fraction of the products of organic matter decomposition under an oxic condition in the underlying sediments is present as opposed to St.3. According to Kaiser and

Sulzberger (2003) observations, chemical reactions involved in stream process and along the continuum appear to be strongly dependent on the chemical composition of riverine DOM.

High molecular weight and hydrophobic components of DOM are derived from the leaching of soils containing highly altered plant material and prokaryotic biomass (Kaiser et al. 2003). The presence is the high molecular compounds at St.2 and St.3 was concomitant with high Fe and Mn concentrations. The recalcitrant nature of DOM, in addition to environmental conditions in the dam reservoir, results in an abundance of both Fe and Mn hence the observation at St.2 and St.3 regardless of the absence of decomposing matter at St.3 (Figure 5-1). The drastic decrease in Mn and Fe concentration between St.3 and St.4 despite inflow from anthropogenic sources (Figure 3-5 and 3-6), is not only related to photo-induced redox cycling but also the nature of DOM. Since DOM character changes seem to be coupled with Fe and Mn concentration change along the stream. DOM around the dams contains high amounts of lignin that are three-dimensional amorphous cross-linked aromatic polymers. The polymers contain some metal-binding functional groups including phenolic, hydroxyl and carboxyl groups making it a suitable adsorbent material for heavy metals. An increase in lignin-type humic acid resulted in higher level of heavy metal content in the sediment (Aryal et al., 2015). Hence the loss of high molecular weight DOM between stations is accompanied by a removal and precipitation of trace metals (Fe and Mn).

Origin of organic matter is important in determining and influencing of its behavior and interaction with other elements, at St.1 and St.4 low molecular weight character. Low molecular weight DOM derived from fresh fine particulate and autochthonous sources is hydrophilic in nature (Kaiser and Sulzberger, 2003) therefore, metal concentration especially Fe and Mn are likely to show and inverse relationship as observed at St.1 and St.4.

During transport from head streams to oceans, metals undergo through various processes transforming from one phase to another. Some metals are impeded and removed by processes such as sorption and precipitation (Luan and Vadas 2015) while other are eliminated via flocculation following water chemistry changes i.e., ionic strength and pH. Most of the changes in surface water result from mixing of water different sources. Metal-DOM interactions trends vary significant between the natural and anthropogenically influenced waters (Biken et al., 2011). Strong affinity exhibited between DOM influenced by anthropogenic factors and metals (Biken et

al., 2011) indicated the presences of other ligands other than natural humic substances. This scenario is evident in variation between the stations (St.1 and St.4). Although CDOM properties revealed characteristics dominated by low molecular weight organic compounds, correlation between trace metals (Fe, Mn and Pb) further showed the difference in DOM composition. Other trace metals (Zn, Cr, Cd and Al) were only associated with CDOM property molecular weight. According to Biken et al., (2011) anthropogenic ligands have limited effect on Zn speciation in surface water, which explains the difference in significant correlations observed for total Zn with C1, C2 and DOM concentration at St.1. Yet no significant correlations were observed at St.4 with any of the DOM properties except $S_{275-295}$ (Table 5A-1).

5.4.2   PCA and cluster analysis results

PCA analysis was used to explain which DOC properties and trace metals explained the observations made at each station. From the PCA loadings, three principal components (PCs 1, 2 and 3) with Eigen values greater than two accounting for 52.9% explained variance were used. The first 2 PCs explaining 42.5% of the total variance were correlated to FeDiss, MnDiss, CDOM properties and PARAFAC components pH (Fig 5-3, Tables 5-1 and A-6)

Table 5-1 Loadings of variables on three principal components

	1 (25.8%)	2 (16.8%)	3 (10.6%)
FeDiss	-.900	.030	.014
CuDiss	.169	-.211	.242
CrDiss	.309	.022	-.462
MnDiss	-.887	.035	-.005
ZnDiss	-.163	.032	.018
AlDiss	.470	-.105	.405
C1	.093	-.602	.340
C2	.186	.861	-.121
C3	.224	.829	-.187
DOC	.266	.798	.209
$SUVA_{254}$	-.708	.348	.355
a350	-.813	.207	.358
E2:E3	.714	-.398	-.230
S_R	.663	-.160	.362
S275295	.777	-.320	.154
DON	-.325	-.490	.260
pH	.559	.400	.414
Temp	.087	.384	.391
DO	.297	.226	-.157
ORP	.483	.342	-.230
EC	.269	.156	.821
Turbidity	.017	.116	.146

Cd, Pb, Ni, were excluded from analysis since most of the values were below QL
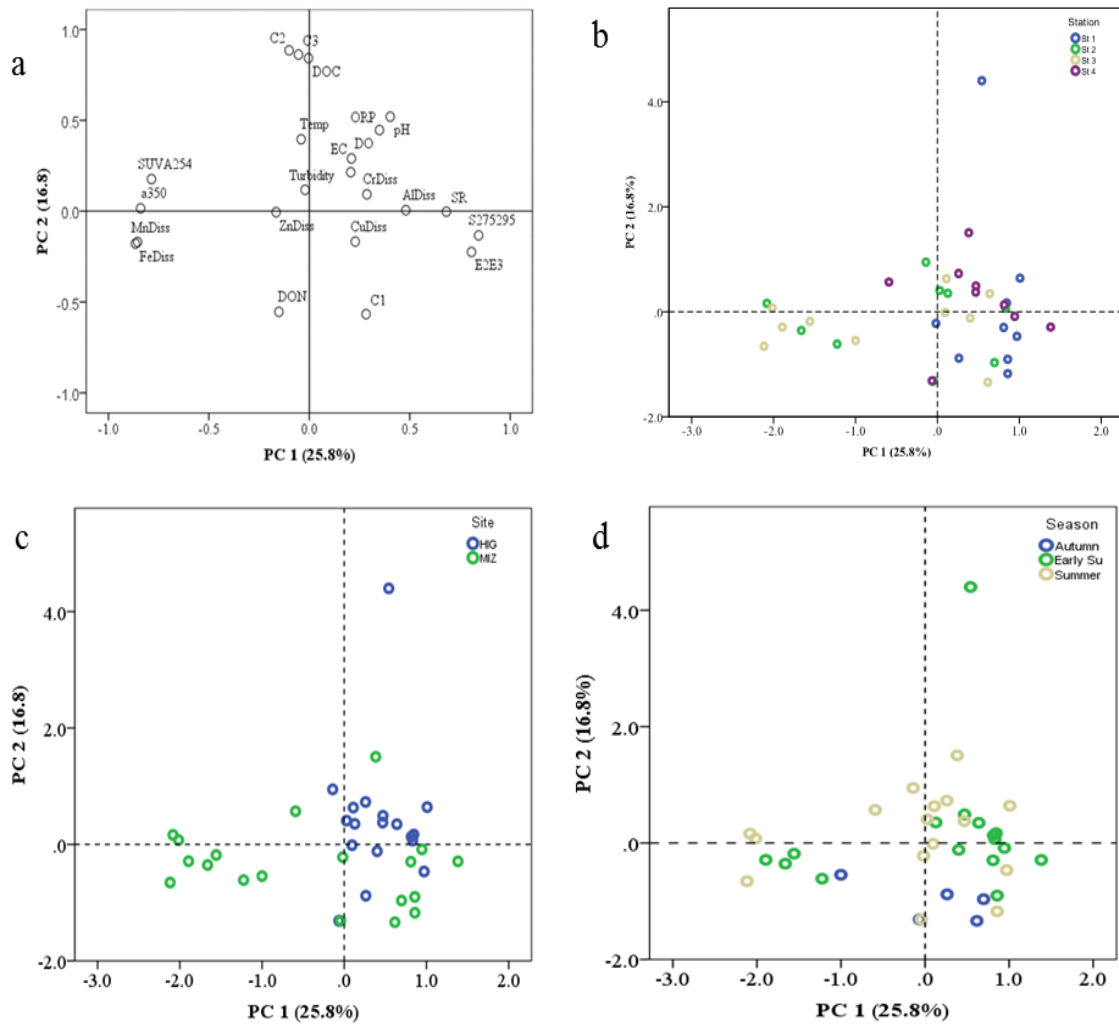
Figure. 5-3 Principal component analysis ordination and score plots of trace metals and DOC properties for sites HIG and MIZ on the first and second PCs, a-Variable loadings score for dissolved trace metals and DOC properties, scores for stations, c-scores for each site, d-scores for
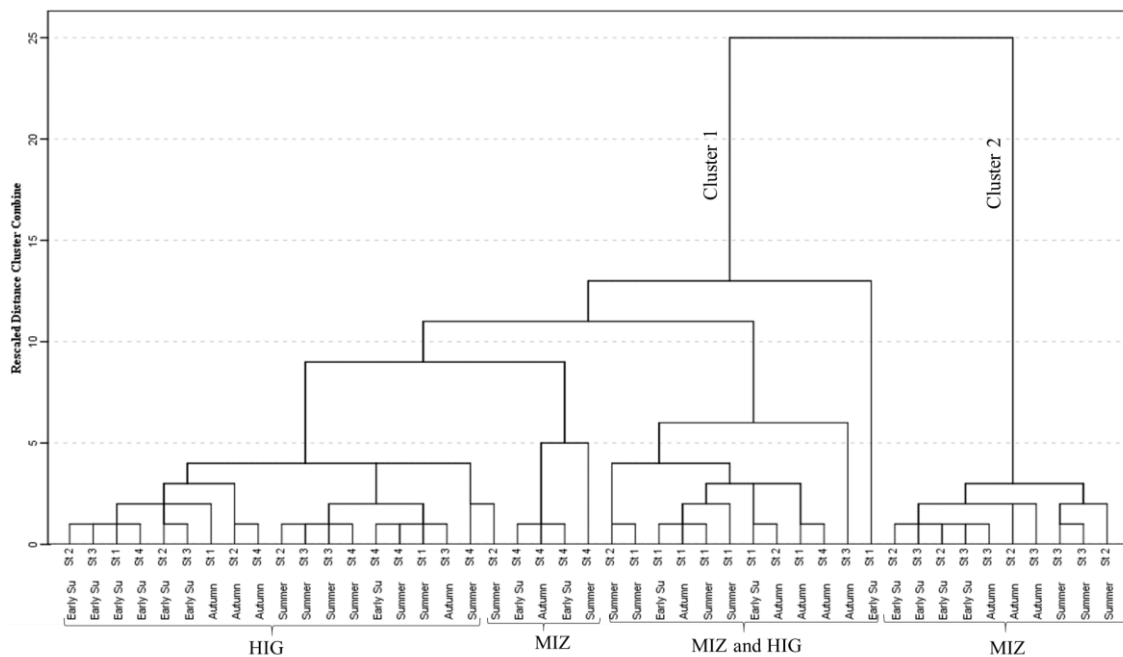
Figure. 5-4 Two clusters for the samples classified by wards method separating St.2 and St.3 at

The first loadings separated dissolved metals Fe, Mn, Cu, Zn, and DON, and DOM properties C1 (humic acid), molecular size (E2:E3, $S_{275-295}$) from environment variables pH, DO, EC, ORP, Temperature and DOM properties C2, C3, $SUVA_{254}$, $a350$ and DOC concentration (Figure 5-3a). Samples from St.2 and St.3 at MIZ were more linked to trace metals and DOM properties (Figure 5-3b, 5-3c) as opposed to samples from the other stations. Scores for samples from HIG had positive factors on the second principal component (PC 2) while samples for autumn sampling were differentiated from other sampling seasons by PC 1 (Figure 5-3c and 5-3d).

The loading on the first and second principal components reveal how important MnDiss, FeDiss and DOM composition are outstanding in the influencing the characteristics of each studied sites. Trace metals (MnDiss and FeDiss) and DOM properties CDOM concentration ($a350$ and aromaticity) with negative factors on PC 1 were distinguished from molecule size and pH which loaded positively on PC 1. The variables with strong loadings on PC 1 and PC 2 as well as environmental variable pH and EC signify the importance of MnDiss and FeDiss and DOM character under changing environmental conditions. Further analysis with hierarchical analysis categorized all the samples into two main clusters (Figure 5-4). The two groups showed St.2 and St.3 at MIZ were significantly different from other sites. Within cluster one, St.4 samples from

MIZ had unique characteristic from HIG samples from all stations and summer sample for MIZ at St.2. These samples characteristics were again different from St.1 samples from both HIG and MIZ majorly influenced by the season.

DOM and trace metals are affected by seasonal variability, type, source and time of release (Carstea et al 2012). The influence of Fe, Mn and Fe revealed by PC 1 further confirms what other studies have observed (Wu et al., 2004). Fe is the most abundant metal in the environment and has high binding strength compared to other metals (Wu et al 2004), in addition the role of Mn oxides have been described in the sections above. From the clusters, MIZ st.2 and St.3 characterized by high Mn and Fe concentrations and high molecular aromatic DOM presented unique characteristics from other stations. These characteristics contrast areas with anthropogenic influences (St.4) indicating a strong influence by dam.

5.5   Summary

In this chapter, the link between changing DOM properties and metals Mn and Fe was investigated in detail. A negative relationship between dissolved forms of Mn and Fe was found in the upstream (St.1) and downstream (St.4) with fulvic acid-like fraction (C1). While around sabo dams, a positive relationship was observed with C1, a more significant interaction between DOM properties with Mn and Fe was evident at St.3 (immediate downstream of the dam). From hierarchical clustering results, the characteristic of around the dam for one of the sites (MIZ) was significantly different from all the stations. This shows that sabo dams influence the characteristics of the streams. However their influence may be site related and more evident in some streams as opposed to others.

References

Aryal R, Furumai H, Nakajima F, Beecham S, Kandasamy J (2015) Characterisation of Prolonged Deposits of Organic Matter in Infiltration System Inlets and Their Binding with Heavy Metals: a PARAFAC Approach Water, Air, & Soil Pollution 226 doi:10.1007/s11270-015-2426-2

Canfield, D.E., Thandrup, B. and Hansen, J.W., 1993. The anaerobic degradation of organic matter in Danish coastal sediments: iron reduction, manganese reduction and sulphate reduction. Geochemica et cosmochemica Acta, 57, 3867-3883.

Cârstea EM, Ghervase L, Pavelescu G, Iojă CI (2012) Correlation of Dissolved Organic Matter Fluorescence and Several Metals Concentration in a Freshwater System Procedia Environmental Sciences 14:41-48 doi:10.1016/j.proenv.2012.03.005

ElBishlawi H, Jaffe PR (2015) Characterization of dissolved organic matter from a restored urban marsh and its role in the mobilization of trace metals Chemosphere 127:144-151 doi:10.1016/j.chemosphere.2014.12.080

Gueguen C, Clarisse O, Perroud A, McDonald A (2011) Chemical speciation and partitioning of trace metals (Cd, Co, Cu, Ni, Pb) in the lower Athabasca river and its tributaries (Alberta, Canada) Journal of environmental monitoring : JEM 13:2865-2872 doi:10.1039/c1em10563a

Ingri, L.J., et al., (2011) Manganese redox cycling in lake Imandra: Impact on nitrogen and the trace metal sediment record. Biogeosciences Discuss, 8,273-321. DOI 10.5194/bgd-8-273-2011

Kaiser E, Sulzberger B (2004) Phototransformation of riverine dissolved organic matter (DOM) in the presence of abundant iron: Effect on DOM bioavailability Limnol Oceanogr 49:540–554

Karbassi AR, Monavari SM, Nabi Bidhendi GR, Nouri J, Nematpour K (2008) Metal pollution assessment of sediment and water in the Shur River Environmental monitoring and assessment 147:107-116 doi:10.1007/s10661-007-0102-8

Kedziorek MAM, Geoffriau S, Bourg ACM (2008) Organic Matter and Modeling Redox Reactions during River Bank Filtration in an Alluvial Aquifer of the Lot River, France

Environmental science & technology 42:2793-2798 doi:10.1021/es702411t

Kostka JE, Luther III GW, Nealson KH (1995) Chemical and biological reduction of Mn (III) -pyrophosphate complexes: Potential importance of dissolved Mn (III) as an environmental oxidant Geochimtca et Cosmochimica Acta S9 5

Leenher JA, Croué J-P (2003) Organic matter characterization. Aquatic organic matter; Understanding the unknown structures is key to better treatment of drinking water Environmental science & technology 19 A

Luan H, Vadas TM (2015) Size characterization of dissolved metals and organic matter in source waters to streams in developed landscapes Environmental pollution 197:76-83 doi:10.1016/j.envpol.2014.12.004

Mohiuddin KM, Otomo K, Ogawa Y, Shikazono N (2012) Seasonal and spatial distribution of trace elements in the water and sediments of the Tsurumi river in Japan Environmental monitoring and assessment 184:265-279 doi:10.1007/s10661-011-1966-1

Montoura RFC, Andrew Dickson, Riley JP (1978) the complexation of metals with humic material in natural waters. Estuarine and coastal marine science 6, 387-408

Mueller KK, Lofts S, Fortin C, Campbell PGC (2012) Trace metal speciation predictions in natural aquatic systems: incorporation of dissolved organic matter (DOM) spectroscopic quality Environmental Chemistry 9:356 doi:10.1071/en11156

Ren Z-L et al. (2015) Effect of dissolved organic matter composition on metal speciation in soil solutions Chemical Geology 398:61-69 doi:10.1016/j.chemgeo.2015.01.020

Shikazono N, Tatewaki K, Mohiuddin KM, Nakano T, Zakir HM (2012) Sources, spatial variation, and speciation of heavy metals in sediments of the Tamagawa River in Central Japan Environmental geochemistry and health 34 Suppl 1:13-26 doi:10.1007/s10653-011-9409-z

Tebo BM, Johnson HA, McCarthy JK, Templeton AS (2005) Geomicrobiology of manganese(II) oxidation Trends Microbiol 13:421-428 doi:10.1016/j.tim.2005.07.009

Terajima T, Moriizumi M (2013) Temporal and spatial changes in dissolved organic carbon concentration and fluorescence intensity of fulvic acid like materials in mountainous headwater catchments Journal of Hydrology 479:1-12 doi:10.1016/j.jhydrol.2012.10.023

Tessier A, Fortin D, Belzile N, R. Devitre R, and G. Leppard (1996) Metal sorption to diagenetic

iron and manganese oxyhydroxides and associated organic matter. Geochimica et Cosmochimica Acta, Vol. 60, No. 3, pp. 387-404

Slaveykova VI, Wilkinson KJ (2005) Predicting the bioavailability of metals and metal complexes: Critical review of the biotic ligand model Environ. Chem. 2, 9-24

Warren LA, Haack EA (2001) Biogeochemical controls on metal behaviour in freshwater environments Earth-Science Reviews 54:261-320 doi:10.1016/s0012-8252(01)00032-0

Worms I, Simon D.F, Hassler CS, Wilkinson KJ (2006) Bioavailability of trace metals to aquatic microorganisms: importance of chemical, biological and physical process on biouptake Biochimie 88, 1721-1731 doi:10.1016/j.biochi.2006.09.008

Wu FC, Cai YR, Evans RD, Dillon PJ. (2004) Complexation between Hg(II) and dissolved organic matter in stream waters: an application of fluorescence spectroscopy. Biogeochemistry 71: 339 351

Youhei Yamashita and Rudolf Jaffe (2008). Characterizing the Interactions between Trace Metals and Dissolved Organic Matter Using Excitation-Emission Matrix and Parallel Factor Analysis. Environ. Sci. Technol. 2008, 42, 7374–7379

Zhang, H., et al., 2002. Localised remobilization of metals in a marine sediment. Science of the Total Environment, 296(1), pp.175-187.

6   Conclusion and recommendations

6.1   Conclusion

The importance of trace metals and role of DOM are widely known. However, there are gaps regarding how these two elements interact and behave in various environments. In this thesis, both DOM and metals behaviors were investigated along the continuum in mountainous streams. Mountainous ecosystems are rich in both micro and macro environment, and along the stream continuum particulate organic matter is broken down and is accompanied by biogeochemical cycles transformation. Water impediment and organic matter retention in sabo dams did not only result in the dissolution of stable hydroxides but also modified DOM composition. The nature and characteristics of DOM are very crucial in determining the fate of many metals by providing suitable ligands.

Both Mn and Fe concentrations were observed to increase drastically in the dam vicinity and this was simultaneous with changes in DOM molecular weight and aromaticity. Although DOM concentration was not significantly affected by the presence of sabo dams, changes in DOM characteristics were evident. These observations were made in the two major study sites (Mizunashigawa (MIZ) and Higashiiwamotogawa (HIG), but other metals did not show such a trend along the stream. Trace metal concentrations were drastically high around sabo dams (Figure 3-5) with more than two fold increase for Mn between upstream sections of the dam. Regarding DOM composition characteristics changes, an increase in aromatic content and molecular weight were more pronounced within the dam vicinity.   Generally, areas around the dam were significantly different from other stations with regard to DOM composition and Fe and Mn concentrations. However, both Fe and Mn were influenced by site and location along the stream (two-way ANOVA at p $\leq$0.001). Also, Fe and Mn were found to have a positive correlation with humic substances in the stations near Sabo dam surrounding as opposed to the upstream and downstream locations (Figure 5-1). Regardless of such changes along the stream, PARAFAC components did not show a similar pattern. Three PARAFAC components were dominated by fulvic-like component 4-4, the ratio of Fulvic like to humic-like was between 2.1 to 3.1. The impact of sabo dams revealed by unique features exhibited around the dams characterized by high Mn and Fe concentrations together with increase DOM aromaticity, and dominated by high molecular weight organic matter. This may influence the function of the stream depending on the

size and length of the stream, and the capacity of the dam. From metal concentration changes and DOM composition along the stream it is evident the dams had a significant impact on the behavior of these elements, however, in some case the impacts may be more as observed at MIZ.

These findings are important in bridging the gaps in studies involving trace metals and DOM in along changing conditions. Furthermore, this opens the door to new questions on specific interactions within the dam reservoir and to what extent do these interactions affect downstream communities and the whole watershed at large.

6.2   Recommendations

In this study, the trend of Mn, Fe, and DOM along sabo dammed streams together with Sabo dam impacts on these elements have been investigated. However, since DOM and metals flux are related to terrestrial environments, it is essential to include temporal and spatial environmental changes in any future research. I recommend long term monitoring of DOM and metal loading in streams and using geographical information systems based techniques together with stable isotopes will elaborate more on sources and sinks of both DOM and metals which are important in determining their ultimate fate.

The association between DOM and metals is enhanced by DOM characteristics and free metals ions. In this study, dissolved metals form was used to represent free ions. Also, DOM was treated as a bulk, hence applying methods that separated and classify DOM such as high-performance liquid chromatography (HPLC) is recommended. Therefore to further understand the dynamics of both DOM and metals, I recommend employing other techniques that can quantify free and bioavailable metals that participate in reactions. The interaction between metals and DOM in the aquatic environment is influenced by various factors such as hydrological events, residence time, light penetration and microorganisms among others, especially in dammed streams. These should, therefore, be integrated into future research along with experimental concepts and models.

Appendix

Table A-1 Sampling sites at the five sites in 2015

Site	2015		
	Early Summer	Summer	Autumn
MIZ	22nd June; 13th July	13th & 28th Aug	14th Sept;22nd
HIG	22nd June; 15th July	13th & 28th Aug	14th Sept;22nd
KSW	2nd June	20th Aug	18th Nov
IMO	19th June	27th Aug	26th Nov
MNK	3rd July	27th Aug	16th Nov

The main study sites (MIZ and HIG) were sampled monthly while KSW, IMO, and MNK samples were collected in June, August and November.
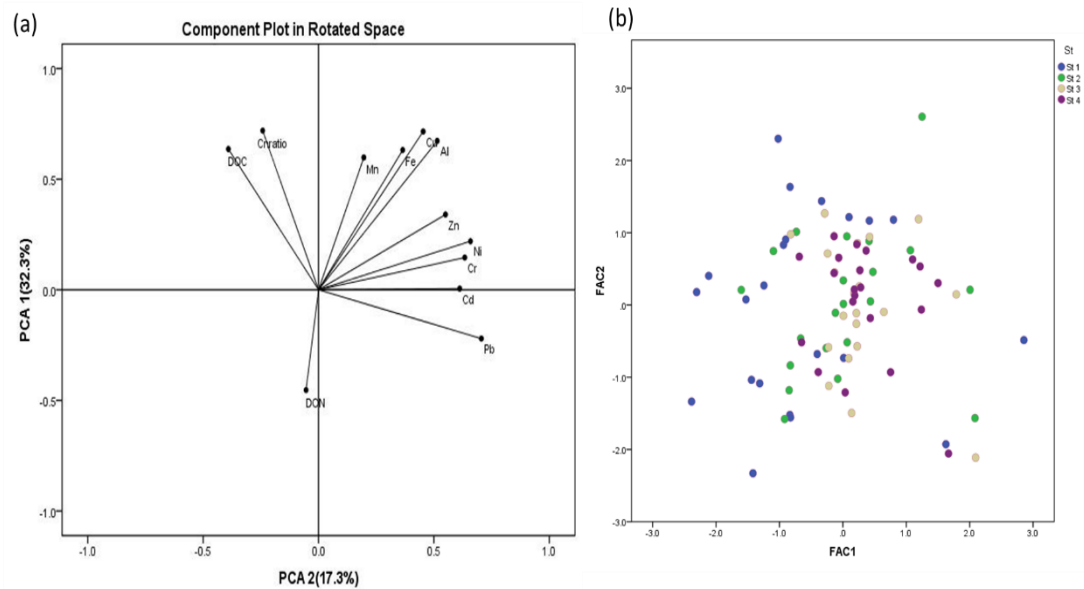
Figure A-1 PCA analysis plots; (a) Variable loading on PCs 1 and 2, (b) shows factor scores for each station on the 1st and 2nd PCs

Table A-2 Total and dissolved metal concentration measured at KSW, MNK and IMO

Site	Date	Station	Total									Dissolved								
			Fe	Cu	Cr	Mn	Ni	Zn	Pb	Cd	Al	Fe	Cu	Cr	Mn	Ni	Zn	Pb	Cd	Al
KSW	6/2/2015	St.1	2910.00	8.41	4.29	56.85	4.28	52.21	1.73	0.06	2293.33	128.07	0.79	0.52	4.13	0.74	11.07	0.21	0.02	92.50
	6/2/2015	St.2	701.85	3.34	6.60	28.56	5.23	24.85	1.82	0.36	481.46	99.07	0.78	0.53	12.80	1.37	6.29	0.27	0.02	69.30
	6/2/2105	St.3	644.81	2.19	1.00	37.08	1.46	18.41	0.49	0.03	410.68	115.10	1.19	0.32	21.42	1.37	8.12	0.21	0.02	56.80
	6/2/2015	St.4	1315.31	10.47	169.97	39.03	91.18	15.00	1.16	0.09	419.92	223.95	153.05	0.52	11.77	2.27	10.36	2.22	0.03	244.98
	20/08/2015	St.1	54.61	1.06	0.20	4.60	0.67	5.67	0.13	0.01	43.66	39.70	1.60	<Q.L.	5.10	1.10	6.70	<Q.L.	<Q.L.	28.60
	20/08/2015	St.2	131.75	0.85	0.16	81.41	0.83	14.22	0.15	0.02	44.53	140.00	1.20	<Q.L.	125.00	1.60	8.30	<Q.L.	<Q.L.	15.30
	20/08/2015	St.3	261.22	0.93	0.17	103.51	0.96	2.91	0.09	0.01	26.19	301.00	1.20	<Q.L.	144.00	1.50	7.00	<Q.L.	<Q.L.	21.30
	20/08/2015	St.4	236.42	0.86	0.17	7.87	0.72	2.32	0.16	0.01	36.67	289.00	1.20	<Q.L.	6.40	1.20	6.80	0.20	<Q.L.	22.30
	18/11/2015	St.1	343.00	1.70	0.90	17.00	1.80	8.10	0.30	<Q.L	148.00	135.00	1.30	0.40	12.10	1.50	7.20	0.20	<Q.L.	60.10
	18/11/2015	St.2	351.00	1.50	2.00	34.80	2.10	6.30	0.30	<Q.L	148.00	144.00	1.00	0.60	33.60	1.60	3.90	0.20	<Q.L.	44.70
	18/11/2015	St.3	453.00	1.60	0.50	46.00	1.70	7.20	0.30	<Q.L	148.00	208.00	1.10	0.20	40.50	1.40	3.90	0.20	<Q.L.	61.60
	18/11/2015	St.4	474.00	1.60	0.70	26.30	1.60	5.00	0.30	<Q.L	196.00	165.00	0.90	0.20	18.80	1.20	2.60	<Q.L.	<Q.L.	41.10
IMO	19/6/2015	St.1	53.15	0.68	2.22	1.87	0.65	7.75	0.41	0.01	58.35	128.00	0.50	<Q.L.	14.10	Q.L.以下	5.50	0.20	<Q.L.	18.90
	19/6/2015	St.2	41.63	0.64	0.74	1.87	0.32	6.95	0.18	0.01	49.04	13.20	0.60	<Q.L.	0.60	Q.L.以下	5.60	<Q.L.	<Q.L.	22.10
	19/6/2015	St.3	138.91	0.61	0.25	11.81	0.52	12.53	0.19	0.01	50.65	187.00	1.50	<Q.L.	4.40	7.00	17.40	1.20	<Q.L.	121.00
	27/08/2015	St.1	19.16	0.46	0.15	0.94	0.27	4.23	0.15	0.01	24.08	408.00	0.50	<Q.L.	31.40	Q.L.以下	17.10	<Q.L.	<Q.L.	13.30
	27/08/2015	St.2	24.80	0.47	0.15	1.85	0.17	3.14	0.18	0.01	14.38	23.06	0.46	1.50	2.07	1.03	3.36	0.17	0.01	18.13
	27/08/2015	St.3	424.56	0.53	0.20	33.67	0.04	3.83	0.18	0.01	20.97	29.60	0.60	<Q.L.	0.70	0.90	4.90	0.20	<Q.L.	25.50
	26/11	St.1	19.90	0.40	<Q.L.	0.60	<Q.L.	3.20	<Q.L.	<Q.L.	20.60	ND	ND	ND	ND	ND	ND	ND	ND	ND

Area	Date	Station																			
	26/11	St.2	23.00	0.30	<Q.L.	0.90	<Q.L.	1.60	<Q.L.	<Q.L.	17.00	ND	ND	ND	ND	ND	ND	ND	ND	ND
MNK	7/3/2015	St.1	280.21	2.13	14.96	5.74	1.98	6.58	0.16	0.01	231.86	11.97	0.43	0.19	0.30	0.27	8.14	0.43	0.01	16.19
	7/3/2015	St.2	258.76	2.02	0.54	26.54	0.65	21.01	0.40	0.04	203.10	26.00	0.31	0.06	21.39	0.14	1.61	0.06	0.01	12.40
	7/3/2015		669.96	5.65	1.06	19.61	1.11	26.71	0.53	0.03	680.83									
	7/3/2015	St.3	183.84	0.90	0.90	36.06	0.46	5.39	0.17	0.01	77.96	87.86	0.29	0.06	47.89	0.26	1.87	0.09	0.01	9.21
	7/3/2015	St.4	163.22	1.02	0.51	32.77	0.64	32.84	1.05	0.08	64.35	77.96	0.60	0.28	25.63	0.28	17.57	0.20	0.04	7.64
	27/08/2015	St.1	30.52	0.50	0.18	0.99	0.21	2.54	0.16	0.01	23.70	12.43	0.32	0.13	0.21	0.17	2.37	0.12	0.01	5.85
	27/08/2015	St.2	41.27	0.57	0.15	20.79	0.24	1.94	0.14	0.02	19.53	38.10	0.60	<Q.L.	13.40	<Q.L.	4.60	<Q.L.	<Q.L.	10.30
	27/08/2015	St.3	322.86	0.94	0.21	76.36	0.25	3.35	0.38	0.03	85.56	245.00	0.60	<Q.L.	113.00	0.60	10.20	<Q.L.	<Q.L.	13.50
	27/08/2015	St.4	169.52	0.55	0.19	14.94	0.24	2.80	0.21	0.02	21.06	186.00	0.60	<Q.L.	17.10	<Q.L.	8.20	<Q.L.	<Q.L.	16.10
	16/11/2015	St.1	189.00	1.50	0.80	4.20	0.70	28.70	5.40	<Q.L.	89.00	42.40	0.50	1.90	0.60	1.00	2.50	<Q.L.	<Q.L.	9.10
	16/11/2015	St.2	136.00	1.10	0.30	9.60	<Q.L.	5.70	<Q.L.	<Q.L.	58.00	55.10	0.70	3.20	6.20	1.50	5.30	<Q.L.	<Q.L.	23.00
	16/11/2015	St.3	1230.00	6.20	2.70	69.80	2.50	18.30	0.70	<Q.L.	555.00	142.00	0.70	1.60	26.70	1.40	4.30	<Q.L.	<Q.L.	15.90
	16/11/2015	St.4	149.00	1.40	0.30	17.50	<Q.L.	9.10	0.40	<Q.L.	56.30	64.10	1.10	<Q.L.	13.40	<Q.L.	8.90	0.30	<Q.L.	26.00

Table A-3 Overall correlations between total metal concentrations for all the sites

	Cu	Fe	Cr	Mn	Ni	Zn	Pb	Cd	Al	DOC	C:N
Cu	1										
Fe	.608[**]	1									
Cr	.484[**]	.315[**]	1								
Mn	.417[**]	.897[**]	.116	1							
Ni	.714[**]	.345[**]	.765[**]	.149	1						
Zn	.606[**]	.401[**]	.275[**]	.273[**]	.474[**]	1					
Pb	.628[**]	.461[**]	.305[**]	.302[**]	.423[**]	.586[**]	1				
Cd	.671[**]	.378[**]	.272[*]	.274[*]	.432[**]	.737[**]	.710[**]	1			
Al	.842[**]	.721[**]	.473[**]	.518[**]	.532[**]	.610[**]	.565[**]	.565[**]	1		
DOC	.146	.112	-.188	.144	.037	.032	-.191	.052	.080	1	
C:N	.202	.105	-.007	.109	.205	.063	-.121	.131	.159	.662[**]	1

**. Correlation is significant at the 0.01 level, * 0.05 level (2-tailed).

A-1 PARAFAC modeling

Initially, the PARAFAC model was run on the complete dataset (62 EEMs) (Figure A-2) to identify outliers and estimate the number of components. After removing outliers, the model was fitted with both negative and non-negative constraints. PARAFAC model can be run with or without non-negativity constraints, when run without non-negativity constraints, it considers negative wavelengths and concentrations, which in real terms are physically meaningless and chemically impossible. When run with non-negativity constraints, the model is restricted to positive wavelengths and concentrations. In both modes, leverage value analysis was used to identify the possible outliers. From leverage values and visual spectra checking, five outliers were identified from the leverages (Figure A-3). The leverage value reveals how far a sample is from the average distribution of all samples and samples with high leverages include St.1 sample for July from MIZ, and, September samples for St.1, St.2 and St.3 from HIG and August sample for St.2 at HIG.
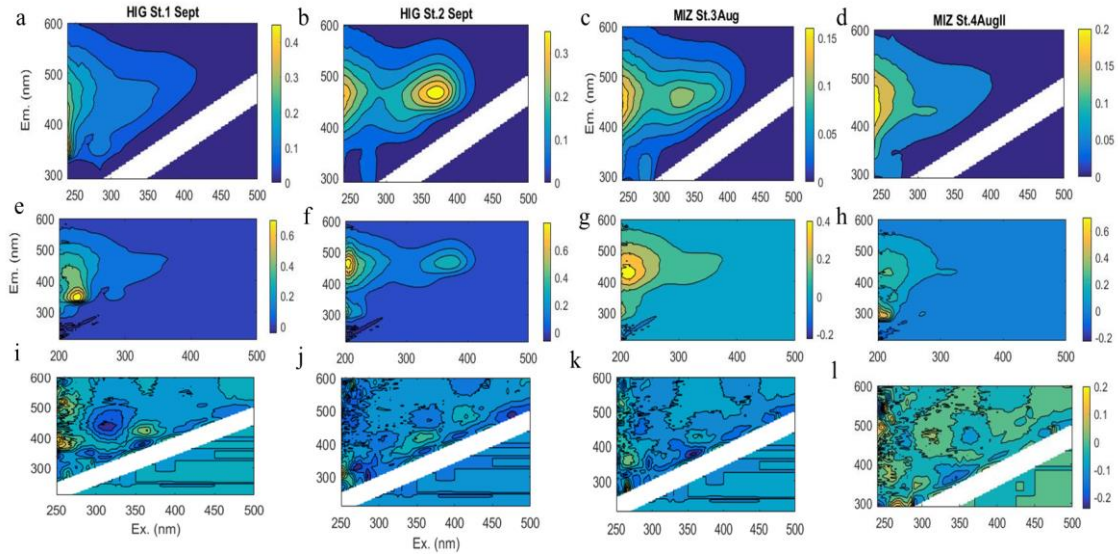
Figure A-2 Examples of EEM figures for different stations (St.1-St.4), a-d Modeled, e-h measured, i-l Residuals. (i) was excluded as an outlier.

Deciding on the number of components was based on core consistency diagnostic results, residual plots, visual checking of residual plots and finally, the data was split into four random sets and validated with split half analysis (Figure A-2 and A-4) (Murphy et al., 2014 and other references within). In the split half analysis, the dataset is divided into equal halves randomly, and then PARAFAC model is run on each pair, the excitation and emission loadings of combined pairs are compared with other pairs alternatingly. Four random splits used in this analysis consisted of 15, 14, 14 and 14 samples in each split.
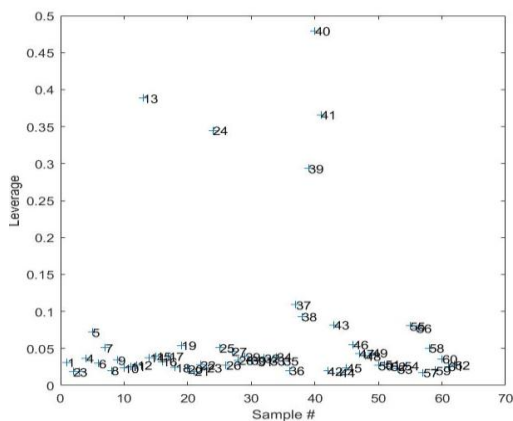
Figure A-3 Leverage scores for 62 samples showing outliers sample #13, #24, #41, #39 and #40.
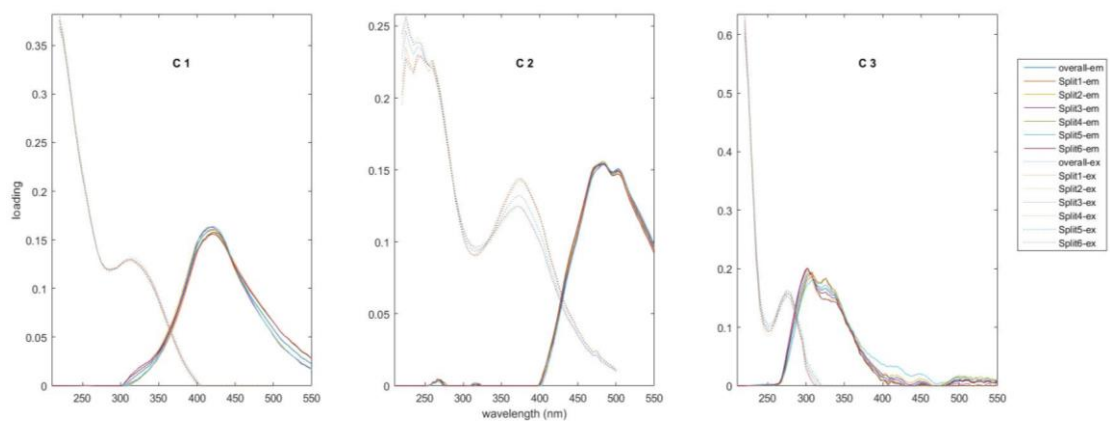
Figure A-4 Validated emission and excitation loading for split half analysis.

Table A-4. Monthly CDOM properties, fluorescence indices, and physicochemical properties of each sampling site

Month	Station	FIX	BIX	HIX	DOC	SD	$SUVA_{254}$	a350	E2:E3	S_R	$S_{275\text{-}295}$	pH	Temp	Turbidity	DO	ORP	Conductivity
6/22/2015	HIG St 1	1.46	0.53	8.57	0.75	0.01	3.03	1.43	4.71	0.77	0.014	7.44	15.5	2.10	8.72	333.0	6.20
	HIG St 2	1.59	0.54	6.12	0.82	0.02	2.79	1.40	4.95	0.68	0.013	7.79	16.1	1.47	9.21	303.0	6.80
	HIG St 3	1.56	0.54	8.65	0.84	0.01	3.07	1.66	4.79	0.67	0.012	7.78	19.8	7.43	8.24	326.0	6.77
	HIG St 4	1.48	0.56	5.37	0.92	0.92	2.90	1.77	4.69	0.81	0.014	7.31	21.5	4.60	8.16	297.7	7.27
7/15/2015	HIG St 1	1.49	0.54	8.53	0.17	0.02	2.88	1.82	4.37	0.86	0.013	7.76	18.5	5.30	10.48	326.7	5.67
	HIG St 2	1.68	0.52	5.35	1.05	0.00	2.85	2.23	4.10	0.64	0.010	7.53	19.3	1.57	10.32	302.0	6.45
	HIG St 3	1.59	0.57	7.81	1.15	0.01	2.42	2.12	3.96	0.73	0.011	7.87	21.3	1.77	9.92	233.7	6.30
	HIG St 4	1.52	0.60	6.39	0.91	0.03	3.32	2.12	4.26	0.85	0.013	7.58	22.8	1.17	9.73	265.3	8.60
8/13/2015	HIG St 1	1.51	0.52	3.67	1.49	0.03	2.39	2.10	5.35	0.78	0.013	7.43	18.0	2.90	8.98	334.0	5.80
	HIG St 2	2.35	0.36	6.17	0.65	0.00	4.01	1.95	4.22	0.62	0.010	7.29	19.2	1.60	8.88	316.0	6.60
	HIG St 3	1.43	0.51	3.69	0.68	0.01	3.73	1.94	4.06	0.70	0.011	7.80	20.0	9.70	9.32	324.0	6.50
	HIG St 4	1.55	0.60	7.60	0.99	0.01	3.06	2.10	4.61	0.78	0.013	7.37	20.6	5.20	9.54	340.0	9.30
8/28/2015	HIG St 1	1.59	0.64	4.77	1.03	0.02	2.11	1.43	4.86	0.84	0.014	7.52	18.8	0.00	9.02	323.0	6.70
	HIG St 2	1.53	0.54	6.59	0.77	0.02	4.28	2.52	4.17	0.76	0.011	7.60	20.3	6.30	9.38	322.0	7.10
	HIG St 3	1.52	0.55	5.34	0.96	0.02	3.32	2.52	3.81	0.74	0.011	7.87	20.8	1.10	8.94	347.0	7.30
	HIG St 4	1.47	0.52	6.05	0.75	0.01	4.20	2.57	3.64	0.97	0.012	7.76	23.7	10.90	8.90	313.0	10.40
9/14/2015	HIG St 1	1.47	0.68	4.84	1.03	0.02	3.33	2.26	4.53	0.79	0.013	7.40	14.3	ND	10.09	319.0	10.11
	HIG St 2	2.36	0.48	6.92	1.22	0.02	2.69	2.39	4.07	0.66	0.011	7.20	15.6	ND	9.14	315.0	8.52
	HIG St 3	1.53	0.81	4.55	1.03	0.03	2.81	2.05	4.23	0.71	0.012	7.40	15.8	ND	7.92	325.0	8.47
	HIG St 4	1.55	0.60	8.21	1.20	0.01	2.99	2.52	4.26	0.75	0.012	7.40	17.8	ND	8.75	290.0	7.86
10/22/2015	HIG St 1	1.60	0.53	8.96	0.76	0.01	2.93	1.40	4.62	0.81	0.012	7.13	10.4	3.00	9.00	ND	6.30
	HIG St 2	1.60	0.54	7.36	0.70	0.01	5.55	3.23	3.54	0.61	0.012	7.06	11.4	14.10	8.95	ND	6.90
	HIG St 3	1.54	0.56	7.70	0.74	0.09	4.54	2.81	3.67	0.63	0.012	7.34	11.1	4.00	9.37	ND	7.70
	HIG St 4	1.53	0.60	7.71	1.31	0.01	3.01	2.80	4.24	0.89	0.012	7.19	15.6	1.20	8.35	ND	10.30
11/11/2015	HIG St 1	1.41	0.51	7.41	1.12	0.01	3.35	2.76	4.17	0.87	0.012	6.96	11.0	5.50	5.70	100.0	0.50
	HIG St 4	1.52	0.57	8.56	1.40	0.03	3.23	3.39	4.10	0.80	0.012	6.98	9.6	4.00	5.56	209.0	4.30
11/22/2015	HIG St 1	1.44	0.53	7.04	0.66	0.01	3.18	1.46	4.39	0.78	0.012	7.05	7.3	1.30	ND	150.0	4.30
	HIG St 2	1.45	0.54	5.96	0.66	0.00	3.21	1.48	4.14	0.78	0.012	7.09	7.2	5.70	ND	160.0	5.50

	HIG St 3	1.45	0.56	7.72	0.61	0.01	3.44	1.48	4.18	0.76	0.012	7.02	7.7	1.50	ND	88.0	5.40
	HIG St 4	1.52	0.61	7.78	1.12	0.01	2.48	2.01	4.14	0.72	0.012	6.89	9.3	2.60	ND	93.0	8.00
6/22/2015	MIZ St 1	1.37	0.48	8.02	0.76	0.03	3.24	1.60	4.96	0.77	0.013	6.95	15.3	0.00	8.61	331.7	3.73
	MIZ St 2	1.53	0.54	7.17	0.85	0.01	6.13	4.48	3.38	0.61	0.010	6.66	16.7	1.60	7.49	173.3	5.63
	MIZ St 3	1.54	0.55	6.96	0.85	0.03	6.80	5.15	3.28	0.57	0.010	6.92	15.9	1.10	9.11	156.0	5.57
	MIZ St 4	1.55	0.60	6.93	1.58	0.04	2.73	2.93	4.45	0.82	0.014	7.59	17.4	5.10	8.74	292.0	33.80
7/15/2015	MIZ St 1	2.43	0.49	9.82	0.83	0.05	2.95	1.46	5.14	0.81	0.014	6.92	17.5	0.00	9.03	301.7	4.73
	MIZ St 2	1.52	0.54	6.02	1.12	0.02	4.42	4.06	3.58	0.66	0.011	6.60	22.1	1.87	9.70	176.0	5.70
	MIZ St 3	1.56	0.56	9.36	1.01	0.00	5.55	4.92	3.34	0.60	0.010	7.19	19.5	3.77	12.00	221.0	5.47
	MIZ St 4	1.54	0.60	4.13	1.90	0.04	2.16	2.73	4.50	0.95	0.014	7.92	22.8	1.77	12.43	244.0	22.40
8/13/2015	MIZ St 1	1.43	0.51	8.46	0.69	0.01	6.56	3.15	4.34	0.87	0.014	6.75	20.3	4.90	3.52	297.0	5.00
	MIZ St 2	1.51	0.53	4.41	0.94	0.01	2.29	1.18	5.64	0.75	0.014	6.76	20.6	5.70	4.14	149.0	7.50
	MIZ St 3	1.58	0.56	7.82	0.85	0.01	7.22	5.45	3.35	0.59	0.010	7.17	19.7	8.80	5.75	123.0	6.60
	MIZ St 4	1.55	0.61	5.85	1.31	0.02	4.32	5.08	3.32	0.58	0.010	7.49	22.4	6.80	4.93	274.0	13.90
8/28/2015	MIZ St 1	1.47	0.55	4.78	1.28	0.02	1.90	1.40	5.51	0.80	0.014	6.89	21.9	2.40	3.74	147.0	6.30
	MIZ St 2	1.54	0.56	7.11	0.70	0.01	8.62	5.25	3.33	0.65	0.010	6.73	19.0	0.00	3.47	362.0	5.20
	MIZ St 3	1.93	0.43	4.05	0.97	0.02	6.77	5.91	3.27	0.61	0.010	7.23	19.7	2.70	4.65	142.0	6.20
	MIZ St 4	1.50	0.57	2.87	0.56	0.02	8.25	3.33	4.20	0.99	0.014	8.56	25.3	4.70	4.44	182.0	36.50
9/14/2015	MIZ St 1	1.41	0.48	12.01	0.97	0.04	2.87	1.66	5.25	0.74	0.014	6.90	14.9	ND	8.60	320.0	6.16
	MIZ St 2	1.50	0.54	5.93	1.05	0.02	3.94	3.04	4.13	0.67	0.012	7.00	16.3	ND	7.10	185.0	7.63
	MIZ St 3	1.50	0.54	8.27	1.03	0.01	4.06	3.10	4.04	0.62	0.011	7.00	15.7	ND	10.31	198.0	7.24
	MIZ St 4	1.55	0.61	7.26	1.34	0.01	2.63	2.31	4.70	0.83	0.014	8.00	17.2	ND	9.67	243.0	26.30
10/22/2015	MIZ St 1	1.43	0.51	14.20	0.75	0.01	3.33	1.77	4.22	0.82	0.013	6.84	11.4	1.40	8.70	ND	5.00
	MIZ St 2	1.50	0.57	6.67	0.81	0.00	2.95	1.78	4.05	0.80	0.010	6.55	12.2	4.00	8.44	ND	5.80
	MIZ St 3	1.50	0.56	9.39	0.71	0.04	3.51	1.75	4.15	0.76	0.011	6.97	12.4	4.90	9.14	118.0	5.60
	MIZ St 4	1.65	0.62	6.28	1.36	0.03	2.24	2.10	4.27	0.74	0.014	8.07	14.9	4.80	8.71	153.0	25.60
11/11/2015	MIZ St 1	1.43	0.50	10.32	1.00	0.02	3.20	2.21	4.37	0.95	0.013	7.12	9.9	5.50	5.79	196.0	3.80
	MIZ St 2	1.47	0.52	7.89	0.98	0.00	2.79	1.80	4.67	0.92	0.013	7.17	10.7	9.30	5.90	136.0	4.50
	MIZ St 3	1.47	0.53	6.01	1.15	0.01	3.20	2.60	4.30	0.95	0.013	7.14	10.8	1.50	5.64	164.0	4.30
	MIZ St 4	1.47	0.55	8.34	1.51	0.01	3.28	3.57	4.20	0.86	0.012	7.48	11.3	288.80	6.70	179.0	6.30
11/22/2015	MIZ St 1	1.41	0.52	12.52	0.66	0.01	3.28	1.38	4.79	0.75	0.013	6.82	8.1	0.10	6.80	251.0	5.00
	MIZ St 2	1.45	0.55	7.51	0.74	0.05	3.66	1.96	4.14	0.66	0.012	7.09	9.1	1.60	5.22	138.0	5.90
	MIZ St 3	1.51	0.56	9.53	0.69	0.02	4.07	2.16	3.94	0.65	0.011	6.64	9.1	1.10	5.90	81.0	6.20
	MIZ St 4	1.53	0.57	7.37	0.97	0.00	3.31	2.21	4.36	0.73	0.012	6.91	9.3	4.90	4.84	169.0	18.90

ND-No data

Table A-5 Correlation index between metals and DOM composition properties

St.1	Fe	Cu	Cr	Mn	Ni	Zn	Pb	Cd	Al	FeDiss	CuDiss	CrDiss	MnDiss	NiDiss	ZnDiss	PbDiss	CdDiss	AlDiss
DOC	.079	.067	.063	.062	-.127	-.666**	-.467	-.582*	.284	-.025	-.089	-.083	.203	-.357	.092	-.130	-.108	-.118
C1	-.434	-.309	-.289	-.226	-.316	.011	.151	.269	-.110	-.442	-.023	.092	-.056	-.298	.120	-.147	.003	-.055
C2	-.116	.097	-.187	-.018	.136	.883**	.822**	.950**	-.035	-.137	.128	.023	-.076	.154	-.106	-.066	-.034	.047
C3	-.029	.148	-.211	.103	.119	.895**	.866**	.954**	.159	-.105	.199	.095	.075	.141	-.128	-.083	-.070	.157
C1C2	.307	.411	.594*	.119	.325	-.028	-.028	.022	.239	-.429	.631**	-.136	.128	-.422	.097	-.195	-.111	.186
SUVA254	-.223	-.052	-.066	-.261	-.061	-.051	.031	-.078	-.066	-.074	-.127	-.145	-.140	-.089	-.092	-.027	-.074	.178
a350	-.223	.327	.017	-.230	.092	-.081	.096	-.017	.383	.021	-.123	-.191	.192	-.265	-.111	-.214	-.275	.295
E2E3	.071	-.203	.039	-.030	-.167	-.225	-.153	-.117	-.238	-.475	.141	-.059	-.337	-.309	.204	-.153	.102	-.419
SR	-.207	.140	.081	-.167	.221	.118	.284	.241	-.039	.081	-.210	-.314	-.019	-.537	-.487	-.409	-.344	.045
S275295	-.418	-.348	-.023	-.501	-.293	-.340	-.175	-.039	-.488	-.843**	-.035	-.389	-.621*	-.569	.097	.015	.273	-.441
DON	-.099	-.195	.162	-.359	-.172	-.562*	-.424	-.417	-.351	-.408	-.083	-.200	-.559*	-.279	-.211	-.201	-.068	-.275
Fe	1	.604*	.532	.917**	.539*	.129	.152	-.058	.700**	.517	.657*	.228	.690**	.103	-.118	.055	-.084	.186
Mn	.917**	.368	.226	1	.356	.182	.248	-.028	.779**	.661*	.460	.361	.902**	.175	-.104	.112	-.075	.112

St .2	Fe	Cu	Cr	Mn	Ni	Zn	Pb	Cd	Al	FeDiss	CuDiss	CrDiss	MnDiss	NiDiss	ZnDiss	PbDiss	CdDiss	AlDiss
DOC	.180	.531*	-.240	.166	.229	.537*	-.106	.299	.282	.103	.194	-.122	.140	.230	.196	.444	.045	.143
C1	.668*	-.218	-.432	.652*	-.132	.064	-.227	.199	-.199	.694**	.092	-.626*	.702**	-.339	.739**	-.521	.563	-.304
C2	-.302	-.065	.145	-.278	.194	.048	-.156	-.140	-.173	-.175	.353	.356	-.240	.329	.079	-.256	-.183	.061
C3	.493	-.032	-.246	.371	-.349	-.064	.242	.275	.241	.471	.057	-.508	.304	-.185	.365	.211	.469	.192
C1C2	.595*	-.239	-.582*	.616*	-.663**	-.321	.091	.426	.009	.570*	-.213	-.679**	.576*	-.473	.006	-.050	.609*	-.049
SUVA254	.360	-.324	-.186	.287	-.130	-.034	-.041	.132	-.165	.402	-.052	-.306	.306	-.334	.497	-.331	.353	-.228
a350	.489	-.125	-.332	.406	-.082	.161	-.027	.313	-.054	.527*	.047	-.428	.403	-.268	.585*	-.196	.475	-.139
E2E3	-.202	.032	.040	-.105	-.113	-.109	-.151	-.136	.018	-.332	-.035	.148	-.090	.031	-.432	-.026	-.268	.074
SR	-.213	-.327	-.310	-.155	-.178	-.308	.011	-.334	-.275	-.143	-.482	.275	-.131	.042	-.204	-.222	-.309	-.109
S275295	-.247	-.282	.061	-.157	-.178	-.105	-.128	-.354	-.236	-.327	-.182	.228	-.147	-.067	-.407	-.320	-.317	-.065
DON	.315	-.624*	-.708**	.439	-.585*	-.187	-.450	-.281	-.591*	.478	-.261	-.192	.462	.075	.195	-.871**	.367	-.286

	Fe	Cu	Cr	Mn	Ni	Zn	Pb	Cd	Al	FeDiss	CuDiss	CrDiss	MnDiss	NiDiss	ZnDiss	PbDiss	CdDiss	AlDiss
Fe	1	.033	-.627*	.957**	-.378	.050	-.061	.357	.096	.923**	.157	-.927**	.945**	-.174	.535*	-.188	.448	-.199
Mn	.957**	-.121	-.707**	1	-.479	.068	-.180	.199	-.103	.947**	.164	-.917**	.990**	-.022	.523*	-.376	.496	-.332

St.3	Fe	Cu	Cr	Mn	Ni	Zn	Pb	Cd	Al	FeDiss	CuDiss	CrDiss	MnDiss	NiDiss	ZnDiss	PbDiss	CdDiss	AlDiss
DOC	.206	.426	-.101	.078	.283	.473	.436	.459	.467	-.070	.488	-.382	-.026	.369	.834**	.514	.600	.344
C1	.592*	-.311	-.277	.642*	-.307	-.508	-.283	-.067	-.343	.453	-.324	-.507	.603*	-.439	-.368	-.472	-.204	-.492
C2	.356	-.119	.012	.406	.037	-.101	-.103	.060	-.135	.437	-.090	-.100	.437	-.124	-.275	-.106	.185	.116
C3	.229	.065	.059	.286	.001	-.016	.070	-.184	.031	.142	.048	.040	.165	.025	-.297	.024	-.135	-.151
C1C2	.154	-.072	-.011	.114	-.189	-.112	-.074	-.141	-.088	-.091	-.105	-.257	.031	-.117	.159	-.067	-.281	-.424
SUVA$_{254}$	.761**	-.203	-.435	.884**	-.315	-.248	-.172	.100	-.224	.656**	-.200	-.430	.785**	-.319	-.479	-.337	-.158	-.402
a350	.792**	-.084	-.479	.855**	-.246	-.103	-.049	.301	-.085	.619*	-.060	-.536*	.751**	-.233	-.165	-.258	.014	-.274
E2E3	-.665**	.264	.617*	-.755**	.606*	.275	.236	-.349	.280	-.589*	.265	.378	-.668**	.375	.237	.407	-.004	.386
SR	-.594*	.760**	.184	-.723**	.548*	.715**	.743**	-.214	.762**	-.456	.733**	.383	-.569*	.837**	.346	.850**	.077	.333
S$_{275295}$	-.879**	.518*	.509	-.919**	.577*	.482	.482	-.343	.516*	-.790**	.504	.517	-.816**	.653*	.324	.678*	-.099	.373
DON	.706**	.529*	-.437	.758**	.233	.436	.559*	.198	.528*	.521*	.554*	-.575*	.486	.509	.108	.611	.363	.070
Fe	1	-.121	-.441	.955**	-.205	.030	.626*	.207	.027	.881**	.108	-.708**	.894**	-.473	-.102	-.211	.013	-.233
Mn	.955**	-.291	-.476	1	-.266	-.047	.507	.111	-.153	.859**	.006	-.646*	.920**	-.347	-.283	-.299	-.052	-.340

St.4	Fe	Cu	Cr	Mn	Ni	Zn	Pb	Cd	Al	FeDiss	CuDiss	CrDiss	MnDiss	NiDiss	ZnDiss	PbDiss	CdDiss	AlDiss
DOC	.368	.032	.160	.184	.047	.568*	-.009	.433	-.179	.294	.175	.066	-.087	.411	-.021	.888**	.067	.302
C1	-.579*	.124	-.101	-.599*	-.074	-.317	.005	-.196	-.012	-.547*	.222	-.187	-.546*	-.481	.072	-.815**	.054	-.232
C2	-.473	.290	-.124	-.488	-.095	-.350	.120	-.167	.300	-.546*	.087	-.251	-.341	-.492	.050	-.876**	-.023	-.241
C3	-.656*	.176	.012	-.555*	.077	.069	.040	.142	-.051	-.606*	.329	-.056	-.637*	-.363	.222	-.449	.462	-.215
C1C2	-.372	-.367	.049	-.417	.077	.160	-.227	-.029	-.696**	.063	.290	.143	-.421	.081	.009	.303	.213	.051
SUVA$_{254}$	-.313	.069	-.228	-.302	-.171	-.323	.084	-.168	.104	-.299	-.063	-.150	-.219	-.434	-.184	-.539	-.202	.068
a350	.185	.122	-.146	-.004	-.239	-.114	.181	-.019	.059	.121	-.028	.224	-.185	-.281	-.272	-.042	-.333	-.015
E2E3	-.162	-.268	.079	-.043	.048	.314	-.299	.133	-.419	-.107	.216	-.418	-.168	.224	.271	.374	.379	.411
SR	-.137	.339	-.026	-.055	-.046	.351	.412	.390	.409	-.383	-.132	-.738**	-.054	-.068	-.033	.177	.245	.305
S$_{275295}$	-.296	.222	.146	-.212	.209	.522*	.062	.436	-.005	-.460	.227	-.677*	-.384	.090	.175	.495	.631*	.580*

114

DON	.394	-.385	-.043	.399	-.130	-.171	-.042	-.104	-.230	.359	-.521*	-.032	.313	-.092	-.487	.031	-.397	.254
Fe	1	.100	.243	.802**	-.071	-.181	-.001	-.261	.364	.753**	-.096	.150	.566*	.419	.069	.303	-.281	.167
Mn	.802**	-.140	.251	1	.071	-.057	.004	-.066	.340	.523*	-.389	.220	.714**	.208	.028	.406	.003	.218

**. Correlation is significant at the 0.01 level (2-tailed), *. Correlation is significant at the 0.05 level (2-tailed).

Table A-6 Results for PCA showing explained variance and Eigen values and explained variance

Component	Initial Eigenvalues			Extraction Sums of Squared Loadings		
	Total	% of Variance	Cumulative %	Total	% of Variance	Cumulative %
1	5.666	25.757	25.757	5.666	25.757	25.757
2	3.691	16.779	42.536	3.691	16.779	42.536
3	2.272	10.327	52.863	2.272	10.327	52.863
4	1.952	8.874	61.737	1.952	8.874	61.737
5	1.675	7.615	69.352	1.675	7.615	69.352
6	1.389	6.314	75.665	1.389	6.314	75.665
7	1.186	5.392	81.057	1.186	5.392	81.057
8	.805	3.660	84.717			
9	.673	3.060	87.777			
10	.634	2.884	90.661			
11	.503	2.286	92.947			
12	.359	1.633	94.580			
13	.345	1.569	96.149			
14	.287	1.306	97.455			
15	.187	.851	98.305			
16	.125	.570	98.875			
17	.100	.454	99.329			
18	.080	.362	99.691			
19	.037	.168	99.858			
20	.015	.067	99.925			
21	.010	.044	99.969			
22	.007	.031	100.000			

Extraction Method: Principal Component Analysis.

Component Matrix[a]

	Component						
	1 (25.8%)	2 (16.8%)	3 (10.6%)	4	5	6	7
FeDiss	-.900	.030	.014	-.044	.108	-.006	-.316
CuDiss	.169	-.211	.242	.253	.571	.262	.080
CrDiss	.309	.022	-.462	-.010	-.037	.519	.498
MnDiss	-.887	.035	-.005	.001	.002	-.132	-.307
ZnDiss	-.163	.032	.018	-.295	.607	-.425	.263
AlDiss	.470	-.105	.405	-.186	.400	.305	-.086
C1	.093	-.602	.340	-.328	.061	.272	-.156
C2	.186	.861	-.121	.313	.189	.056	-.157
C3	.224	.829	-.187	.334	.178	.073	-.120
DOC	.266	.798	.209	.293	.136	-.013	-.126
SUVA254	-.708	.348	.355	.174	.020	-.135	.345
a350	-.813	.207	.358	-.029	.066	.186	.171
E2E3	.714	-.398	-.230	.165	-.087	-.312	-.138
SR	.663	-.160	.362	.453	.030	-.104	-.062
S275295	.777	-.320	.154	.267	.038	-.371	-.072
DON	-.325	-.490	.260	.439	.121	.031	.194
pH	.559	.400	.414	-.312	-.160	.205	.083
Temp	.087	.384	.391	-.430	-.303	-.446	.098
DO	.297	.226	-.157	-.573	.151	.209	-.450
ORP	.483	.342	-.230	-.405	.082	-.195	.386
EC	.269	.156	.821	-.103	-.106	.037	-.009
Turbidity	.017	.116	.146	.221	-.728	.233	.016

Extraction Method: Principal Component Analysis.

a. 7 components extracted.

Acknowledgement